

RD-A150 336

SOME CHARACTERISTICS OF AUTOMOTIVE GASOLINES AND THEIR
PERFORMANCE IN A L. (U) MICHIGAN UNIV ANN ARBOR DEPT OF
MECHANICAL ENGINEERING AND AP. K M MORRISON ET AL.

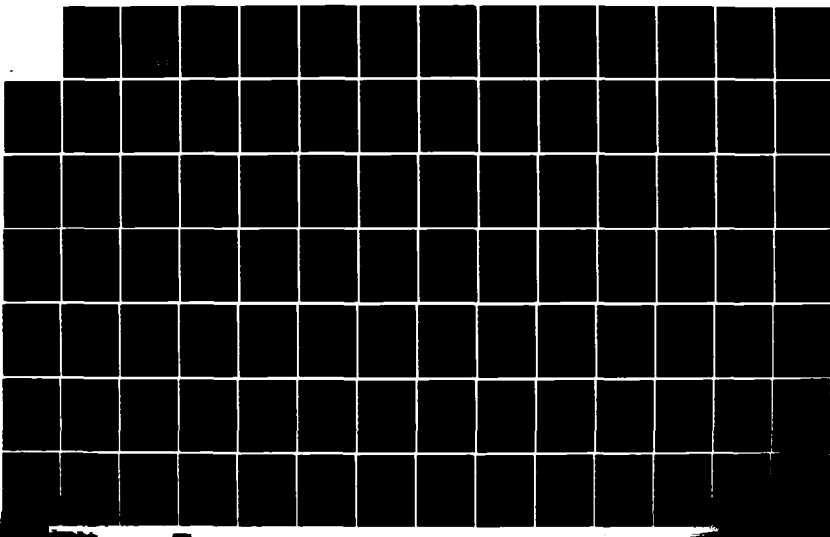
1/2

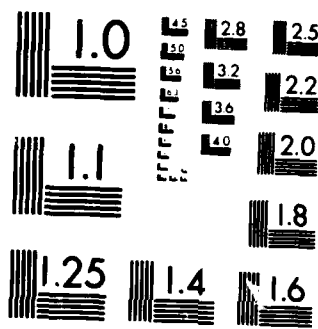
UNCLASSIFIED

NOV 84 DOT/FAA/CT-84/12 DOT-FA79NA-6083

F/G 21/4

NL





MICROCOPY RESOLUTION TEST CHART
NATIONAL BUREAU OF STANDARDS 1963 A

AD-A150 336

12

DOT/FAA/CT-84/12

Some Characteristics of Automotive Gasolines and their Performance in a Light Aircraft Engine

K. M. Morrison
Nak W. Sung
D. J. Patterson
University of Michigan

Final Report
November 1984

This document is available to the U.S. public through the National Technical Information Service, Springfield, Virginia 22161.

NOTICE

This document is disseminated under the sponsorship of the Department of Transportation in the interest of information exchange. The United States Government assumes no liability for the contents or use thereof.

The United States Government does not endorse products or manufacturers. Trade or manufacturer's names appear herein solely because they are considered essential to the object of this report.

Technical Report Documentation Page

| | | | |
|--|--------------------------------------|--|-----------|
| 1. Report No. | 2. Government Accession No. | 3. Recipient's Catalog No. | |
| DOT/FAA/CT-84/12 | | | |
| 4. Title and Subtitle | | 5. Report Date | |
| Some Characteristics of Automotive Gasolines and Their Performance in a Light Aircraft Engine | | November 1984 | |
| 6. Performing Organization Code | | | |
| 7. Author(s) | | 8. Performing Organization Report No. | |
| K. M. Morrison, Nak W. Sung, D. J. Patterson | | | |
| 9. Performing Organization Name and Address | | 10. Work Unit No. (TRAIS) | |
| The University of Michigan Department of Mechanical Engineering 309 Automotive Laboratory, North Campus Ann Arbor, Michigan 48109 | | 11. Contract or Grant No. | |
| 12. Sponsoring Agency Name and Address | | 13. Type of Report and Period Covered | |
| Federal Aviation Administration Technical Center Atlantic City Airport, New Jersey 08405 | | Final Report October 1982 - March 1984 | |
| 14. Sponsoring Agency Code | | | |
| 15. Supplementary Notes | | | |
| <p>16. Abstract</p> <p>The primary purpose of this extensive test effort was to observe real-time operational performance characteristics associated with automotive grade fuel utilized by piston engine powered light general aviation aircraft. In fulfillment of this effort, baseline engine operations were established with 100LL aviation grade fuel followed by four blends of automotive grade fuel.</p> <p>A comprehensive sea - level - static test cell/flight test data collection and evaluation effort was conducted to review operational characteristics of a carbureted light aircraft piston engine as related to fuel volatility, fuel temperature, and fuel system pressure. Presented herein are results, data, and conclusions drawn from test cell engine operation as well as flight test operation on 100LL aviation grade fuel and various blends of automotive grade fuel.</p> <p>Sea - level - static test cell engine operations were conducted utilizing an AVCO Lycoming 0-320 engine connected to an eddy current dynamometer which facilitated data collection under various engine load conditions. Test cell instrumentation was utilized to obtain operational data (temperatures, pressures, flow rates, torque, horsepower, exhaust emissions, etc.) from idle through cruise to maximum power with fuel grades having Reid vapor pressures of 6.7, 8.0, 11.7, 14.0, and 14.4. In addition, real-time inflight performance data was obtained utilizing a Cessna 150/Continental 0-200A engine, while operating on test fuels No. 1 and No. 2 which had Reid vapor pressures of 14.4 psi and 8.0 psi, respectively.</p> | | | |
| 17. Key Words | | 18. Distribution Statement | |
| General Aviation Automotive Fuel Aviation Fuel Vapor Lock Vapor-Liquid Ratio | | Document is available to the U.S. public through the National Technical Information Service, Springfield, VA 22161 | |
| 19. Security Classif. (of this report) | 20. Security Classif. (of this page) | 21. No. of Pages | 22. Price |
| Unclassified | Unclassified | | |

Preface

The authors wish to acknowledge the contribution of Thomas Slopsema, who performed the vapor to liquid ratio tests. We appreciate the contributions of equipment and advice of Dr. Larry Duke of Avco-Lycoming, Williamsport Division, Williamsport, Pennsylvania and the donation of special test fuels from, and the advice of, Mr. Larry Meyer of Phillips Petroleum Co. of Bartlesville, Oklahoma. We also appreciate the suggestions of Harry Zeisloft of Experimental Aircraft Association (EAA) and Keith Biehl of Federal Aviation Administration (FAA).

| | |
|--------------------|-------------------------------------|
| Accession For | |
| NTIS GFA&I | <input checked="" type="checkbox"/> |
| DTIC TAB | <input type="checkbox"/> |
| Unclassified | <input type="checkbox"/> |
| Ja 177401 2 | |
| By | |
| Distribution/ | |
| Availability Codes | |
| Avail and/or | |
| Dist | Special |
| A-1 | |



LIST OF ILLUSTRATIONS

| Figure | | Page |
|--------|--|------|
| 1 | Distillation Curve for Five Fuels | A-6 |
| 2 | Vapor to Liquid Ratio Test Arrangement | A-7 |
| 3 | Vapor to Liquid Ratios at Different Temperatures - Calculated and Measured | A-8 |
| 4 | Vapor to Liquid Ratios at Altitude for 100LL Fuel | A-9 |
| 5 | Vapor to Liquid Ratio at Altitude for No. 1 Fuel | A-10 |
| 6 | Vapor to Liquid Ratio at Altitude for Wet 100LL Fuel | A-11 |
| 7 | Schematic Diagram of Two Fuel Delivery Systems | A-12 |
| 8 | Fuel Pump Flow Versus Engine Speed | A-13 |
| 9 | Pressure Variation Inside Fuel Pump | A-14 |
| 10 | Pressure Drop Through the Gravity Fuel System and Carburetor | A-15 |
| 11 | Equivalence Ratio Distribution With 100LL Fuel | A-16 |
| 12 | Equivalence Ratio Distribution With No. 1 and No. 2 Fuels | A-17 |
| 13 | Inlet Air Temperature Effect on Mixture Distribution | A-18 |
| 14 | Vapor Lock Development | A-19 |
| 15 | Torque Variation as Vapor Lock Develops | A-20 |
| 16 | Vapor to Liquid Ratio When Vapor Lock Occurs- With Fuel Pump System | A-21 |
| 17 | Vapor to Liquid Ratio When Vapor Lock Occurs- Gravity Feed System | A-22 |
| 18 | Time for Vapor Lock - With Fuel Pump System | A-23 |
| 19 | Time for Vapor Lock - Gravity Feed System | A-24 |
| 20 | Fuel Temperature When Vapor Lock Occurs- With Fuel Pump System | A-25 |
| 21 | Fuel Temperature When Vapor Lock Occurs- Gravity Feed System | A-26 |

| | | |
|----|--|------|
| 22 | Heat Added per Pound of Fuel versus Vapor to Liquid Ratio - Fuel No. 1 | A-27 |
| 23 | Heat Added per Pound of Fuel versus Vapor to Liquid Ratio - Wet 100LL | A-28 |
| 24 | Heat Added per Pound of Fuel versus Vapor to Liquid Ratio - Dry 100LL | A-29 |
| 25 | Weight Percent Vaporized versus Temperature for No. 1 Fuel | A-30 |
| 26 | Weight Percent Vaporized versus Temperature for Wet 100LL | A-31 |
| 27 | Weight Percent Vaporized versus Temperature for Dry 100LL | A-32 |
| 28 | Vapor to Liquid Ratio versus Weight Percent Vaporized | A-33 |
| 29 | Density Ratio Between Liquid and Total Vapor Evolved up to Different Vapor to Liquid Ratios- No. 1 Fuel and Dry 100LL | A-34 |
| 30 | Density Ratio Between Liquid and Total Vapor Evolved up to Different Vapor to Liquid Ratios- Wet 100LL | A-35 |
| 31 | Measured Flow Characteristics of Gravity Fuel System Components | A-36 |
| 32 | Float Bowl Vacuum versus Engine Speed | A-37 |
| 33 | Calculated Radiant and Convective Heat Transfer to Strainer (Baseline and Insulated) and Carburetor Line | A-38 |
| 34 | Calculated Radiant Heat Transfer to Strainer (Baseline and Insulated) versus Distance from Exhaust Pipe for Various Surface Temperatures | A-39 |
| 35 | Effect of Strainer Size on Fuel System Pressure Drop - Calculated | A-40 |
| 36 | Effect of Carburetor Line Inside Diameter on Total System Pressure Drop and Total Pressure Head Available - Uninsulated Strainer | A-41 |
| 37 | Effect of Carburetor Line Inside Diameter on Total System Pressure Drop and Total Pressure Head Available - Insulated Strainer | A-42 |

| | | |
|----|--|------|
| 38 | Source of Pressure Drops as Carburetor Line Inside Diameter is Changed - Uninsulated Strainer | A-43 |
| 39 | Source of Pressure Drops as Carburetor Line Inside Diameter is Changed - Insulated Strainer | A-44 |
| 40 | Vapor to Liquid Ratios Present at Various Places in Fuel System versus Engine Speed- Uninsulated Strainer | A-45 |
| 41 | Vapor to Liquid Ratios Present at Various Places in Fuel System versus Engine Speed- Insulated Strainer | A-46 |
| 42 | Breakdown of Sources of Fuel Head Available and Pressure Drops - Uninsulated Strainer | A-47 |
| 43 | Effect of Carburetor Inlet Valve Area on Pressure Drop | A-48 |
| 44 | Effect of Fuel System Modification on Initial Fuel Temperature Producing Vapor Lock | A-49 |
| 45 | Effect of Water in 100LL Fuel and Effect of Carburetor Inlet Valve Modification on Initial Fuel Temperature Producing Vapor Lock | A-50 |
| 46 | Effect of Fuel Tank Temperature Drop Before Hot Fuel Handling Test | A-51 |
| 47 | Effect of Agitation of Fuel in Tank | A-52 |
| 48 | Effect of Altitude on Vapor Lock with Different Fuel Tank Cooling Rates | A-53 |
| 49 | Effectiveness of "Ideal" Boost Pump | A-54 |
| 50 | Measured Fuel Consumption Rate versus Engine Speed | A-55 |
| 51 | Measured Cylinder Head and Cooling Air Temperatures versus Engine Speed | A-56 |

LIST OF TABLES

| Table | | Page |
|-------|---|------|
| 1 | Properties of Fuels | 3 |
| 2 | Standard Deviations of Equivalence Ratio | 6 |
| 3 | Standard Deviation of Equivalence Ratio for Different Inlet Air Temperatures | 7 |
| 4 | Engine Test Conditions | 9 |
| 5 | Baseline Conditions Representative of a Typical Gravity Feed Fuel System used with Lycoming O-320 Engine | 21 |

EXECUTIVE SUMMARY

This report, "Some Characteristics of Automotive Gasolines and Their Performance in a Light Aircraft Engine", presents observations/data obtained by the University of Michigan for the Federal Aviation Administration Technical Center under contract DOT-FA79NA-6083. As part of the contract effort, the University conducted engine tests on a FAA Technical Center provided AVCO Lycoming O-320 light aircraft piston engine. In addition, the University subcontracted with the Experimental Aircraft Association for real-time flight test performance data which was obtained with a Cessna 150/Continental O-200A engine. Performance data were obtained on both engines with 100LL aviation grade fuel and four blends of automotive fuel. Reid vapor pressures were of 6.7, 8.0, 11.7, 14.0 and 14.4 psi for these fuels.

Standard engine test cycles which encompassed flight conditions of; idle, full power, cruise (rich and lean), descent and approach were established for the O-320 engine operated in a sea-level test cell. Flight test cycles were established to cover taxi/engine warm-up, takeoff/landing, cruise (rich/lean), and maximum performance climb. The test cell cycles were run on all fuels while the flight test cycles were performed on 8.0 and 14.4 Reid vapor pressure fuel blends. Conclusions reached as a result of this extensive test effort are:

1. The more volatile automotive fuels tended to give slightly worse mixture distribution when compared to 100LL.
2. A modification of the ASTM test for vapor to liquid ratio in which the gasoline was permitted to become wet, significantly increased the vapor to liquid ratios and thereby indicates the tendency to vapor lock is greater when a small amount of liquid water is present in the fuel.
3. Exhaust air/fuel ratio, fuel pressure, vapor to liquid ratio, fuel system temperatures and engine output torque all provided indications of vapor lock.
4. For a given engine speed and load the critical vapor to liquid ratio was constant regardless of fuel volatility.
5. Under controlled heating of the fuel supply line, the time interval for vapor lock was found to be related to fuel volatility with the more volatile fuels vapor locking in shorter time.
6. A computer analysis largely based on experimental data was successful in explaining complex relationships of variables affecting vapor lock. It was also useful for evaluating possible fuel system modification to reduce vapor lock.
7. The phenomenon of vapor release due to agitation of the fuel was observed and found to be beneficial if the vapor was released in the fuel tank and detrimental if agitation of the fuel occurred while in the fuel system. Such agitation may arise from resonance vibration of fuel lines or mechanical agitation from an in-line pump.
8. Flight and ground performance with both automotive fuel blends was found to be normal in the one aircraft tested.

INTRODUCTION

In recent years, the price of aviation gasoline has increased sharply and some shortages have arisen. As a result, there has been increased interest in the potential suitability of automobile gasoline for light aircraft. To address this question, a comprehensive study of the existing literature on fuel-related problems in both aviation and automotive engines has been performed at the University of Michigan under contract with the Federal Aviation Administration Technical Center (contract no. DOT-FA79NA-6083) (reference 1).

Principal concerns in the operation of aircraft piston engines are safety, performance, and durability. Several potential problems involved with the use of autogas in light aircraft were identified and classified as either short-term or long-term in nature. Knock, preignition, vapor lock, carburetor icing, and hot restart were identified as potential short-term problems. Loss of performance due to maldistribution, valve sticking, material degradation, lubrication, wear, and fuel storage stability were identified as potential long-term problems. The problems of vapor lock, icing, and maldistribution are directly related to fuel volatility.

Volatility affects engine performance through its influence on the degree of fuel evaporation in the fuel delivery system, intake manifold, and cylinder prior to the combustion process. The American Society for Testing and Materials (ASTM) distillation procedure 90 percent point temperature indicates the amount of heavy, high boiling point, components in the gasoline, and the 10 percent point temperature indicates the amount of light components. Since automobile gasolines have higher ASTM 90 percent point temperatures and lower 10 percent point temperatures than aviation gasolines, it was expected that aviation engines would exhibit increased maldistribution when automobile gasoline was used. Also more volatile fuels are expected to generate more vapor in the fuel delivery system. The serious safety problem of vapor lock occurs when fuel vapor and dissolved air evolve in the fuel system to such an extent that the flow of liquid gasoline is reduced below that required to maintain engine operation. Engine stalling results and restart can be extremely difficult.

The amount of vapor formed from volatile fuel is governed by fuel temperature and pressure. The amount of air evolved from the fuel is increased as fuel pressure decreases. Aldrich et al. (reference 2) correlated the fuel temperature to the amount of vapor formation expressed as vapor to liquid ratio for fuels of different Reid vapor pressure. At high altitudes, vapor formation is increased substantially, due to increased boiling of light fuel components and due to evolution of dissolved air.

York et al (reference 3) performed vapor lock tests in an airplane. They found that a pressure feed system employing a diaphragm pump experienced earlier incipient vapor lock than a gravity feed fuel delivery system. They recommended changing the fuel system to reduce the pressure drop. Piggot (reference 4) demonstrated techniques for calculating pressure drops in the fuel delivery system for different lines, fittings and pumps under two phase flow conditions. He correlated the results to the vapor to liquid ratios. He also indicated how these calculations could be used to analyze a fuel system for limiting fuel tank temperature and limiting altitude.

An experimental program at the University of Michigan has been conducted to evaluate some aspects of use of automobile fuels for light aircraft piston engines. An Avco Lycoming O-320 carbureted engine was employed. The first portion of the experimental program was mixture distribution and its resulting effects on the torque output when various blends were used. This study has been reported in reference 5 to the Federal Aviation Administration (FAA).

The present report summarizes the second portion of the experimental program which covered vapor and liquid-fuel flow characteristics in the fuel delivery system. Two fuel delivery systems, a pressure feed fuel pump system and a gravity feed fuel system, were studied. Reported herein are the vapor-forming tendencies of each of four automotive-type gasolines and one aviation gasoline. Also included in this report are additional results from mixture distribution tests for two specially blended fuels not included in the previous report (reference 5).

EXPERIMENTAL STUDY

FUELS

For the experimental study, two automobile gasolines designated 15B and 12A, two specially blended fuels designated No. 1 and No. 2, and one aviation gasoline (commercial 100LL) were employed. The properties of these are listed in table 1, and the distillation curves are shown in figure 1. The two automotive-type gasolines, 15B and 12A, were blended in an attempt to match volatility extremes of commercially available autogas. Mixture distribution data on these fuels were included in the earlier report (reference 5). Commercial automotive gasoline volatility extremes are shown in the figure also.

In the present study two new specially blended fuels, No. 1 and No. 2, were designed by Remondino (reference 6) and prepared by the Sun Tech Corporation. These fuels not only included extremes in volatility but also composition. They were formulated to be within the autogas specification, ASTM D-439-78 (reference 7) and were blended to have a (R+M)/2 of 87 octane. No. 1 fuel was formulated with ~0 percent catalytically cracked stocks together with a small amount of light straight-run, as necessary, to meet the distillation specifications. It was pressurized with butane and n-pentane to a Reid vapor pressure of 15 psi. This fuel had an overall volatility and minimum boiling temperature which approximately matched the minimum temperature of the Department of Energy survey for winter lead-free gasoline (reference 8). This fuel had especially low end-point volatility. No. 2 fuel was composed of catalytic reformate plus light straight-run for front-end volatility and pressurized with butane and pentane to a Reid vapor pressure of 8 psi.

In comparing these two fuels, No. 1 was expected to be critical in an aircraft engine that is operated at high mean effective pressure cruise conditions at low altitude. The high concentration of olefins might be expected to produce knock or preignition under lean operation conditions. Further its high volatility would promote potential vapor lock or icing problems. No. 2 fuel was expected to uncover situations where maldistribution was likely to occur. It would aggravate maldistribution upon takeoff in engines with cold intake manifolds where the intake manifold passed through an oil sump which was not yet warm. The fuel front-end was expected to have a very low octane number, since the aromatics in the back-end

Table 1
PROPERTIES OF FUELS

| | <u>100LL</u> <u>Avgas</u> | <u>12A</u> <u>Autogas</u> | <u>15B</u> <u>Autogas</u> | <u>No. 1</u> <u>Fuel</u> | <u>No. 2</u> <u>Fuel</u> |
|-----|------------------------------|------------------------------|------------------------------|-----------------------------|-----------------------------|
| H/C | 0.185 | 0.162 | 0.175 | -- | -- |
| RVP | 6.7(6.8) | 11.7 | 14.0 | 14.4 | 8.0 |
| MON | 101.55 | 90.66 | 90.01 | 81.5 | 83.6 |
| RON | 104.14 | 99.57 | 99.57 | 93.1 | 90.0 |
| SG | 0.705 | 0.739 | 0.704 | 0.735 | 0.753 |

Distillation Temperatures (°F)

| | | | | | |
|--------------|-----------|------|------|------|------|
| IBP | 108(108)* | 84 | 80 | 79 | 99 |
| 5% | 129(138) | 93 | 84 | 93 | 124 |
| 10 | 148(152) | 105 | 89 | 102 | 139 |
| 15 | 162(-) | 118 | 95 | -- | -- |
| 20 | 175(172) | 134 | 101 | 124 | 167 |
| 30 | 194(186) | 172 | 116 | 151 | 195 |
| 40 | 207(200) | 205 | 137 | 181 | 226 |
| 50 | 213(208) | 226 | 169 | 212 | 252 |
| 60 | 218(214) | 243 | 211 | 248 | 274 |
| 70 | 223(218) | 263 | 242 | 285 | 294 |
| 80 | 230(224) | 290 | 279 | 320 | 314 |
| 90 | 244(234) | 329 | 338 | 366 | 340 |
| 95 | 260(248) | 361 | 368 | 398 | 364 |
| FBP | 334(294) | 415 | 412 | 443 | 418 |
| Recovery(ml) | 98(98) | 96.4 | 96.5 | -- | -- |
| Residue (ml) | 0.1(1.0) | 0.3 | 0.1 | -- | -- |
| Loss (ml) | 1.9(1.0) | 3.3 | 3.4 | --** | --** |
| TEL (ml/gal) | -- | 3.0 | 3.0 | 0 | 0 |

Hydrocarbon Distribution

| | | | | | |
|--------------|---------|----|----|------|------|
| Aromatic (%) | (16.6)* | -- | -- | 26.5 | 40.3 |
| Olefin (%) | (0.1) | -- | -- | 24.0 | 1.6 |
| Paraffin (%) | (83.3) | -- | -- | 49.5 | 58.1 |

*Data inside parenthesis are for second batch of fuel.
**The fuel run in the University of Michigan Lycoming O-320 engine had an addition of 3.0 ml/gal TEL to ensure the 90/97 octane requirement of this engine was met.

would contribute most of the anti-knock quality. This can result in the high and low octane components of the fuel becoming separated in the intake manifold with possible knock resulting in one or more cylinders. Moreover the boiling range in this fuel would tend to worsen mixture distribution. The knock tendency of these fuels was not evaluated in our tests.

VAPOR TO LIQUID BENCH TESTS

Since gasolines are composed of many different hydrocarbons having different boiling temperatures, each component contributes different amounts of vapor at a given temperature. To determine the vapor formation characteristics of each fuel, vapor to liquid ratio bench tests were conducted following the procedures specified in ASTM D2533-67 (reference 7).

Figure 2 shows the test apparatus. A fuel sample of 1.0 milliliter, which was taken from a closed container kept on ice, was carefully introduced into the vapor to liquid burette by a 1.0 milliliter hypodermic syringe. (A 4.0 milliliter sample size was used for better precision at low vapor to liquid ratios below 7:1.) The hypodermic syringe was also kept cold on ice. The vapor to liquid burette was completely filled with water-free glycerin. After the sample fuel was injected in the burette, the burette was immersed in a water bath. The water temperature in the bath was controlled by addition of hot or cold water. A magnetic stirrer was used to provide uniform water bath temperature. Both liquid fuel and vapor were held at each temperature until equilibrium was reached and the vapor to liquid ratio was determined from readings of volume of vapor for the 1.0 milliliter of liquid. To simulate altitude and for control, the pressure at the vapor to liquid interface was controlled by a vacuum pump and the height of glycerin in the leveling bulb following Hodges' test modifications (reference 9).

Figure 3 shows the relationship between temperature and vapor to liquid ratio for each fuel at standard atmospheric pressure. All fuels showed a moderate vapor formation at lower temperatures up to a vapor to liquid ratio of about 2. Over a ratio of 4, vapor generation increased sharply with a small increase of temperature. These test data are indicated as solid lines in figure 3.

Computational results using ASTM D439x1.2 (reference 7) are shown by the discrete points in figure 3. This method employs ASTM distillation data and the Reid vapor pressure. A listing of the computer program used is in the appendix. This was written in "basic". While Hodges (reference 9) reported significant differences between experimental and calculated values, our computations were in excellent agreement with the data.

Two fuels, 100LL and No. 1, were tested at a pressure lower than standard atmospheric pressure of as much as 20 inches of mercury vacuum, the pressure at 27,000 feet altitude. The results are shown in figures 4 and 5. Reduced pressure increased vapor to liquid ratios significantly. For the 100LL fuel the effect of altitude up to 10,000 feet was to reduce boiling temperature about 3° F for every 1,000 feet for vapor to liquid ratios above 3. This effect was amplified for the vapor to liquid ratios below 2. For the No. 1 fuel, the effect was about 2.7° F reduction in boiling temperature for every 1,000 feet.

Since commercial gasolines are commonly saturated with water, it is of interest to determine the increase in vapor to liquid ratio for saturated fuel. For this the

glycerin in the vapor to liquid burette was replaced by water and the same altitude tests were repeated for the 100LL fuel whose Reid pressure was 6.8 psi. The presence of water-vapor increased the total vapor volume significantly as the comparison in figure 6 reveals. For example, at 10,000 feet a vapor to liquid ratio of 4 was reached at 127.4° F with water and 145.4° F with glycerin. This is an effect about equal to use of a dry 10 psi Reid vapor pressure autogas. Very little undissolved liquid water is required to produce this effect, as the following example suggests. At 122° F the ratio of the specific volume of water vapor to that of liquid water is 12530. Thus 0.1 percent by volume of liquid water at this temperature could form 12.5 volumes of vapor per volume of liquid mixture.

This large vapor to liquid effect is due to the additive characteristics of the vapor pressures of immiscible liquids (reference 9). The relative effect for higher vapor pressure fuels is less because the vapor pressure of water is much lower at the lower temperatures where the more volatile fuels generate significant volumes of vapor.

FUEL SYSTEM FLOW CHARACTERISTICS

Fuel flowrates are determined by the fuel delivery system and engine demand. Gonzalez (reference 10) discussed different fuel delivery systems for light aircraft engines, and indicated design changes which affect fuel flow. In the present study two fuel delivery systems were evaluated, an engine-driven diaphragm type fuel pump system and a gravity feed fuel system. Figure 7 shows schematics of the two systems.

For the fuel pump system, the maximum output flow rate of the fuel pump was measured for various engine speeds and two different fuels, the No. 1 and 100LL gasolines. This was done by collecting fuel in a container of known volume and measuring the filling time with a stopwatch. During this time, the engine was fueled by a completely separate gravity system. The gravity fuel head at the pump inlet was 18 inches, the same as for the majority of the testing with the fuel pump system. Figure 8 shows flow results for 100LL and No. 1 fuels at different engine speeds. The lower flow rate when pumping the volatile No. 1 fuel can be attributed to vapor formation inside the fuel pump. To show the reduced pressure inside the pump, a piezoelectric pressure transducer was installed in the pump cavity.

The pressure variation inside the diaphragm pump at 1000 rpm during normal engine operation on 100LL fuel is shown in figure 9. During the suction stroke, the pressure inside the pump fell to 3 psi below atmospheric pressure. Two curves are shown in figure 9. These are results for unrestricted and restricted inlet conditions. The lower curve (restricted inlet) shows a greater vacuum for a longer time. This resulted from enough blockage on the suction side of the fuel pump to cause the output pressure to fall from the normal 4 psi to 3 psi above atmospheric pressure. Such lower inlet pressure can arise from increased vapor formation with volatile fuels.

The pressure drop across various components of the gravity feed fuel system was quantified for different fuel flowrates. This was done by measuring flowrates of 100LL fuel into a container of known volume and timing the event with a stopwatch for various gravity heads. The measured flowrates for various pressure drops through the fuel line and carburetor are shown in figure 10. The majority of the pressure drop was found to be across the carburetor inlet needle valve. The

analytical formula suggested by Piggot (reference 4, equation 4) was used to calculate the pressure drop, and this was compared to the measured values on figure 10. The significance of these flow restrictions will be discussed in the analysis section.

MIXTURE DISTRIBUTION STUDY

The tests for mixture distribution reported in reference 5 were repeated for the two new fuels, No. 1 and No. 2. The 100LL fuel was retested also. The Lamdascan instrument was used for determining equivalence ratio in each cylinder exhaust. The results are shown in figures 11 and 12. From the equivalence ratio values for each cylinder, the standard deviations of equivalence ratio were calculated in order to quantify the degree of maldistribution. These values are listed in table 2.

Table 2

STANDARD DEVIATIONS OF EQUIVALENCE RATIO

Standard Deviations

| <u>RPM</u> | <u>100LL</u> | <u>No. 1</u> | <u>No. 2</u> |
|------------|--------------|--------------|--------------|
| 1000 | 0.027 | 0.033 | 0.042 |
| 1620 | 0.028 | 0.038 | 0.046 |
| 2000 | 0.046 | 0.076 | 0.064 |
| 2200 | 0.065 | 0.087 | 0.084 |
| 2200* | 0.061 | 0.086 | 0.093 |
| 2350 | 0.118 | 0.092 | 0.052 |
| 2350* | 0.114 | 0.121 | 0.122 |
| 2700 | 0.043 | 0.029 | 0.029 |

*Lean mixture.

For speeds below 2350 revolutions per minute the results showed more maldistribution for both No. 1 and No. 2 fuels when compared to 100LL fuel. At

speeds of 2000, 2200 and 2350 revolutions per minute, all fuels showed relatively poor distribution.

In this testing the different speed conditions were run on a number of different days because the distribution data was taken during the beginning of the vapor lock test runs. Each fuel was compared to the others, for each speed, on the same day and as close to the same time as possible. The average ambient temperature (and intake temperature) was about 50° F for all tests.

The inlet air temperature was found to affect mixture distribution for both 100LL and No. 1 fuels as shown in figure 13 and table 3. The mixture distribution was improved somewhat as inlet air temperature was increased. In the previous report (reference 5) the mixture distribution of both the baseline and experimental fuel 12A were worse than that of the baseline and experimental fuel 15B. The main difference in experimental conditions in the two sets of tests (conducted on different days) was the ambient (and inlet air) temperature, which was significantly lower for the baseline-12A pairing.

Table 3

STANDARD DEVIATION OF EQUIVALENCE RATIO
FOR DIFFERENT INLET AIR TEMPERATURES

At 2200 rpm, 100LL Fuel

| <u>Inlet Air Temp</u> <u>°F</u> | <u>Standard</u> <u>Deviation</u> |
|------------------------------------|-------------------------------------|
| 50 | 0.077 |
| 74 | 0.054 |
| 81.5 | 0.053 |
| 90 | 0.052 |
| 95.5 | 0.042 |
| 100 | 0.040 |

At 2200 rpm, No. 1 Fuel

| | |
|-----|-------|
| 48 | 0.073 |
| 60 | 0.061 |
| 82 | 0.067 |
| 90 | 0.049 |
| 100 | 0.052 |

VAPOR LOCK STUDY

For the vapor lock study the fuel system reported in reference 5 was modified to accommodate two fuel delivery systems, a gravity feed and fuel pump pressure system according to the schematic in figure 7. The gravity feed fuel system was constructed simply by bypassing the fuel line around the fuel pump and replacing all of the 5/16 inch inside diameter tubing of the pump system with 3/8 inch inside diameter tubing. The purpose was to more closely simulate the gravity system of a high wing aircraft. Subsequent flow testing showed that the pressure drop across the tubing was low compared to the other system elements, in particular the carburetor.

A vapor to liquid ratio meter was designed and built to measure vapor to liquid ratio while the engine was running. This meter was made of 5/16 inch inside diameter copper tubing for the pump system, and 3/8 inch inside diameter tubing for the gravity system. The total length of 86 inches of 5/16 inch tubing (66 inches for 3/8 inch tubing) was coiled, insulated and mounted on a plate. A 10 pound maximum capacity strain gage load cell was used to measure the total weight of copper tubing, plate and fuel in the tubing. A flexible rubber line was run to the rigid tubing of the vapor to liquid ratio meter to supply and return the fuel flow while minimizing any effect on the readings. Also all the tubing of the vapor to liquid meter was arranged with a slight slope to the engine so that it was self draining, and no fuel would puddle in the test section. The load cell detected the change of total weight. As more of the fuel vaporized, the weight decreased. The weight change was correlated to the change of liquid and vapor volumes inside the unit. Assuming that the vapor was weightless, the vapor to liquid ratio was calculated by the following equation:

$$\frac{V}{L} = \frac{W_T - W_A}{W_A} = \frac{(V_F - V_E) - (V_M - V_E)}{V_M - V_E} = \frac{V_F - V_M}{V_M - V_E}$$

where: $\frac{V}{L}$ = vapor to liquid ratio, volumes vapor/volume liquid

W_T = total weight of fuel in the meter without vapor
(voltage full - voltage empty)

W_A = actual weight of fuel in the meter (measured voltage - voltage empty)

V_F = voltage full

V_E = voltage empty

V_M = measured voltage

This vapor to liquid ratio meter was installed between the fuel pump and the carburetor. It was necessary to shield it from the engine cooling air stream in order to prevent signal fluctuations due to the air flow.

The vapor formation from the fuel varied with fuel temperature and pressure. For control of fuel temperature, a heat exchanger was immersed in a water bath equipped with two 2500 watt electric heaters (figure 7). These heaters could be turned on or off from the engine control panel. For cooling the bath, the heaters were turned off and cold tap water was added. The cold water flow could be started from the control panel. A drain near the top of the bath drained away the mixed water

and held a constant level. For the pressure fuel system thermocouples were located before the fuel pump, after the fuel pump, before the carburetor inlet and in the float bowl. For the gravity system, the pump inlet and outlet thermocouples were moved - one to the bath, the other was tied into the line after the heat exchanger. The locations of the thermocouples are shown in figure 7 also.

Using the 8 different engine operating modes listed in table 4, which were used in the previous testing for the distribution study, the 5 different fuels were tested for vapor lock characteristics. For each fuel system, each fuel was run at a given engine speed. At the onset of each run, the fuel temperature was kept below 65° F to ensure no vapor in any portion of fuel system. In some runs, ice was poured in the water bath to shorten cooling time. Signals from the vapor to liquid ratio meter, thermocouples, and Lamdascan equivalence ratio meter were recorded using a Nicolet Model 206 digital oscilloscope. This data was later transferred to a Hewlett Packard Model 9830 computer for processing and plotting. One oscilloscope channel was used for equivalence ratio meter data and vapor to liquid ratio meter data, the other channel was used to record the 4 temperature signals. To accommodate more than one signal per channel, electronically timed switches were used.

Table 4
ENGINE TEST CONDITIONS

| <u>Mode</u> | <u>RPM</u> | <u>HP</u> |
|-------------------------|------------|-----------|
| 1. Idle | 1000 | 8 |
| 2. Normal approach | 1600 | 32 |
| 3. Normal decent | 2000 | 65 |
| 4. Economy cruise, rich | 2200 | 87 |
| 5. Economy cruise, lean | 2200 | 87 |
| 6. Normal cruise, rich | 2350 | 107 |
| 7. Normal cruise, lean | 2350 | 107 |
| 8. Maximum power | 2700 | 160 |

Figure 14 shows a typical result as vapor lock developed for the 12A fuel at 2350 rpm, lean condition, with the fuel pump system. Shown are the fuel temperatures (4 locations), vapor to liquid ratio, equivalence ratio, and pressure at the carburetor. In viewing the vapor to liquid ratio curve, note slow vapor formation initially followed by a rapid increase of vapor in the fuel line. In

turn this is followed by a short plateau which ends abruptly with rapid vapor development. Vapor lock was defined as a substantial or complete loss of power output. Figure 15 shows torque output variation as vapor lock developed for 12A fuel at 2350 rpm. In this test the entire vapor lock process took about 300 seconds (5 minutes). In figure 14 note the correspondence between the increasing vapor to liquid signal, the leaning of the engine as indicated by the Lamdascan meter, the rising fuel temperatures, and the decreasing fuel supply pressure associated with the greater volume flow of vapor to liquid mixture required to keep the engine running and the fuel pumps limited volumetric capacity.

Three fuels, 100LL, 12A and 15B are compared in figure 16 in which is plotted the vapor to liquid ratio at vapor lock onset with the fuel pump system. The vapor to liquid ratio at which vapor lock occurs has been termed the critical value. Critical vapor to liquid ratios decreased as engine speed increased. At 2700 rpm, vapor lock occurred at a vapor to liquid ratio of about 6, regardless of the fuel. The solid line is a curve fit of the data. The error in determining vapor to liquid ratio for one percent error in weight was estimated and indicated by the magnitude of the bars in figure 16. All the data fell within this one percent band. For comparison the critical vapor to liquid ratio was calculated from the equation below from reference 4. The measured fuel pump output (figure 8) and fuel flow requirements (figure 50) measured and reported previously (reference 5) are plotted as points on figure 16, labeled expected $\frac{V}{L}$ ratio for 100LL and 15B fuels.

They show good correlation with the actual measured critical vapor to liquid ratios. The equation below relates the pump flow and engine requirement to the onset of vapor lock.

$$\frac{Q_S}{Q_R} = 1 + \left(\frac{V}{L} \right)_{\text{critical}}$$

where: $\frac{Q_S}{Q_R}$ = the ratio of excess pump capacity
 Q_S = maximum fuel pump capacity, gal/hr.
 Q_R = liquid fuel flow required by engine, gal/hr.

The literature indicates that the vapor to liquid ratio existing in any part of the fuel system can be determined from the vapor to liquid ratio versus temperature (and pressure) characteristics as measured or calculated for a particular fuel together with the local pressure and temperature in the fuel system component of interest. At various operating conditions, knowing the vapor tolerance of a particular aircraft fuel system would allow one to determine how close the aircraft was to vapor lock during flight testing. This can be estimated by measuring pressure and temperature conditions at various critical places in the fuel system. For this technique to be accurate, the temperatures and pressures must be measured quite accurately. A one degree F error represents approximately a 1.5 ratio error in vapor to liquid ratio in the region of rapid vapor formation, above vapor to liquid ratios of 8. For vapor to liquid ratios less than 8, errors due to temperature measurement errors are smaller. The digital temperature measurement device used in our tests (Doric Model 400A type T for copper constant thermocouples) read to the nearest 1° F and the manufacturer specified $\pm 1^{\circ}$ F accuracy. However we saw day to day drift of $\pm 2^{\circ}$ F upon calibration checks with

an ice bath. While this might be sufficient to have some usefulness in estimating how close an aircraft of known vapor to liquid tolerance is to vapor lock, it is not good enough to absolutely determine the vapor to liquid ratio tolerance. Another confounding factor in flight testing to determine vapor to liquid tolerance is weathering or venting of fuel vapors as the fuel tank temperature and/or altitude increase. This changes the temperature-vapor to liquid ratio characteristics. Weathering is addressed in the analysis section. Errors in pressure measurement of ± 0.1 psi would represent an uncertainty of ± 0.9 vapor to liquid ratio for vapor to liquid ratio equal to 8 or greater.

Vapor lock data for the gravity fuel feed system are shown in figure 17. A comparison with figure 16 shows the vapor to liquid ratios at vapor lock were lower than those for the fuel pump system.

The time for the onset of vapor lock is another criteria. It is defined as the time interval for the fuel temperature at the carburetor inlet to rise from 85° F to a level high enough to cause vapor lock. The time required for vapor lock at higher speeds was less than at lower speeds. These results are shown in figures 18 and 19. The time required for vapor lock at each engine operating condition should be used only for comparison among the different test fuels. The times to vapor lock shown are for a rate of heat transfer which increased directly with the water bath temperature and which in turn rises due to the fixed rate of heat input from the electric heaters. On an aircraft the heat input to the fuel system changes as a function of engine operation condition. Therefore no attempt to apply these times to flight conditions should be made.

Figure 20 shows the fuel temperatures at the carburetor inlet when vapor lock occurred for the different operating modes and fuels for the fuel pump system. The highest temperature for vapor lock was with the 100LL fuel and the lowest temperature was for the most volatile 15B fuel. With the gravity fuel system, the same trends existed and these are shown in figure 21 for the five different fuels. Fuel temperatures before the carburetor were decreased with increased engine speeds, since the vapor tolerance of the fuel system was lower at the high fuel flow rates required at these speeds. It should be pointed out that all the heat addition to the fuel pump was at one place, on the suction side of the fuel pump. This was probably the most sensitive area, since with this system the fuel pump is the component limiting the mass flow of fuel to the engine. (In an aircraft installation the heat addition would be more evenly distributed. The large, uninsulated fuel pump with hot lubricating oil splashing on the linkage side is a likely spot for a large fraction of the heat transferred to the fuel). The idea of increasing the pumping capacity of the engine driven pump is evaluated in the following example and determined to be impractical. The fuel temperature required to produce vapor lock can be increased by this same amount (19.2° F) by adding an in-tank boost pump (without danger of increasing the engine compartment heat transfer area) which will pressurize this system to 3 psi.

Increasing the fuel line pressure at the tank has the same effect as reducing the rvp of the fuel an equal amount. This was tested for the gravity feed system at the 2350 rpm condition. An "ideal" boost pump was simulated by pressurizing the fuel supply can to 2 and 4 psi with compressed air. The effect of this on time to vapor lock and carburetor inlet temperature at vapor lock are shown on figures 19 and 21 for the 2350 rpm condition.

EXAMPLE CALCULATION - EFFECT OF INCREASING ENGINE DRIVEN PUMP CAPACITY

If a larger capacity engine driven fuel pump were installed such that 3 psi fuel pressure could be maintained at the 2700 rpm condition, the carburetor would be the device limiting the fuel mass flow when the vapor to liquid ratio of the fuel exceeded 8. (This is based on the equation below, developed in the analysis section). A 3 psi increase would raise the fuel temperature for vapor lock by 3° F (for Fuel No. 1 going from $V/L = 5$ to $V/L = 8$ on figure 5). In addition the increased pressure would increase the temperature for this vapor to liquid ratio by $5.4^{\circ} F/\text{psi}$ (derived from figure 5) $\times 3 \text{ psi} = 16.2^{\circ} F$ for Fuel No. 1. Together this gives a total increase in fuel temperature for vapor lock of $19.2^{\circ} F$.

$$\Delta P = CQ^2 \left(1 + \frac{V}{L}\right)$$

$$\Delta P = 3 \text{ psi} \times 39 \text{ inch gasoline/psi}$$

$$C = 0.0928$$

$$Q = 12.2 \text{ gal/hr at 2700 rpm}$$

$$\text{Substituting and solving for } \frac{V}{L} \text{ gives } \frac{V}{L} = 8$$

To raise the vapor lock temperature by $19.2^{\circ} F$, the fuel pump capacity at this speed would have to be increased from 14.6 gal/hr to about 110 gal/hr. This is based on rate of fuel pressure drop versus vapor to liquid ratio from data similar to that contained in figure 14. Once the fuel pressure begins to fall then we know that the pump capacity at that pressure is:

$$\begin{aligned} Q \text{ existing pump capacity} &= Q \text{ liquid flow required} \times \\ &\quad (1 + V/L \text{ of existing system} \\ &\quad \text{at 3 psi from } V/L \text{ versus pressure} \\ &\quad \text{data as on figure 14}) \\ &= 12.2 (1 + 0.2) = 14.6 \text{ gal/hr} \end{aligned}$$

and the new pump capacity required is:

$$\begin{aligned} Q \text{ new capacity at 3 psi} &= Q \text{ liquid flow required} \times \\ &\quad (1 + V/L \text{ desired of new system}) \\ &= 12.2 (1 + 8) = 110 \text{ gal/hr} \end{aligned}$$

This is assuming that a pump with a larger pumping capacity would receive the same amount of heat transfer. In all likelihood this would not be the case and the additional heat transfer to the larger fuel pump may completely counteract the gains obtained by increasing the pump capacity.

ANALYTICAL MODEL OF GRAVITY FEED FUEL SYSTEMS

The purpose of this section is to show how a vapor-lock analysis of a fuel system can be made that will facilitate decisions about fuel system design or modification, and show the severity of response to fuel volatility.

This model, which has been implemented on a TRS 80 personal computer in "basic", is based heavily on experimental data. The results which are presented are based on data from the Lycoming O-320 engine dynamometer testing performed at the University of Michigan and the flow characteristics and dimensions of a typical gravity feed fuel system such as found in a Cessna 172. Fuel data used in the model were based on measurements made at the University of Michigan. Three fuel types were entered into this model. They were commercial avgas (RVP = 6.8 psi); commercial avgas with undissolved liquid water present (1 percent H_2O added); and high vapor pressure autogas No. 1 (rvp = 14.4 psi)..

The curves which were entered in the computer model are heat added to fuel per pound (initial fuel temperature of 32° F) versus vapor to liquid ratio, figures 22, 23 and 24. These curves were calculated based on the temperature versus vapor to liquid curves, figures 4, 5 and 6, combined with the measurements of weight percent vaporized versus temperature, figures 25, 26 and 27. The measurement of weight percent vaporized versus temperature was performed by slowly heating (about 1 hour per test) approximately 250 ml of fuel sample in a 250 ml Erlenmeyer flask submerged in a water bath on a heater/stirrer unit. A two-hole rubber stopper held a thermometer and vented the flask through a 1/4 inch hole. Tests were performed at atmospheric pressure and at 19.9 inches of mercury absolute pressure corresponding to an altitude of 10,000 feet. The vacuum pump arrangement from the previous vapor to liquid bench test was used to provide the reduced pressure. At appropriate temperature intervals, the flask was weighed to determine the percent weight loss. This was done both with and without a magnetic stirrer (A 3/8 by 1 1/2 inch octagonal spinbar run at 420 RPM) agitating the fuel. It was found that agitation of the fuel lowered the temperature for the formation of a given mass of vapor an average of 5° C. This is shown on the weight percent loss versus temperature curves. Combining the vapor to liquid ratio versus temperature and weight percent vaporized versus temperature curves for agitated fuel gives a vapor to liquid ratio versus weight percent vaporized curve, figure 28. This allowed us to calculate the BTU/lb versus vapor to liquid ratio curves for fuel which is both agitated and not agitated, as explained below. The standard vapor to liquid ratio versus temperature test determines the vapor formation with a small (1 ml) fuel sample in equilibrium with the vapor. The stirring of the large sample in the weight percent versus temperature test brings the fuel and vapor closer to equilibrium conditions. This is why the stirred weight percent vaporized versus temperature curve is used with the vapor to liquid ratio versus temperature curve to produce the vapor to liquid versus weight percent vaporized curve, even though the fuel is not stirred in the vapor to liquid ratio versus temperature test. Density ratio between liquid fuel and fuel vapor has been plotted in figures 29 and 30. This can be calculated as:

$$\text{density ratio} = \text{vapor to liquid ratio} \times \frac{100 - \text{weight percent vaporized}}{\text{weight percent vaporized}}$$

The large density ratio at low vapor to liquid ratios is most likely due to air evolution. Liquid fuel is 630 times more dense than air at 60° F and 1 atm

pressure. Hydrocarbon vapors are more dense than air, with butane vapor about twice as dense as air under these same temperature and pressure conditions. Water vapor has an extremely low density and this effect is indicated for the case of wet 100LL in figure 30 in which is evident almost an order of magnitude increase in the ordinate. The heat required to produce the various vapor to liquid ratios was calculated by the following equations:

$$\frac{\text{BTU}}{\text{lb}} \text{ for each } \frac{V}{L} \text{ ratio} = \text{sensible heat} + \text{latent heat}$$

$$\frac{\text{BTU}}{\text{lb}} = \text{fuel temperature difference} \times C_p \text{ (specific heat of liquid)} \\ + \text{weight percent evaporated at that temperature} \\ \times \text{apparent latent heat at that vapor to liquid ratio}$$

For fuel No. 1

$$\frac{\text{BTU}}{\text{lb}} = ({}^{\circ}\text{F} - 32) \times 0.50 \frac{\text{BTU}}{\text{lb} \cdot {}^{\circ}\text{F}} + \frac{\text{wt \% fuel evap}}{100} \times 95.3 \frac{\text{BTU}}{\text{lb}}$$

For fuel 100LL

$$\frac{\text{BTU}}{\text{lb}} = ({}^{\circ}\text{F} - 32) \times 0.50 \frac{\text{BTU}}{\text{lb} \cdot {}^{\circ}\text{F}} + \frac{\text{wt \% fuel evap}}{100} \times 101.6 \frac{\text{BTU}}{\text{lb}}$$

For fuel 100LL with undissolved H_2O added

$$\frac{\text{BTU}}{\text{lb}} = ({}^{\circ}\text{F} - 32) \times 0.50 \frac{\text{BTU}}{\text{lb} \cdot {}^{\circ}\text{F}} + \frac{\text{wt \% fuel evap}}{100} \times 101.6 \frac{\text{BTU}}{\text{lb}} \\ + \frac{\text{wt \% water evap}}{100} \times 1015 \frac{\text{BTU}}{\text{lb}}$$

Wt % fuel evap = total wt % evap - wt % water evap

$$\text{Where wt \% water evap} = \frac{V}{L} \times \frac{\text{partial press } \text{H}_2\text{O}}{\text{atmospheric press}} \times \frac{\rho_{\text{H}_2\text{O vapor}}}{\rho_{\text{liquid fuel}}} \times 100$$

The apparent latent heat is determined by Hodge's method (reference 9) from the vapor to liquid bench test data.

The computer modeling will be explained by following the fuel on its path to the engine. We know that the engine must have a predetermined mass flow rate of fuel to run at a given operating condition. Since the density of fuel vapor is much less than that of liquid fuel (see figure 29, density ratio of fuel vapor), we are dependent on the flow rate of the liquid portion. The mechanism for moving the fuel to the engine is the pressure differential across the fuel system from fuel tank to carburetor bowl. The carburetor float valve controls the pressure drop of the system allowing only the flow rate needed by the engine to enter the carburetor bowl. Other elements of the fuel system produce various pressure drops also. The components considered in the model, from tank to carburetor are:

1. Fuel tank
2. Tank line and selector valve
3. Fuel strainer/sediment bowl located in engine compartment
4. Strainer to carburetor line
5. Carburetor inlet valve

Once the fuel is in the carburetor bowl, the vapor formed at that point is of little concern except for idle and hot restart. The carburetor bowl makes a very good vapor separator with the vapor venting to the intake manifold. Also the intake air flow and vaporizing fuel in the venturi tend to limit temperature extremes in the float bowl (except during idle and hot soak).

It is assumed here that the fuel tank acts as a vapor separator and that the fuel entering the tank line contains no vapor. The program contains two inputs for fuel tank temperature, fuel tank temperature at altitude and maximum temperature the fuel has experienced while on the ground. Also input is needed as to whether or not the hot fuel has been agitated. These inputs allow a determination of the loss of vapor forming potential before the fuel enters the fuel system.

As the fuel passes through the various components of the fuel system it picks up or rejects heat depending on the surrounding ambient air temperature, another variable input. For the tank line a thin, conductive material such as aluminum tubing is assumed which offers a negligible resistance to the flow of heat. Also since the heat transfer coefficient between the low viscosity boiling fuel and tubing wall is very high (approximately 500 BTU/sq ft/hr/deg F) then the main factor limiting the heat transfer to the fuel is the natural convection between the outside of the tubing and the air. We calculate the heat transfer then by multiplying the exposed tubing surface area and the temperature difference between fuel and air; and then by the heat transfer coefficient for natural convection (here assumed to be 1.5 BTU/hr/sq ft/deg F). This gives the heat transferred to the fuel in BTU/hr. By taking the heat transfer rate and dividing by the fuel flow rate we get the heat input per pound of fuel.

We can now use our BTU/lb versus vapor to liquid ratio curves (figures 22, 23 and 24) to find the average vapor to liquid ratio in this part of the fuel system. To get the average vapor to liquid ratio we will assume that the heat is transferred uniformly along its length and that the average heat energy per pound is 1/2 the difference between the heat per pound at the beginning and the heat per pound at the end. In the model the BTU/lb versus vapor to liquid ratio curves are shifted up or down according to the pressure conditions existing in the line. (These are affected by altitude, fuel tank pressure, fuel head, etc.) The amount was determined experimentally, assuming a linear change between the curves for high and low pressure (low and high altitude) curves plotted on the BTU/lb versus vapor to liquid ratio figures. The volumes of vapor per volume of liquid which have escaped from the fuel tank are determined the same way (based on temperature, pressure and agitation) and subtracted from the previous value to give the true average vapor to liquid ratio in the line.

This average vapor to liquid ratio can now be used to calculate the pressure drop through the tank line and selector valve. The pressure drop versus flow characteristics of the components can be found experimentally. This is done by breaking the fuel line connection before the strainer and measuring the time required for a measured volume flow into a container, and measuring the gravity head which provided this flow.

The literature indicates (reference 4) that the pressure drop (for aircraft fuel systems) should be proportional to the flow rate to the 1.75 power. This was verified experimentally for the piping used for the University of Michigan gravity feed system testing. This shown in figure 31 and for the system consisting of 22 feet of 3/8 inch tubing, some rubber, some copper with fittings, bends, etc.

This data was plotted on log-log paper. A line with a slope of 1.75 drawn thru the data points shows a good fit. Also notice that a line with a slope of 2.0 fits the flow data for the carburetor inlet valve (taken with the bowl removed). This is to be expected since the pressure drop thru an orifice increases with the square of the flow rate.

The pressure drop thru the tank line, strainer and carburetor line, as well as the carburetor valve increase linearly with vapor to liquid ratio according to Pigott's equation (reference 4) for the pressure drop through tubing. This is developed for a slug flow regime, common for low viscosity liquids with vapor to liquid ratios near 0 to over 10.

$$\Delta P = \frac{3.417 \times 10^{-5} \mu^{.25} \rho^{.75} v^{1.75}}{d^{1.25}} (1 + \frac{v}{L})$$

where: ΔP = pressure drop in psi
 l = length of pipe, ft.
 ρ = density of fluid, lb/cu-ft.
 v = mean fluid velocity, fps
 μ = viscosity, English units ($CP \times 0.000672$)
 d = inside pipe diameter, ft.

The carburetor inlet valve shows flow behavior similar to an orifice where:

$$\Delta P = C \rho Q^2$$

If the effective density decreases by a factor of $\frac{1}{(1 + \frac{v}{L})}$ then the average velocity must increase by a factor of $(1 + \frac{v}{L})$ to maintain the same mass flowrate to the engine, therefore:

$$\Delta P = C \frac{\rho}{(1 + \frac{v}{L})} (Q(1 + \frac{v}{L}))^2 = C \rho Q^2 (1 + \frac{v}{L})$$

Thus the carburetor inlet valve shows the same linear increase in pressure drop with vapor formation, as the equation for slug flow in a pipe.

When all of the pressure drops through the various components of the fuel system have been determined, they are added up to see if the head loss would exceed the total fuel head available. If so, then the fuel system would be in a state of vapor lock. In a gravity system the fuel pressure head available is the total of:

1. Ram air pressure from vent tube calculated from $\Delta P = \frac{1}{2} \rho v^2$

where ρ is the air density
 v is the velocity
 P is the dynamic pressure in inches of gasoline

2. Fuel head from fuel liquid level to carburetor inlet valve. Since this depends on the density of the liquid gasoline and the vapor effectively reduces this density, the calculated fuel head is then reduced by a factor of $\frac{1}{(1 + \frac{v}{L})}$ where

the vapor to liquid ratio is the average vapor to liquid ratio calculated to be in the tank line.

3. From this number we must subtract the riser heights (in inches) of any isolated high spots in the fuel plumbing. These are the vertical dimensions of any places where air or vapor can be trapped such as vertical loops.

4. Carburetor bowl pressure. Depending on the bowl vent arrangement this could be positive or negative. Figure 32 shows that for the O-320 with no air filter the bowl was under a slight vacuum. Since this is on the down stream side of the fuel system it has the beneficial effect of adding to the available head across the fuel system.

Total fuel head available =

$$\text{Ram air pressure} + \frac{\text{Fuel head}}{(1 + \frac{v}{L})} + \text{Bowl vacuum} - \text{Riser heads}$$

The heat transfer to the fuel as it flows through the fuel strainer and carburetor line are calculated with similar heat transfer equations. Since these parts are mounted in the engine compartment there is both convective and radiation heat transfer. The proximity of the hot exhaust system makes the radiation heat transferred significant. The radiation heat transfer varies with the temperature to the fourth power and with the reciprocal of the distance for the parallel cylinders assumed. For this model it was assumed that the cylinders, (strainer and carburetor line) had combined radiation and convection heating for the one-third of the surface which is exposed to the exhaust pipe and two-thirds which has only convective heat transfer.

The equation used for the convection only calculation was the classical heat flow through a cylinder. (reference 11)

$$Q = \frac{T_{\text{air}} - T_{\text{fuel}}}{\frac{1}{2\pi r_i h_i} + \frac{\ln(r_o/r_i)}{2\pi k l} + \frac{1}{2\pi r_o h_o}}$$

where: Q = heat transfer rate in BTU/hr
 T = temperature in degrees F
 l = length in feet
 r_i = inside radius in feet
 r_o = outside radius in feet
 h_o = inside heat transfer coefficient in BTU/hr/sq-ft/deg F
 h_i = outside heat transfer coefficient in BTU/hr/sq-ft/deg F
 k = thermal conductivity of cylinder in BTU/hr/ft/deg F

The outside heat transfer coefficient was calculated by classical empirical correlations for air flow crosswise over cylinders, (reference 11). The average air velocity was based on the cross-sectional flow area of the cowling around the fuel system, the measured temperature rise above ambient of the cooling air and the flow rate required to carry off the coolant load of the engine. This was assumed to be 1/3 of the fuel energy content. The inside heat transfer coefficient for low viscosity, boiling liquid is very high, approximately 500 BTU/hr/sq-ft/deg F, so the resistance to flow of heat from fuel to the tube is very low. In a case where a composition wall is used, such as an aluminum tube covered with insulation, the effect of the highly conductive metal layer can be neglected and the entire tube can be considered to be made of the insulating material.

The calculation of the combined convection and radiation heat transfer to the side of the tubing exposed to the exhaust pipe was made by assuming simultaneous radiation and convection heat transfer. The calculation was made for the complete cylinder then multiplied by 1/3 to get the actual heat transfer rate. In the case of a cylinder made of a conductive material almost all of the radiation heat flux is added to the fuel as is the convection heat transfer. For a well-insulated cylinder the radiation causes the surface temperature to increase above the air temperature. The air blowing over the surface then acts to reduce the radiation heat transferred. See Appendix D for the method used to find the outside surface temperature. The heat transfer was then calculated from:

$$\dot{Q} = \text{convection + radiation heat transfer rate}$$

$$\dot{Q} = 2\pi r_o l h_o (T_{\text{air}} - T_{\text{outside}}) + VF A C \epsilon (T_{\text{exhaust}}^4 - T_{\text{outside}}^4)$$

where: \dot{Q} = heat transferred to the fuel in Btu/hr
 r_o = outside radius in feet
 l = length in feet
 h_o = outside heat transfer coefficient
 in Btu/hr/sq-ft/deg F calculated previously
 $C = 0.17 \times 10^{-8}$ Btu/sq-ft/hr/deg R⁴ (Stefan-Boltzman constant)
 $\epsilon = 0.5$ = emissivity of exhaust pipe-oxidized steel
 $A = \text{area} = 2\pi r_o l$ in square feet
 $VF = \text{view factor} = 1/\text{distance between exhaust pipe centerline and cylinder surface.}$
 T_{exhaust} = exhaust pipe surface absolute temperature,
 in degrees Rankine.

Figure 33 shows the calculated heat transfer rates at the various engine speed-load points. This figure indicates the effectiveness of insulation in reducing the heat transfer to the strainer unit. The heat transfer through the carburetor line is already quite low due to the low thermal conductivity of the material it is made of. Figure 34 shows how the distance from the exhaust pipe affects the heat transfer to the strainer. This emphasizes the extreme importance of keeping uninsulated fuel system components some minimum distance from the exhaust system.

Once we know the heat transfer rate to the strainer and carburetor line, we can again find the average vapor to liquid ratios existing in these locations by dividing 1/2 the heat transfer rate to that component by the fuel mass flowrate to

get BTU/lb of fuel, adding the heat which existed in the tank plus that which had been transferred to the fuel as it passed through the previous components, then determining the vapor to liquid ratio from the BTU/lb versus vapor to liquid ratio curve.

The pressure drops across each component may now be found by substituting into the appropriate equation. They are:

$$1. \text{ Tank line } \Delta P = CKQ^{1.75} (1 + VK)$$

where ΔP = pressure drop in inches of gasoline
 CK = flow constant, experimentally determined
 $= \frac{KH}{KG^{1.75}}$
 KH = measured liquid fuel head in inches from fuel level to carburetor inlet
 KQ = measured flowrate out supply line at strainer inlet, at this head, in gal/hr
 VK = average vapor to liquid ratio in tank line
 Q = liquid fuel flow requirement in gal/hr
 $= \text{mass flow in lb/hr} \times \frac{\text{specific gravity}}{8.3 \text{ lb/gal}}$

$$2. \text{ Strainer } \Delta P = CSQ^{1.75} (1 + VS)$$

where $CS = \left(\frac{SH}{SQ^{1.75}} - \frac{KH}{KQ^{1.75}} \right)$
 SH = measured liquid fuel head, fuel level to strainer outlet in inches
 SQ = measured flow rate out strainer outlet at this head in gal/hr
 VS = average vapor to liquid ratio thru strainer
 Q = liquid fuel flow requirement in gal/hr

3. Carburetor line

$$\text{Pigott's equation } \Delta P = \frac{3.417 \times 10^{-5} \mu^{.25} l \rho^{.75} v^{1.75}}{d^{1.25}} (1 + \frac{V}{L})$$

where VL = average vapor to liquid ratio in carburetor line
 ΔP = pressure drop in psi
 $\text{where 1 psi} = 27.7 \text{ inches of gasoline/specific gravity}$

4. Carburetor inlet valve

$$\Delta P = \frac{1}{CF^2} \left(\frac{CH}{CQ^2} Q^2 - \frac{SH}{SQ^{1.75}} Q^{1.75} \right) (1 + VC)$$

where ΔP = pressure drop in inches of gasoline
 CH = measured liquid fuel head, tank level to carburetor inlet.

CQ = measured fuel flow rate
at this head in gal/hr

CF = inlet valve area modification factor,
is to be used to determine effect of
valve size on pressure drop. Above one,
the area is larger than original size,
below one is smaller.

VL = vapor to liquid ratio at carburetor inlet
Q = liquid fuel flow requirement in gal/hr

In order to evaluate the fuel strainer sizing a reasonable assumption would be that for a given strainer material (nylon mesh, metal mesh, paper) and geometry, the pressure drop decreases with the square of the area.

$$\text{New } \Delta P = \text{baseline } \Delta P \frac{\text{Baseline surface area}^2}{\text{New surface area}^2}$$

while making the strainer larger decreases the pressure drop thru the strainer, it also increases the heat transfer area, causing vapor formation, which increases the pressure drop thru all the rest of the fuel system.

Figure 35 shows the effect of various strainer housing sizes (with reference to the baseline case) for both an insulated (1/2 inch fiberglass) and non-insulated (usual) case. The possibility of decreasing the strainer housing surface area may be limited by the requirement for separation of water/sediment. Another factor which should be considered in strainer design is increase of pressure drop due to dirt build up. The baseline conditions for all figures by this computer model are as listed in table 5.

This size versus pressure drop analysis can also be applied to the carburetor line. Again increasing the diameter of the line tends to decrease the pressure drop through the line while the increased heat transfer tends to increase the pressure drop through the line and carburetor inlet valve. Figure 36 shows the total pressure drop through the fuel system (as well as the total fuel head available at each speed) with various sizes of tubing, (0.150 inch wall thickness, and thermal conductivity, $K = 0.08$). Note how the sizing has the most effect at high fuel demand conditions (takeoff power 2700 rpm). Shown for all speeds is the case of the baseline system uninsulated strainer and carburetor line. Figure 37 shows these same curves but with the strainer insulated with 1/2 inch of fiberglass insulation. This curve shows these effects more prominently since most of the heat transfer is now through the line. These curves were made for temperatures which were near critical for the baseline conditions, when using the No. 1 fuel. Figures 38 and 39 provide more detail about how the pressure drops are distributed as the line size is changed, for the engine speed load condition nearest to vapor lock, 2700 rpm. Figure 38 also shows what the pressure drops would be if no vapor were present (i.e. cold fuel). Figures 40 and 41 show how much vapor would be present in the various places at each engine speed and load.

Figure 40 is for the baseline conditions and No. 1 fuel, while Figure 41 is the same but with the strainer insulated. Vapor to liquid ratios which would produce vapor lock would be somewhat higher than those shown at the lower speeds, since the initial fuel temperature used, which is critical for 2700 rpm is not critical at

Table 5

Baseline Conditions
(Representative of a Typical Gravity Feed Fuel)
System used with Lycoming O-320 Engine

Airport Altitude - 1000 feet
Aircraft Altitude - 1000 feet
Airspeed - 1000 rpm = 0 knots/1620 = 70, 2000 = 100, 2200 = 90,
2350 = 100, 2700 = 90
Fuel Flow Rate - lbs. per hr., Figure 50
Air Temperature Rise above ambient degree F - Figure 51
Maximum Fuel Temperature = Fuel Temperature at Altitude =
Ambient Temperature
Area of Duction over fuel system parts - 2 square feet
Thermal Conductivity of carburetor line - 0.08 BTU/hr ft² °F
Distance from exhaust pipe to strainer - 10 inches
Distance from exhaust pipe to fuel line - 10 inches
Exhaust pipe diameter - 2 inches
Exhaust pipe surface temperature - 1200 °F
Specific gravity of fuel - 0.7
Thermal conductivity of uninsulated strainer - 130 BTU/hr ft² °F
Strainer wall Thickness - 0.2 inch
Baseline strainer diameter - 2.25 inch
Baseline strainer length - 3.25 inch
Carburetor line inside diameter - 0.25 inch
Carburetor line wall thickness - 0.15 inch
Carburetor line length - 1 foot
Number of fuel tanks turned on - 2
Tank line lengths, tank to selector valve - 6.5 feet
Line length, selector valve to strainer - 1.5 feet
Baseline tank line outside diameter - 0.5 inch
Fuel tank depth - 3 inches
Carburetor bowl vacuum, inches of water, Figure 32
Total Isolated Riser Heights - 0 inches

Fuel flow measurements of a Cessna 172 fuel system measured at
Federal Aviation Administration Technical Center:

Measured Flow Rate, fuel tank to strainer inlet - 63.3 gal/hr.
Fuel head, fuel level to strainer inlet - 39 inches
Measured flow rate, fuel tank to strainer outlet - 59.6 gal/hr.
Fuel head, fuel level to strainer outlet - 39 inches
Measured flow rate, fuel tank thru carburetor float valve
(bowl removed) - 20.5 gal/hr
Fuel head, fuel tank level to carburetor float valve - 39 inches

the lower speeds. Figure 42 shows a breakdown of sources of fuel head available and pressure drops at various engine speeds for the baseline conditions.

Figure 43 shows the effect on total pressure drop versus carburetor inlet valve area referenced to baseline. This shows that it would be beneficial to increase the area as much as possible. All Lycoming O-320 engines equipped with the Marvel Schebler MA-4SPA have the same inlet valve part number (233615). According to the engine manufacturer this was designed to work with any type of fuel supply system as long as the pressure is below 8 psi and above a minimum of 0.5 psi under maximum flow demand condition, preferably it should be between 2 to 5 psi.

Since the float force must balance the pressure acting on the area of the valve, through a lever, it stands to reason that an area four times larger could be used for a gravity fuel system with only 80 inches gasoline head (2 psi). This would increase the vapor to liquid ratio tolerance by a factor of 4 (at the most critical condition - 2700 rpm takeoff power - the critical vapor to liquid ratio would be increased from 2 to 8). Figures 44 and 45 show the effect of increasing the carburetor inlet valve area by four times and also the effect of insulating the strainer unit, both compared to baseline conditions at the 2700 rpm takeoff power condition. For test fuel No. 1, the fuel tank temperature that would give incipient vapor lock (at 2700 rpm, takeoff power) could be increased from 87 to 102° F by increasing the carburetor valve area while for Dry 100LL it could be increased from 136 to 146° F. Insulating the strainer would increase the temperature from 87 to 94 for fuel No. 1. Making both changes would raise the critical fuel temperature to 115° F.

One important assumption made was that the flow through the gravity fuel feed system is not agitated and so the BTU/lb versus vapor to liquid ratio curves obtained for fuel that was not stirred were used. If the fuels were agitated while flowing through the line (such might be the case when passing through an in-line fuel pump or if the fuel line goes into a resonant vibration) then the curves measured for stirred fuel should be used. This would have the effect that vapor lock would be predicted to occur at fuel temperatures up to 10° F lower.

The procedure normally followed for evaluating the hot fuel handling capability of aircraft fuel systems has been evaluated to see how this fuel system would respond to such a test. In order to determine the capability of a fuel system to handle hot fuel without the necessity of waiting for special weather conditions, the hot fuel test involves pre-heating the fuel in the fuel tank. This tank temperature must be high enough so that the fuel in the coldest part of the system is at least 110° F, under the flight test conditions (takeoff power). The tank is usually heated with heat lamps in a paint hanger to a high enough temperature to cover temperature losses during ground operation before testing. Figure 46 shows that for this fuel system, if the fuel in the tank is allowed to cool more than 6° F from the peak fuel tank temperature (heated without agitation) then vapor lock will be prevented from occurring no matter how hot the fuel is to start with. This is due to the venting and loss of some of the more volatile components of the fuel.

If the fuel was heated with agitation then it is much less likely that vapor lock could be made to occur during the test. Figure 47 shows that with the fuel in the fuel tank having been agitated, test fuels No. 1 and 100LL would not vapor lock during a hot fuel test (fuel above 110° F), but that fuel No. 1 would if the fuel in the tank happened to be near 92° F and the ambient air temperature were 110° F, or above. To ensure a valid hot fuel handling test, that is a test which will

determine which systems have a proper margin of safety, the fuel must not be agitated as it is heated (i.e. not heated first then poured in while hot) and must not drop in temperature between being heated and the test flight. In order to meet these requirements modification of the test procedure is probably required in the form of on-board fuel heating. For example, one possibility might be to incorporate a low pressure drop, thermostatically controlled, electrically heated, liquid to liquid heat exchanger between the tank outlet and fuel system.

The effect of altitude is shown on figure 48. A rate of atmospheric temperature reduction with altitude of 3.5° F per 1000 feet was assumed. Fuel pressure drop versus fuel head available was plotted for three different fuel tank temperature reduction rates. They are 1/4, 1/2 and 3/4 the atmospheric temperature reduction rates. This figure indicates that in the case of a large fuel tank isolated from the outside air, the pressure reduction due to altitude would tend to cause vapor lock at a lower altitude because, in this case, the fuel temperature falls at a lower rate than the atmosphere (This assumes the fuel in the tank starts at or above the ground ambient temperature).

On sizing the ram type fuel tank vent tube, an important factor is the pressure drop versus venting vapor flow rate. Some pressurization is desirable to reduce the likelihood of vapor lock. One psi of pressurization gives the equivalent of using a fuel of 1 psi lower Reid vapor pressure (This effect can best be achieved by using an in-tank boost pump). In sizing the fuel tank vent, one must be careful that the tank (and wing) is not distorted by excessive pressures. Current automotive technology for pressure/vacuum gas caps allow vacuum relief at 1/4 psi and pressure relief at 1 psi. It should be remembered that at this pressurization the force on the side of a 2x2 foot tank is $1 \text{ lb/sq-in} \times 4 \text{ sq-ft} \times 144 \text{ sq-in/sq-ft} = 576 \text{ lbs of force.}$

The effectiveness of an "ideal" in-tank boost pump was evaluated, and the results are shown in figure 49. An ideal boost pump is one that would increase the pressure of the fuel in the tank outlet line without generating any vapor in the pumping process. This figure shows that there is a wide margin of safety (for this system) even with a boost pressure of only 2 psi. A real pump, while generating some vapor in the line, would also provide a large agitation of the fuel tank providing the beneficial vapor loss effects discussed previously.

FLIGHT TEST DATA OF EXPERIMENTAL FUELS 1 AND 2

Testing of the two test fuels under actual flight conditions was performed in a Cessna 150 with a Continental O-200 engine by the Experimental Aircraft Association for the University of Michigan (reference 12).

Data recorded were:

Individual exhaust gas and cylinder head temperatures. Engine compartment, carburetor bowl, intake manifold, right and left fuel tank, cabin and ambient temperatures. Throttle plate travel, altitude, barometer, engine and air speed, and general observations by pilot.

The tests were conducted at ground level ambient temperatures from 28 to 93° F. Operations included touch and go's with a high temperature soak plus economy and maximum cruise conditions at various altitudes.

In conclusion this report stated "Flight and ground performance of the Cessna 150 airplane was satisfactory when using either of the two special blend autogas test fuels identified as lot number 1, or A, and lot number 2, or B. Operation, performance and function were found to be normal."

CONCLUSION

Experiments and calculations have been made on an O-320 Lycoming engine and fuel system employing 100LL avgas and four automotive type gasolines. The following conclusions were reached.

1. In general the more volatile automotive fuels tended to give slightly worse mixture distribution when compared to 100LL.
2. A modification of the ASTM test for vapor to liquid ratio in which the gasoline was permitted to become wet, significantly increased the vapor to liquid ratios and thereby indicates the tendency to vapor lock is greater when a small amount of liquid water is present in the fuel.
3. Exhaust air to fuel ratio, fuel pressure, vapor to liquid ratio, fuel system temperatures and engine output torque all provided indications of vapor lock.
4. Within experimental error, for a given speed-load condition, vapor lock always occurred at the same vapor to liquid ratio regardless of fuel volatility. The more volatile fuels reached this critical value at lower fuel system temperatures.
5. With controlled heating of the fuel supply line (at a non-linear rate) the time interval for vapor lock was found to be related to fuel volatility with the more volatile fuels vapor locking in shorter times.
6. A semi-empirical computer analysis largely based upon experimental data was found to explain complex relationships leading to vapor lock. This model predicted that an increase in carburetor inlet valve area together with insulation of the fuel strainer or the use of an in-tank fuel pump would significantly reduce vapor-lock tendency.
7. The effect of fuel agitation on vapor evolution was quantified in a thermogravimetric bench test, and the computer analysis indicates that increased vapor evolution caused by agitation has a large beneficial effect if it occurs prior to the fuel entering the fuel supply line or a significant detrimental effect if it occurs in the supply line, such as from resonant vibration of the line.
8. Flight and ground performance with both special test automotive fuel blends was found to be normal in the one Cessna 150 aircraft tested.

REFERENCES

1. Patterson, D. J., Morrison, K., Remondino, M., and Slopsema, T., "Light Aircraft Engines, The Potential and Problems for Use of Automotive Fuels, Phase 1-Literature Search," U.S. DOT Report No. FAA-CT-81-150, Dec. 1980.
2. Aldrich, E. W., Barber, E. M. and Robertson, A. E., "Occurrence of Vapor Lock as Related to the Temperature - V/L Characteristics of Motor Gasolines," SAE Journal (transactions), Vol. 53, No. 7, July 1945, 392-401.
3. York, L. L., Hundere, A. and Coit, R. A., "Recommendations for Fuel System Design for Personal Aircraft with Regard to Vapor Lock," SAE Paper 541, Nov. 9-10, 1950.
4. Pigott, R. J. S., "Vapor-Lock-or Dumb Engineering," SAE Journal, Vol. 52, No. 7, July 1944, 310-317.
5. Sung, N. W., Morrison, K., and Patterson, D. J., "Effect of Volatility on Air-Fuel Ratio Distribution and Torque Output of a Carbureted Light Aircraft Piston Engine," U.S. DOT Report, No. DOT/FAA/CT-82/117, March 1982.
6. Remondino, Michael A., "Automotive Gasoline as a General Aviation Fuel - Design of Test Fuel Specifications," Report to University of Michigan, Oct. 1982.
7. American Society for Testing and Materials, ASTM National Standards, Philadelphia, ASTM, 1979.
8. Shelton, E. M., "Motor Gasolines, Winter 1978-1979," U.S. DOE Report, No. DOE/BETC/PPS-79, 1979; and "Motor Gasolines, Summer 1979," U.S. DOE Report No. DOE/BETC/PPS-80/1, 1980.
9. Hodges, R. J., "Vapor Pressure Analysis of Avgas and Mogas, Related to Use in Light Aircraft," Gippsland Institute of Advanced Education (Australia), July 1982 Report.
10. Gonzalez, Cesar, "Functional Compatibility Analysis of Aircraft Engine Fuel Systems," SAE Paper 690308, March 26-28, 1969.
11. Kreith, F., "Principles of Heat Transfer," International Textbook Co., Scranton, Pa., 1958, pg. 36.
12. Zeisloft, Harry, "FAA Autogas Flight Test Report - Special Blend Autogas," Report No. AFR 83-3 to University of Michigan, October 26, 1983.

APPENDIX A

FIGURES

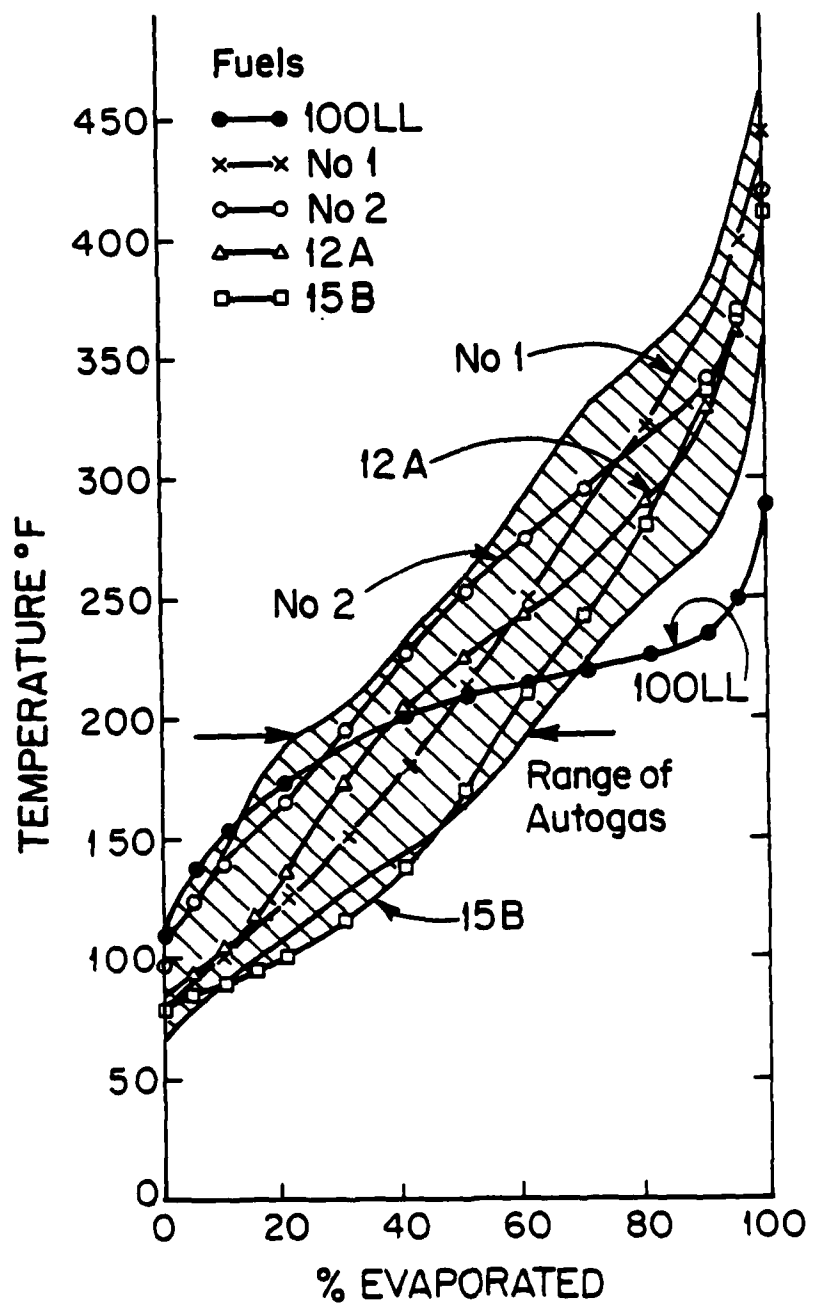


FIGURE 1. DISTILLATION CURVE FOR FIVE FUELS.

The shaded area gives the summer and winter range of autogas data from 1978-79 survey. (Refs. 8)

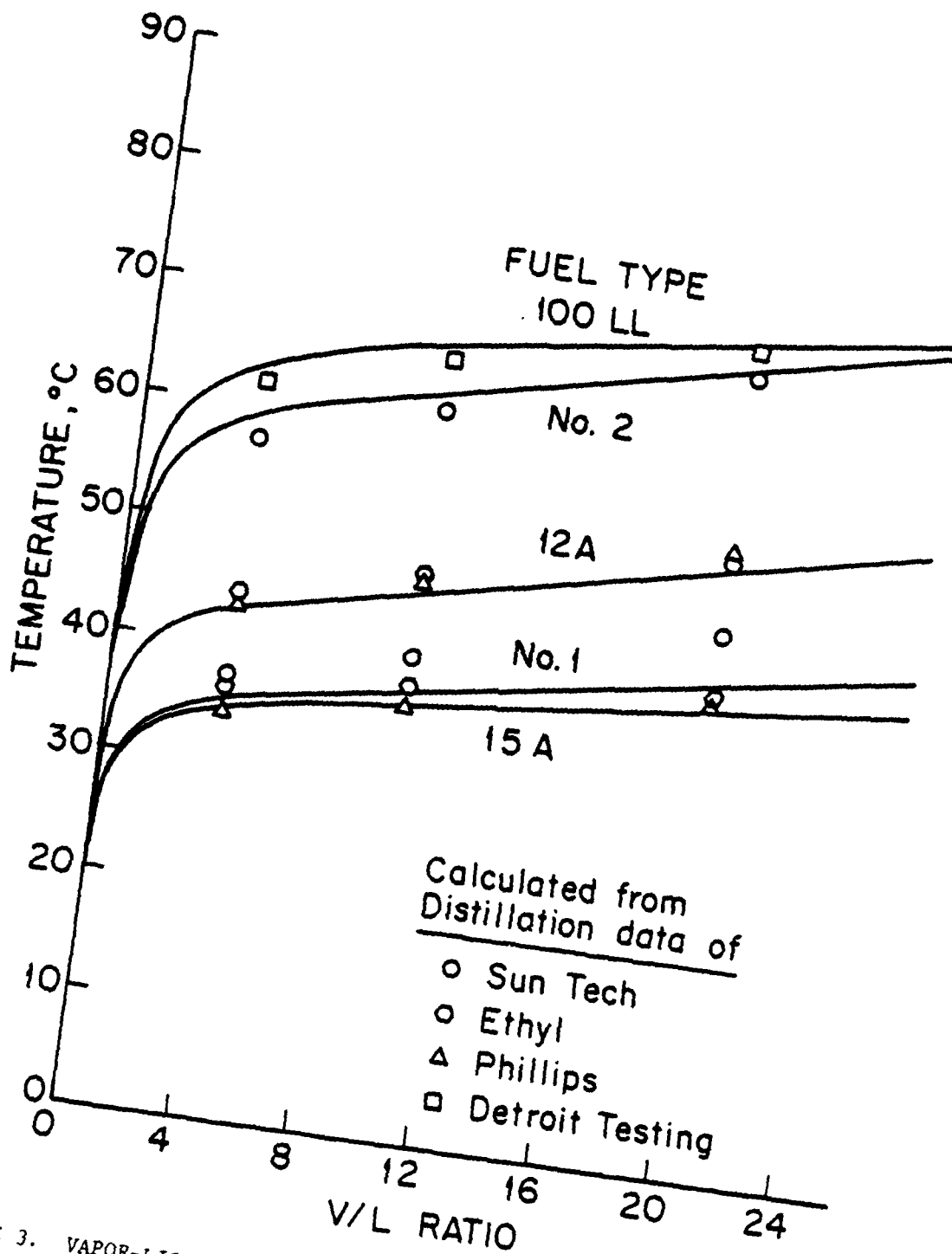


FIGURE 3. VAPOR-LIQUID RATIOS AT DIFFERENT TEMPERATURES.
SOLID LINES ARE EXPERIMENTAL. POINTS ARE CALCULATED.

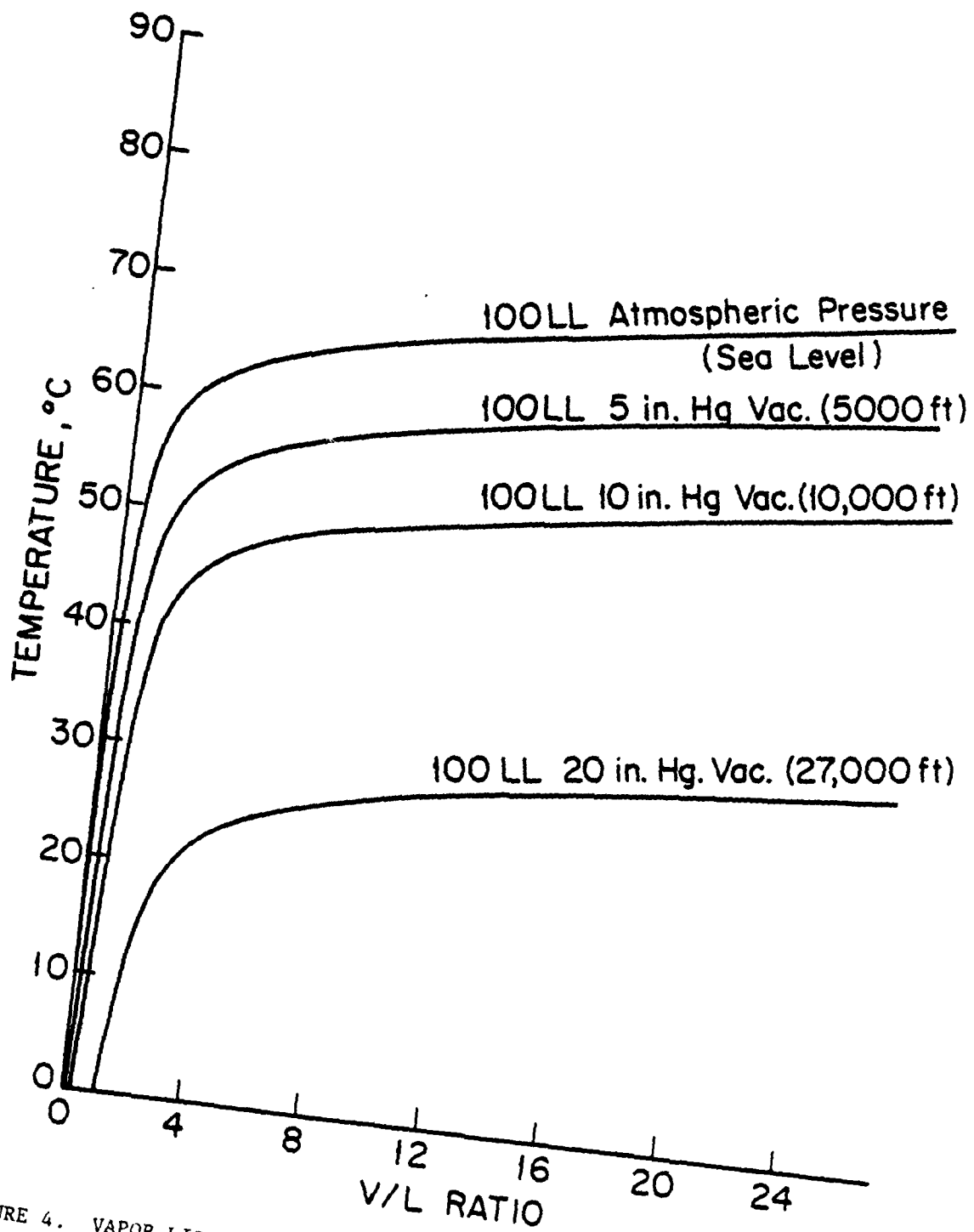


FIGURE 4. VAPOR-LIQUID RATIOS AT ALTITUDE FOR 100LL FUEL

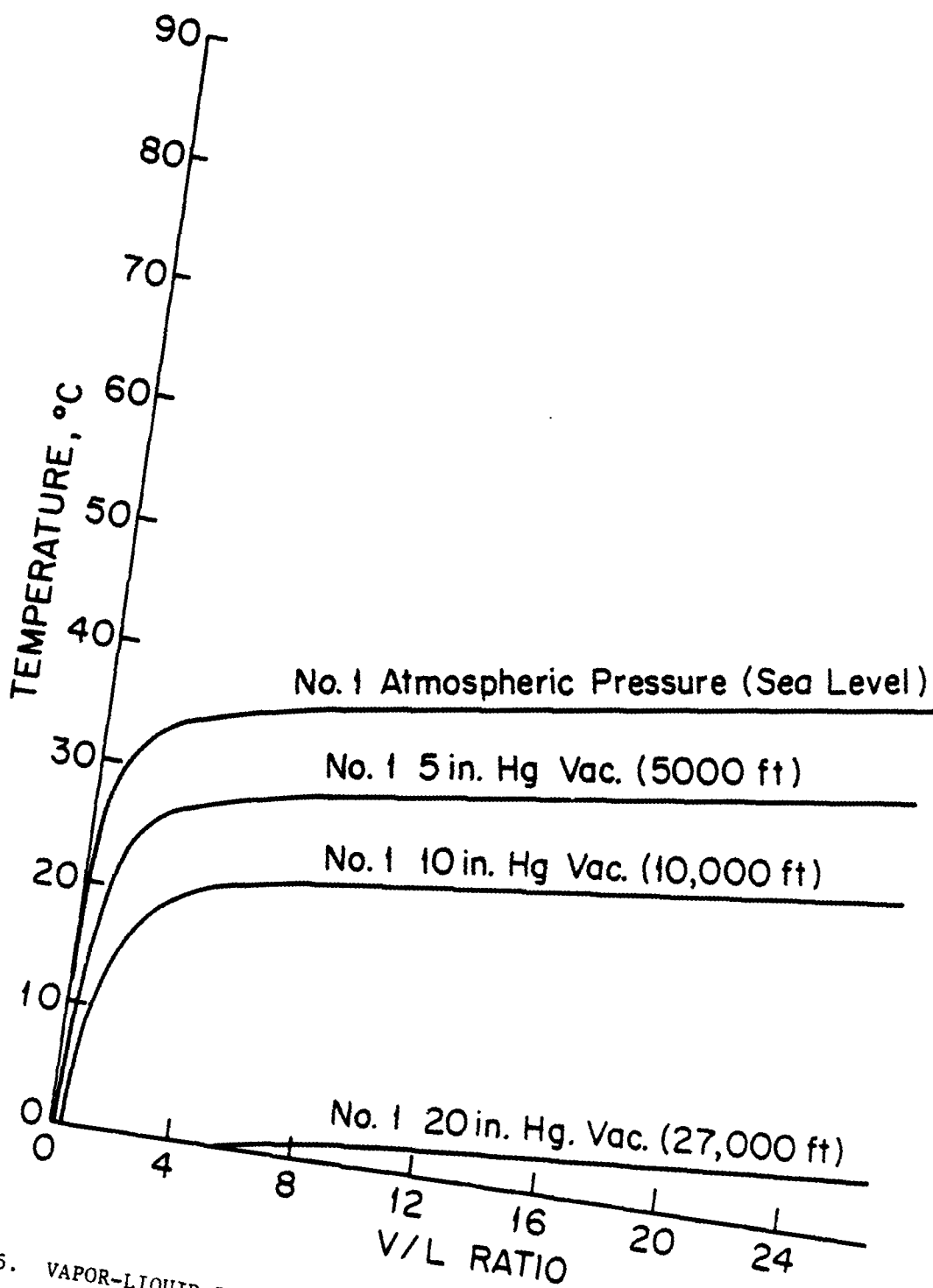


FIGURE 5. VAPOR-LIQUID RATIO AT ALTITUDE FOR NO. 1 FUEL.

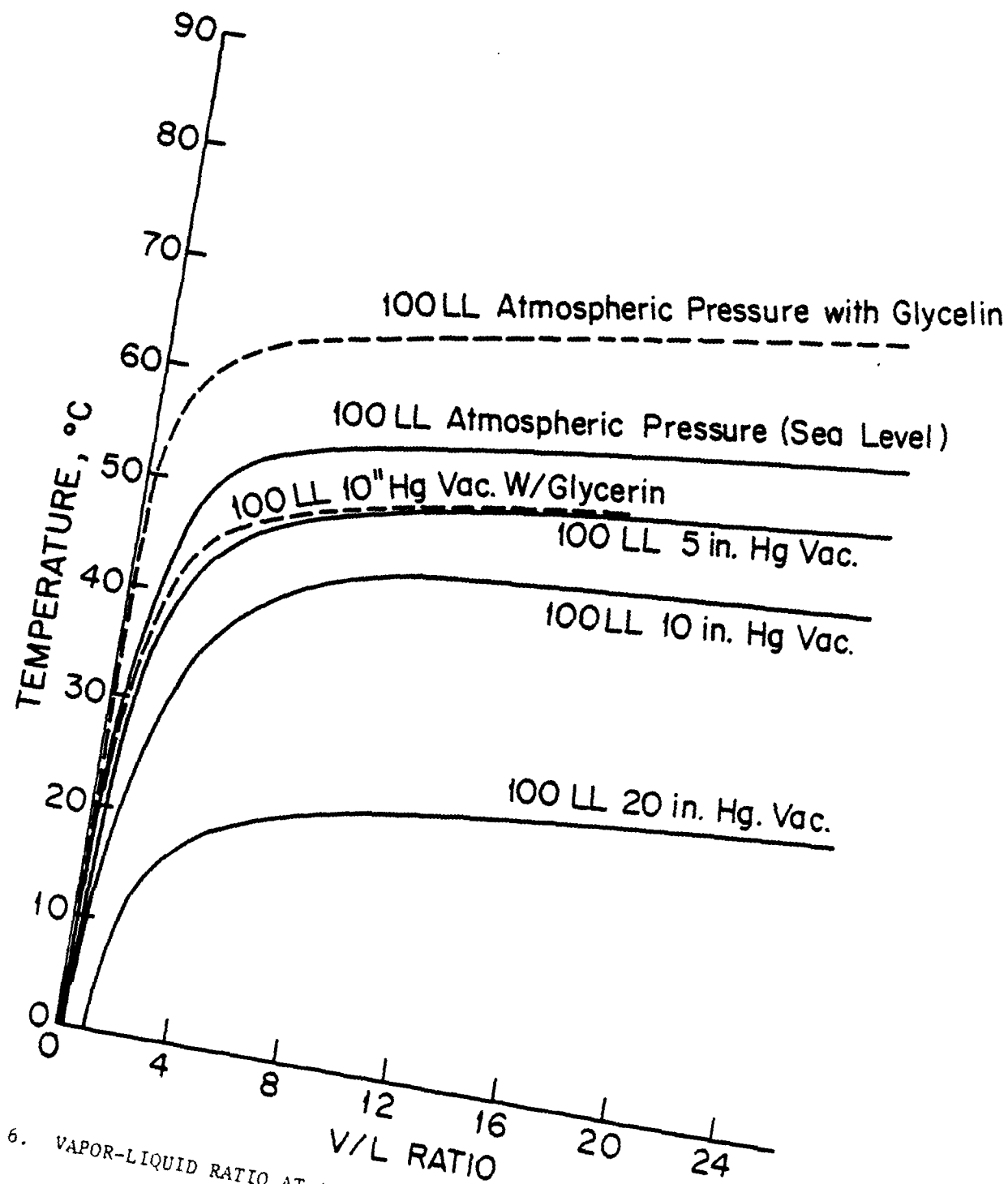


FIGURE 6. VAPOR-LIQUID RATIO AT ALTITUDE FOR 100LL FUEL WITH WATER

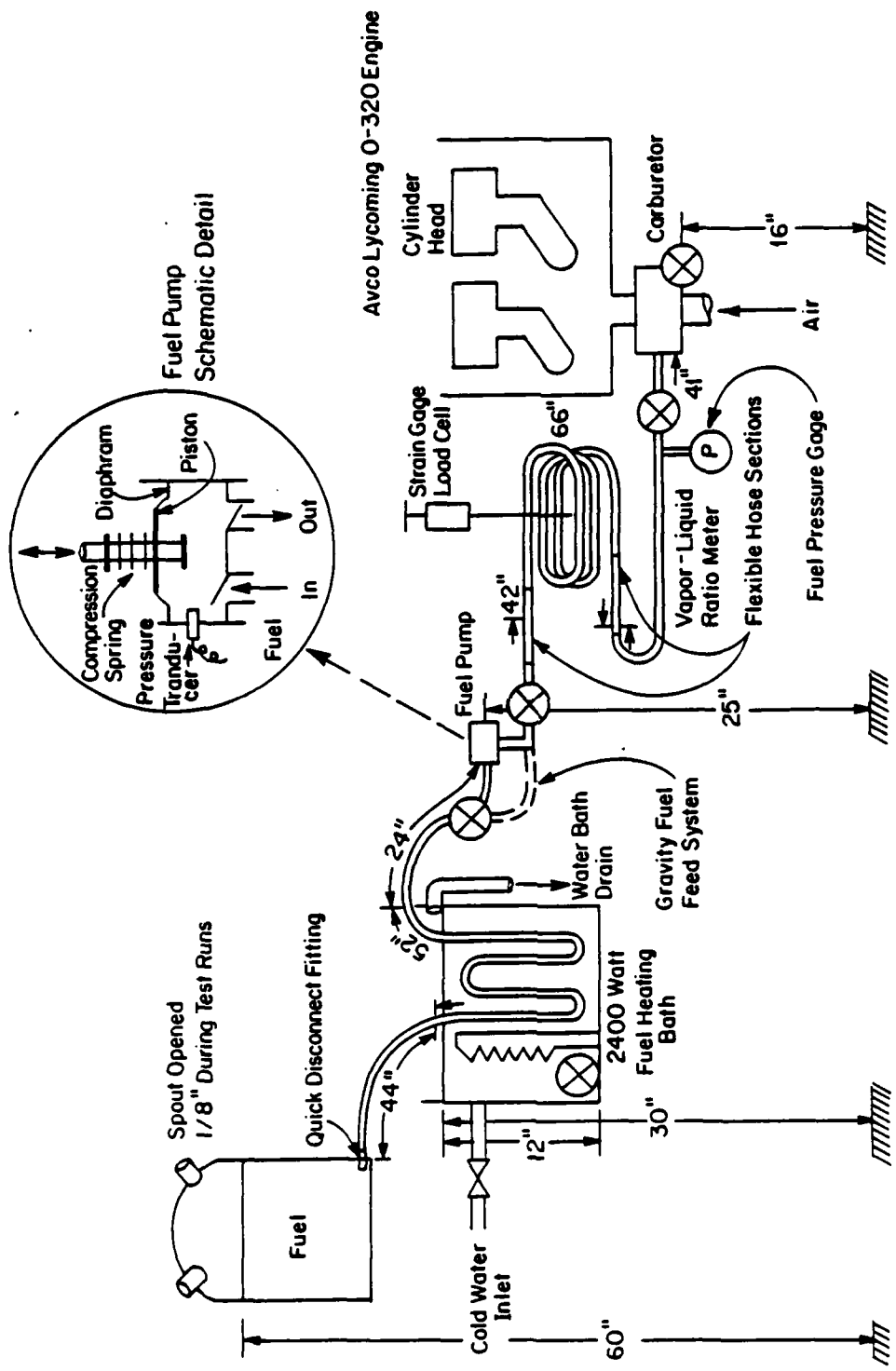


FIGURE 7. SCHEMATIC DIAGRAM OF TWO FUEL DELIVERY SYSTEMS.

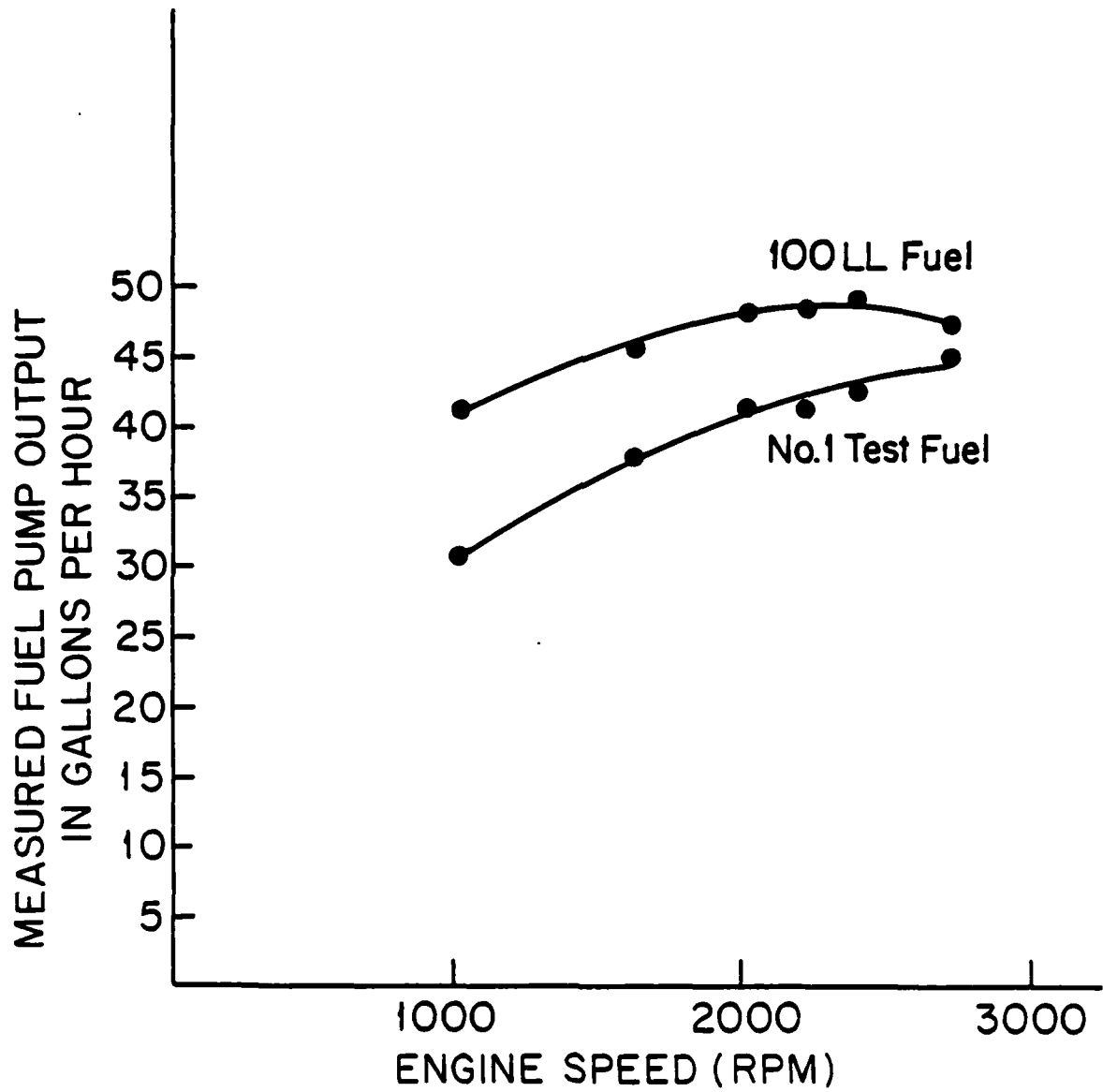


FIGURE 8. FUEL PUMP FLOW AT VARIOUS ENGINE SPEEDS.

No flow restriction at pump outlet, fuel supply 18 inches above inlet, 70°F fuel temperature.

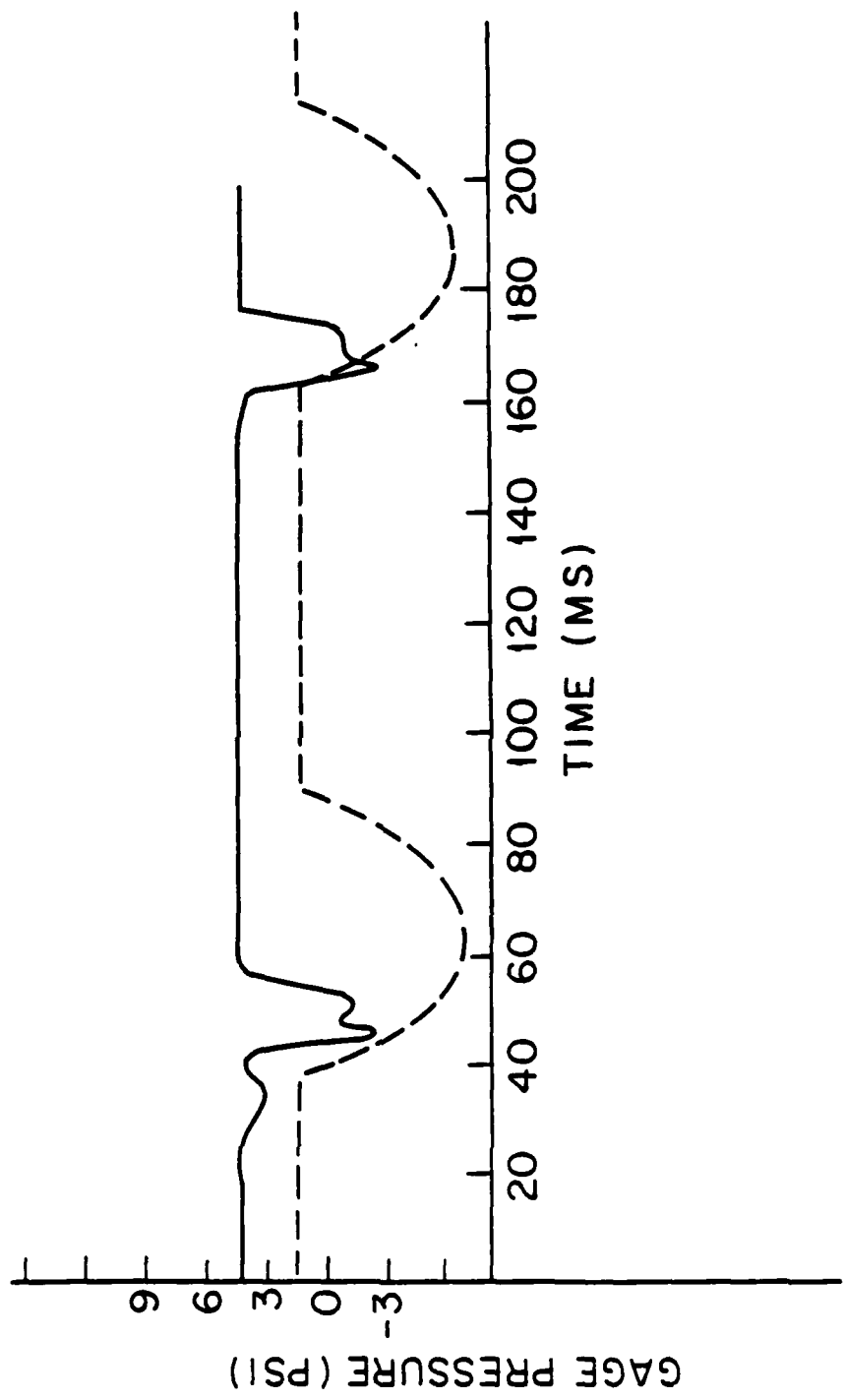


FIGURE 9. PRESSURE VARIATION INSIDE FUEL PUMP.
Upper curve - unrestricted pump inlet,
lower curve - restricted pump inlet.

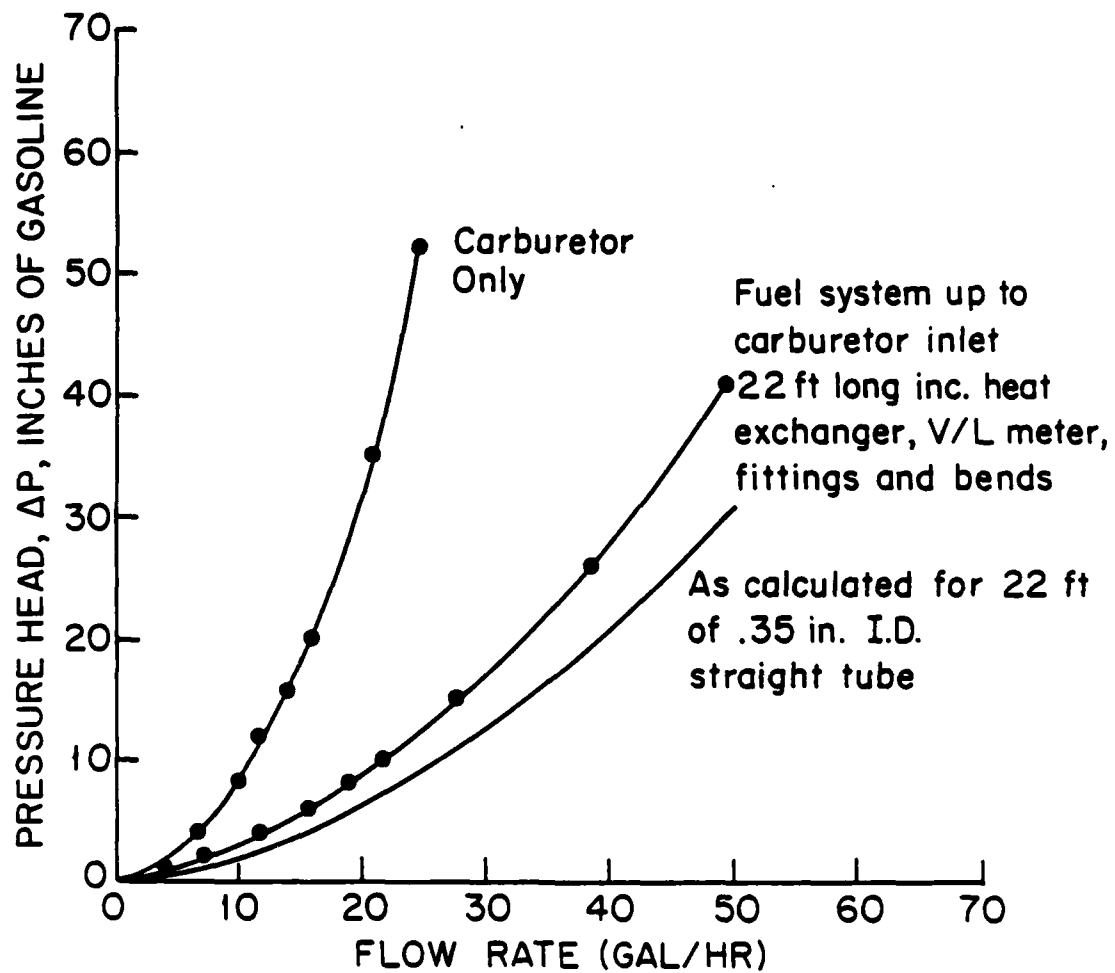


FIGURE 10. PRESSURE DROP THROUGH THE GRAVITY FUEL SYSTEM AND CARBURETOR.

Measured with 100 LL, S.G. = .718, no vapor.

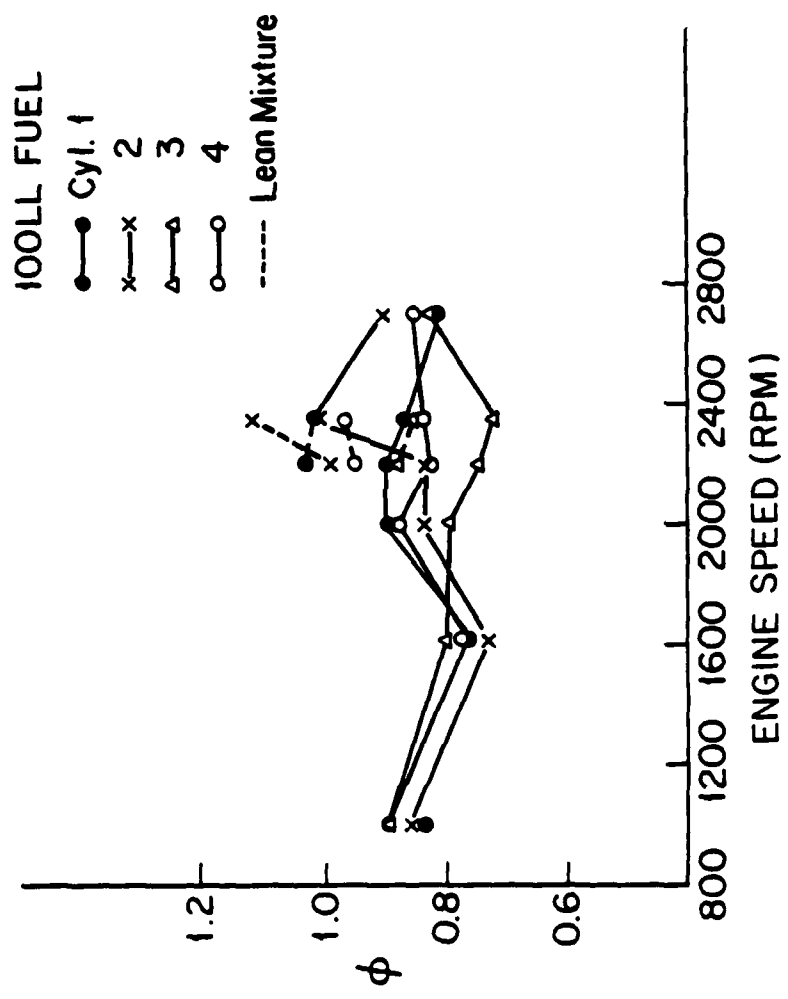


FIGURE 11. EQUIVALENCE RATIO DISTRIBUTION WITH 100 LL FUEL.
 Equivalence ratio (ϕ) = actual air-fuel ratio/
 stoichiometric air-fuel ratio.

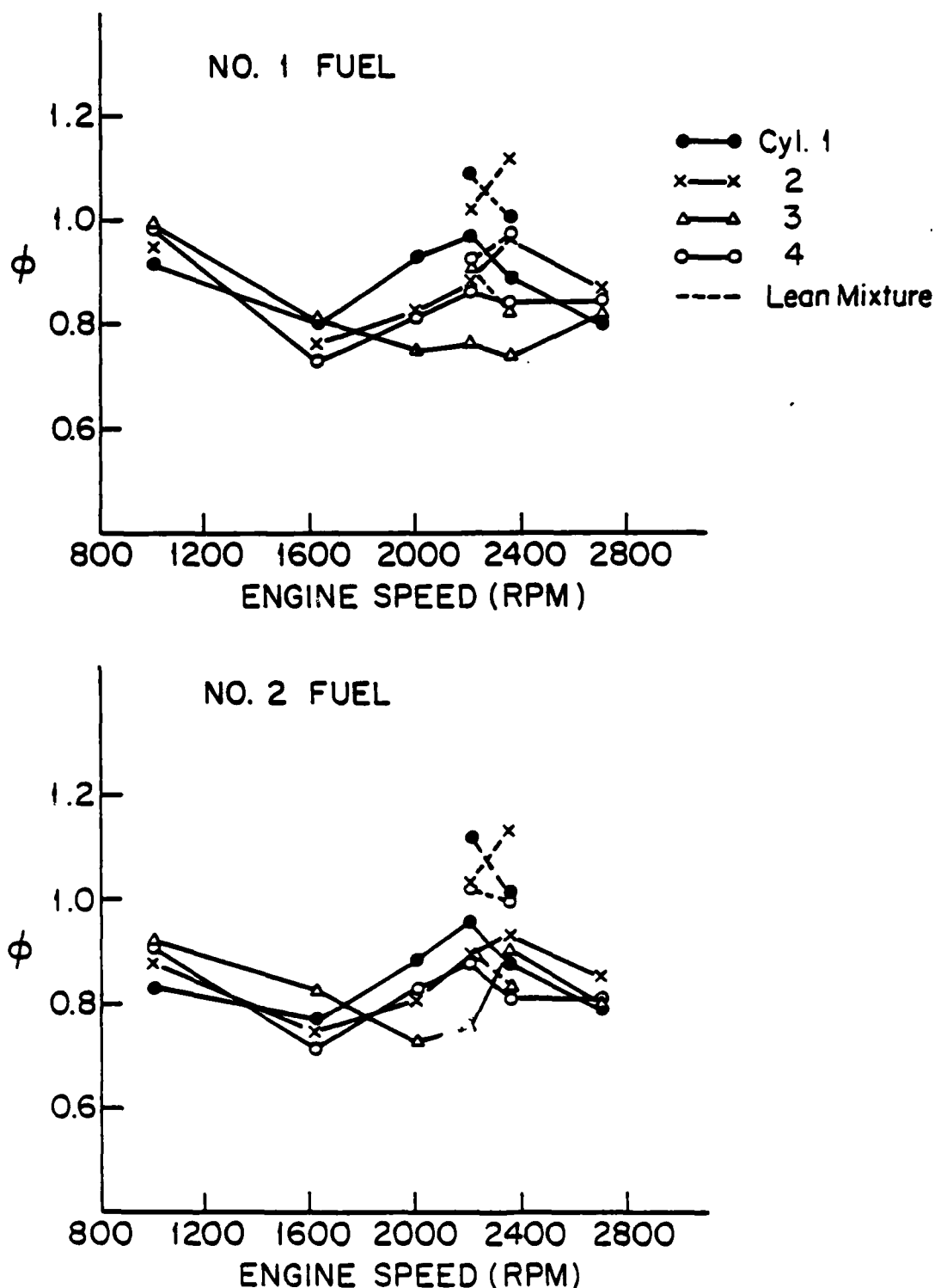


FIGURE 12. EQUIVALENCE RATIO DISTRIBUTION WITH NO. 1 and NO. 2 FUELS.

Equivalence ratio (ϕ) = actual air-fuel ratio/
stoichiometric air-fuel ratio.

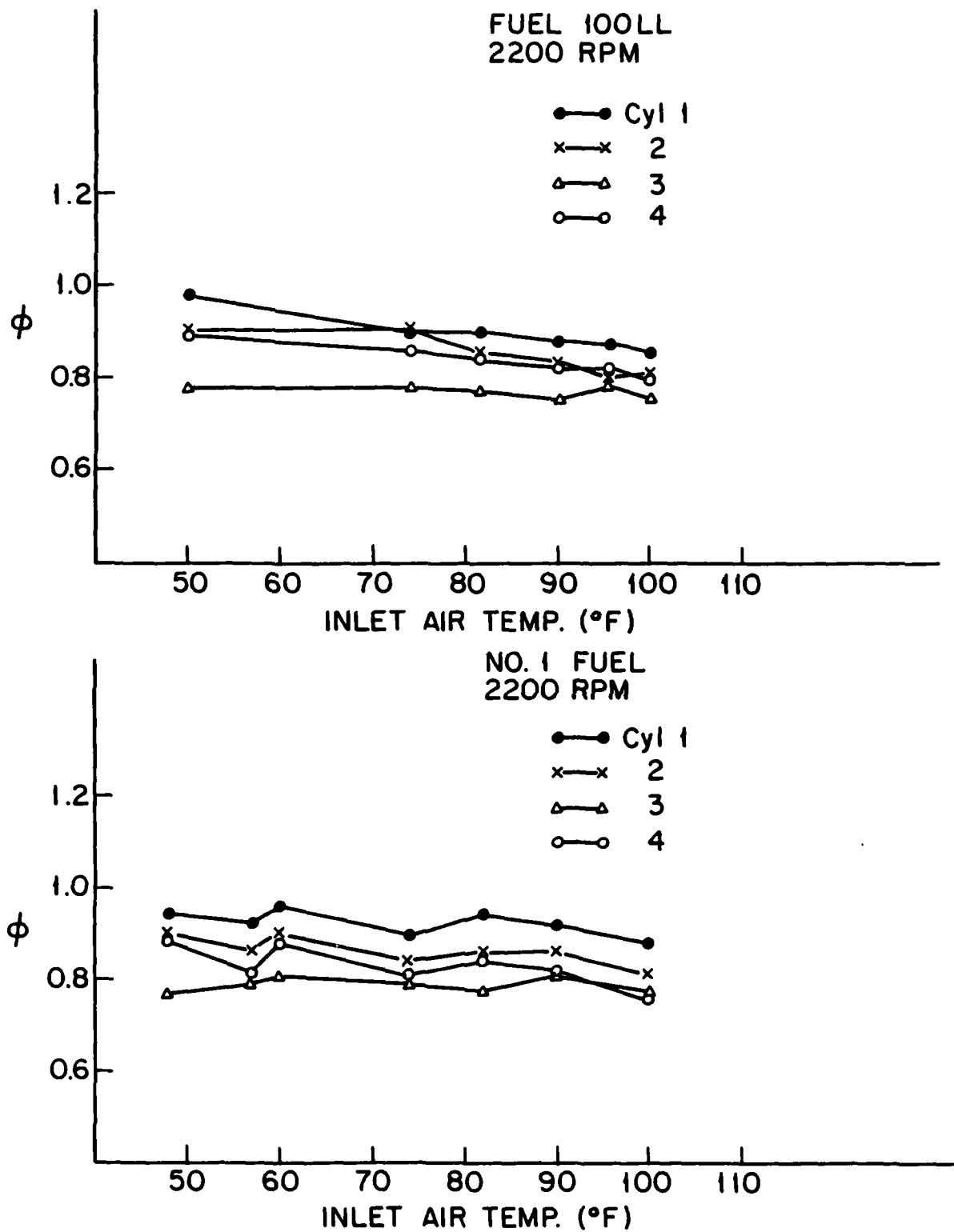


FIGURE 13. INLET AIR TEMPERATURE EFFECT ON MIXTURE DISTRIBUTION.

Equivalence ratio (ϕ) = actual-fuel ratio/stoichiometric air-fuel ratio.

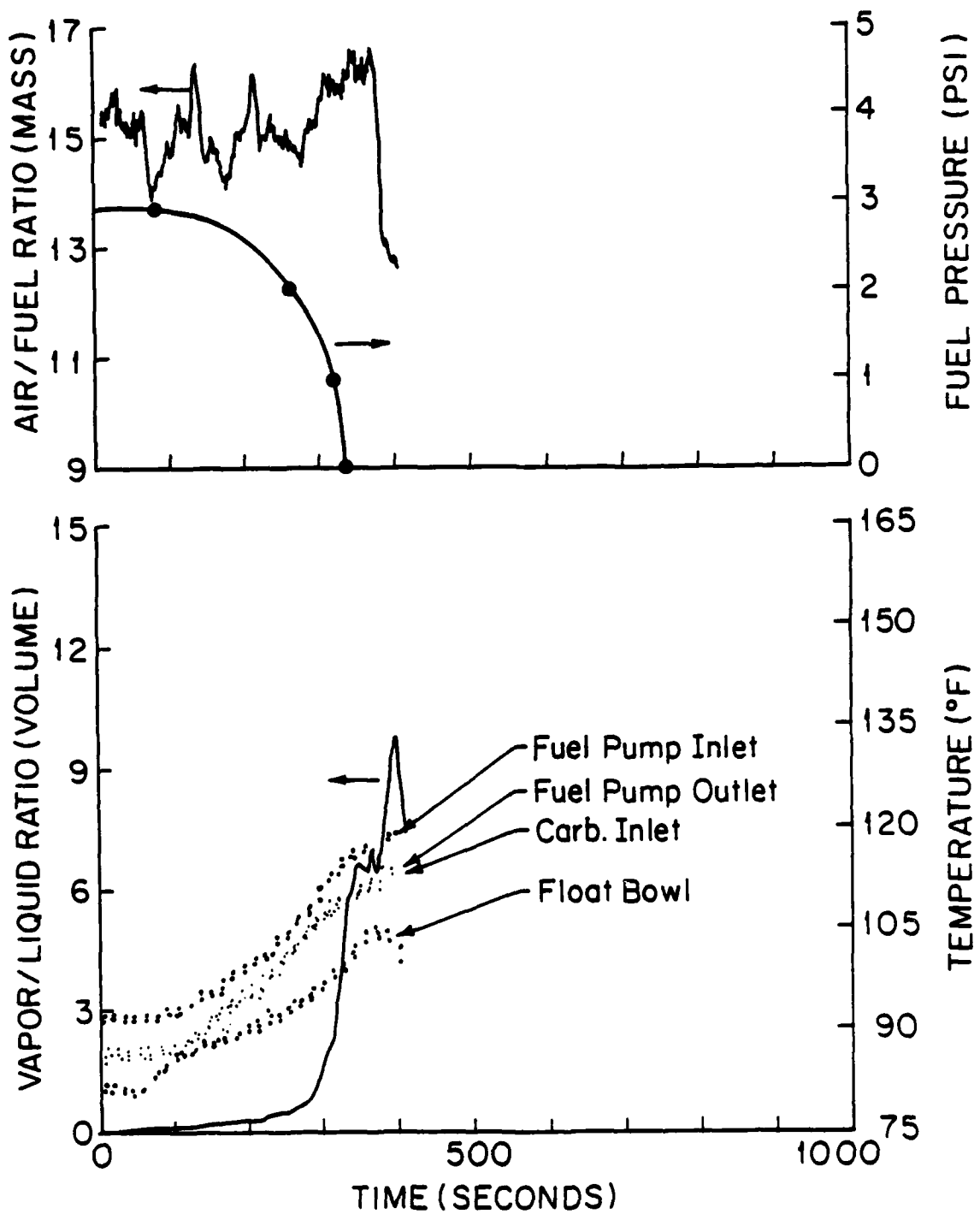


FIGURE 14. VAPOR LOCK DEVELOPMENT.

Fuel 12A, 2350 rpm, lean mixture.

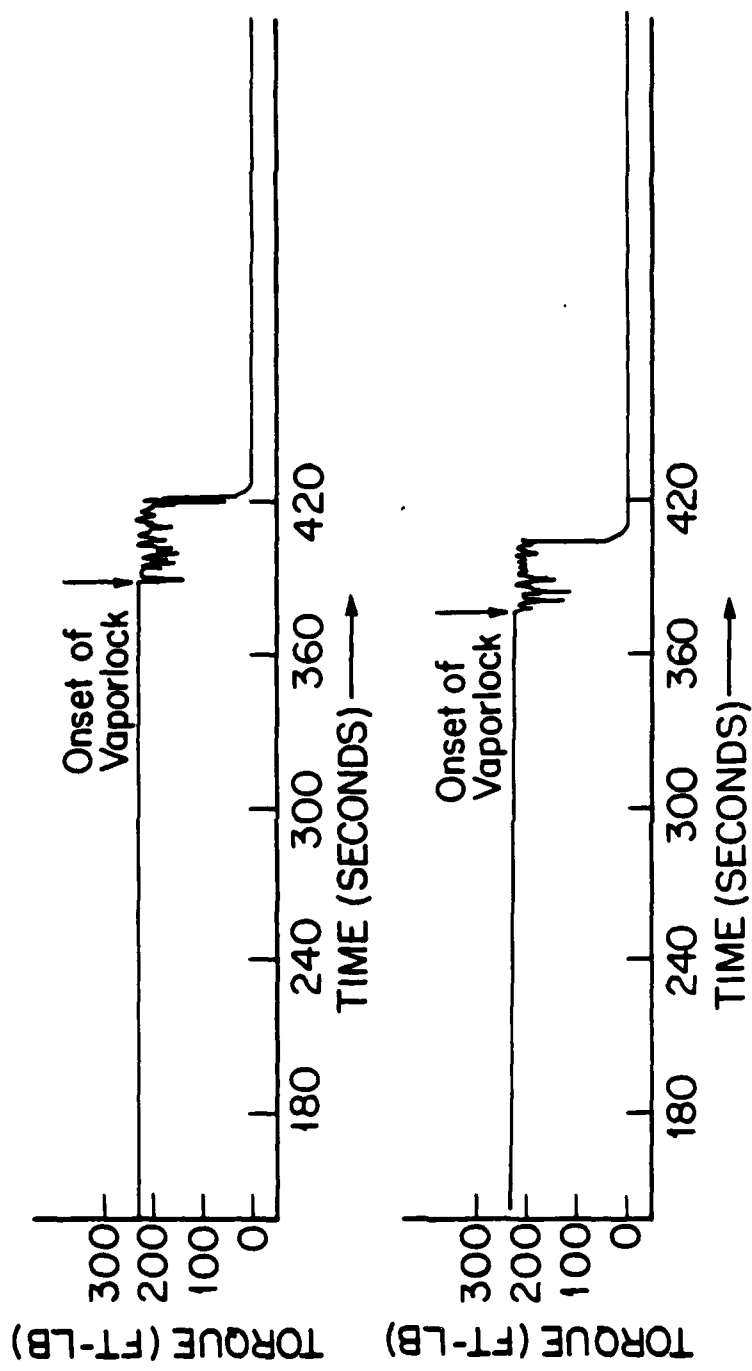


FIGURE 15. TORQUE VARIATION AS VAPOR LOCK DEVELOPS.
 Fuel 12-A, brake torque output at 2350 rpm, lean mixture,
 fuel level 18 inches above pump inlet (top), 18 inches
 below inlet (bottom).

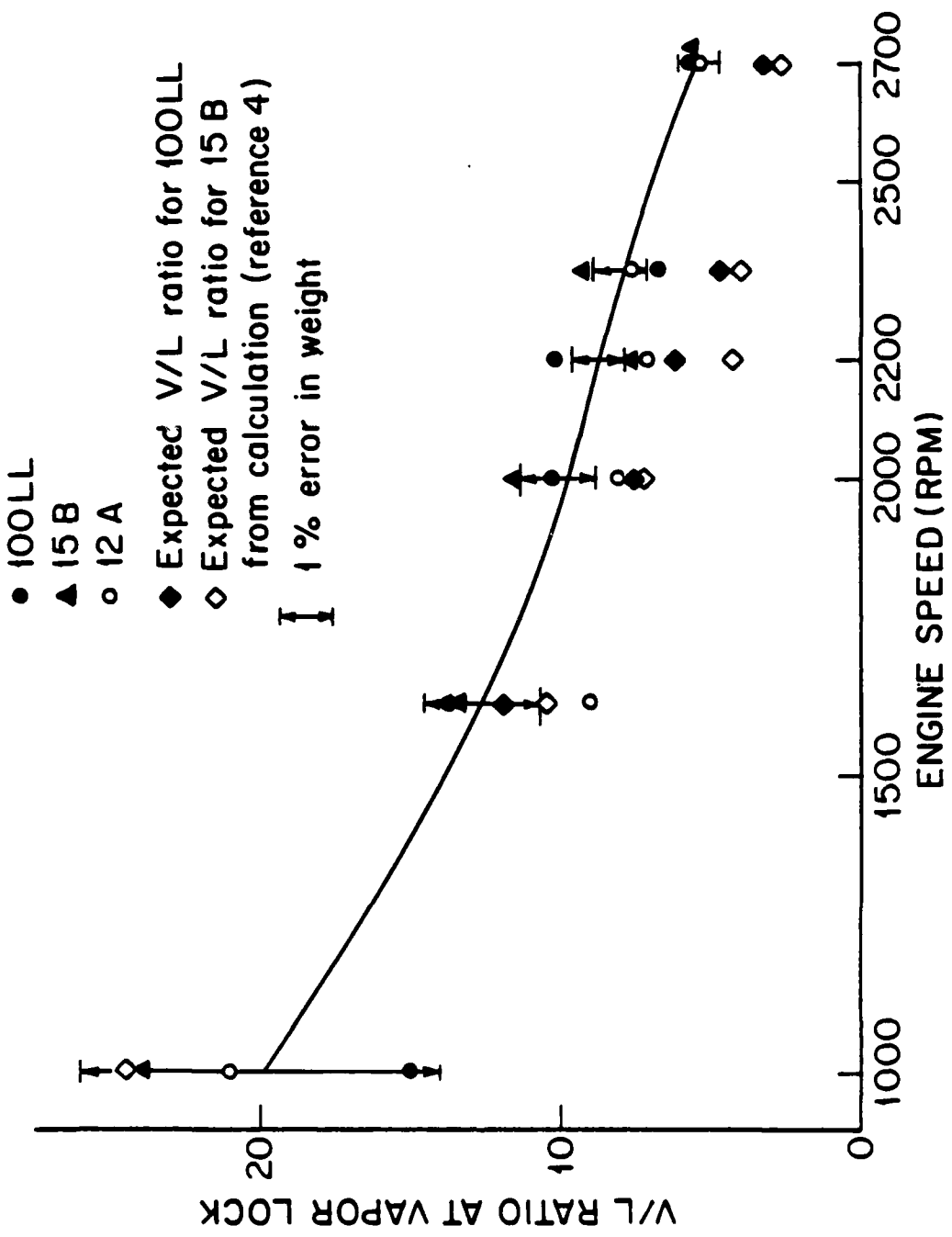


FIGURE 16. VAPOR TO LIQUID RATIO WHEN VAPOR LOCK OCCURS (WITH FUEL PUMP)

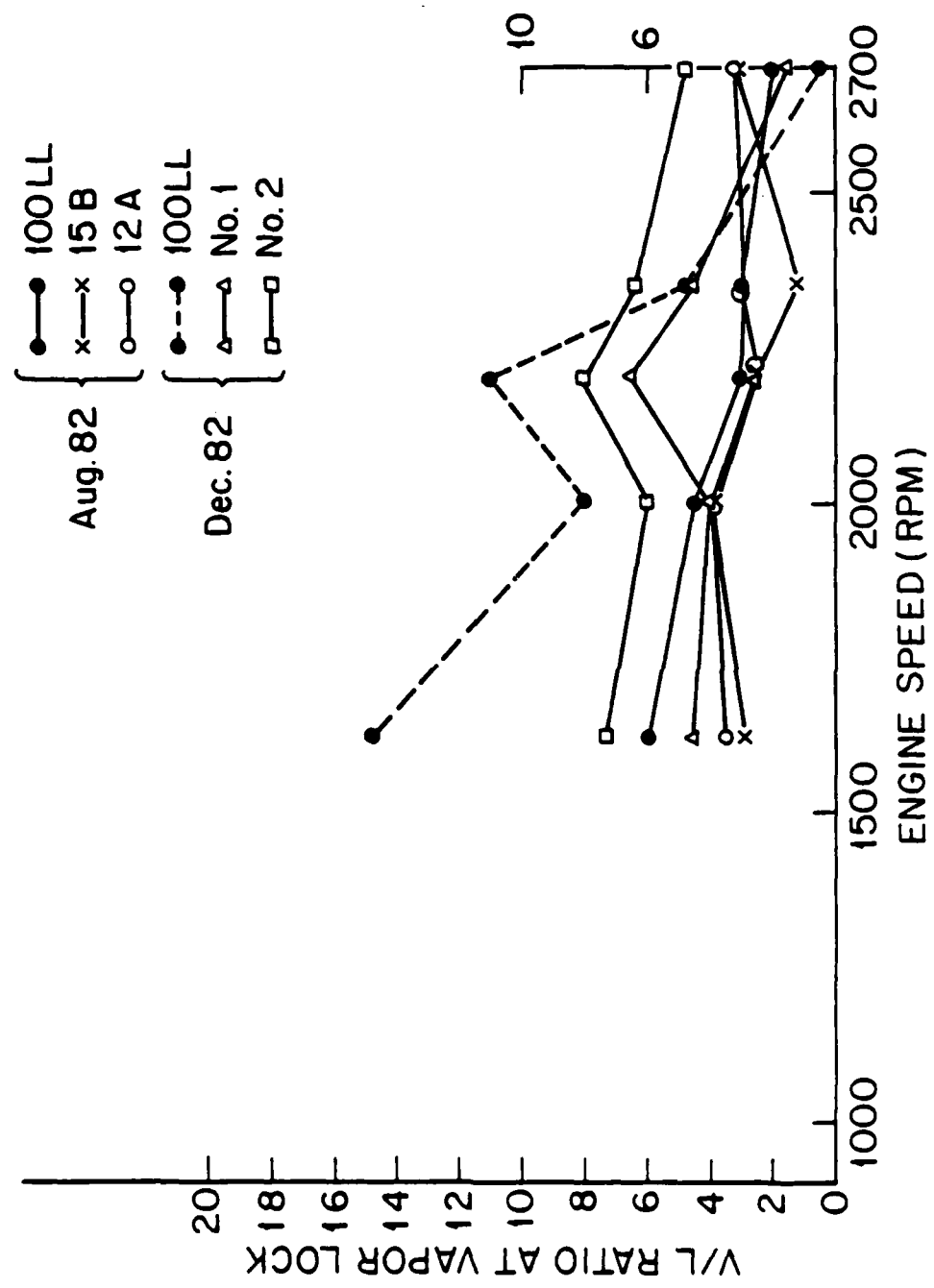


FIGURE 17. VAPOR TO LIQUID RATIO WHEN VAPOR LOCK OCCURS (GRAVITY FEED SYSTEM, NO PUMP).

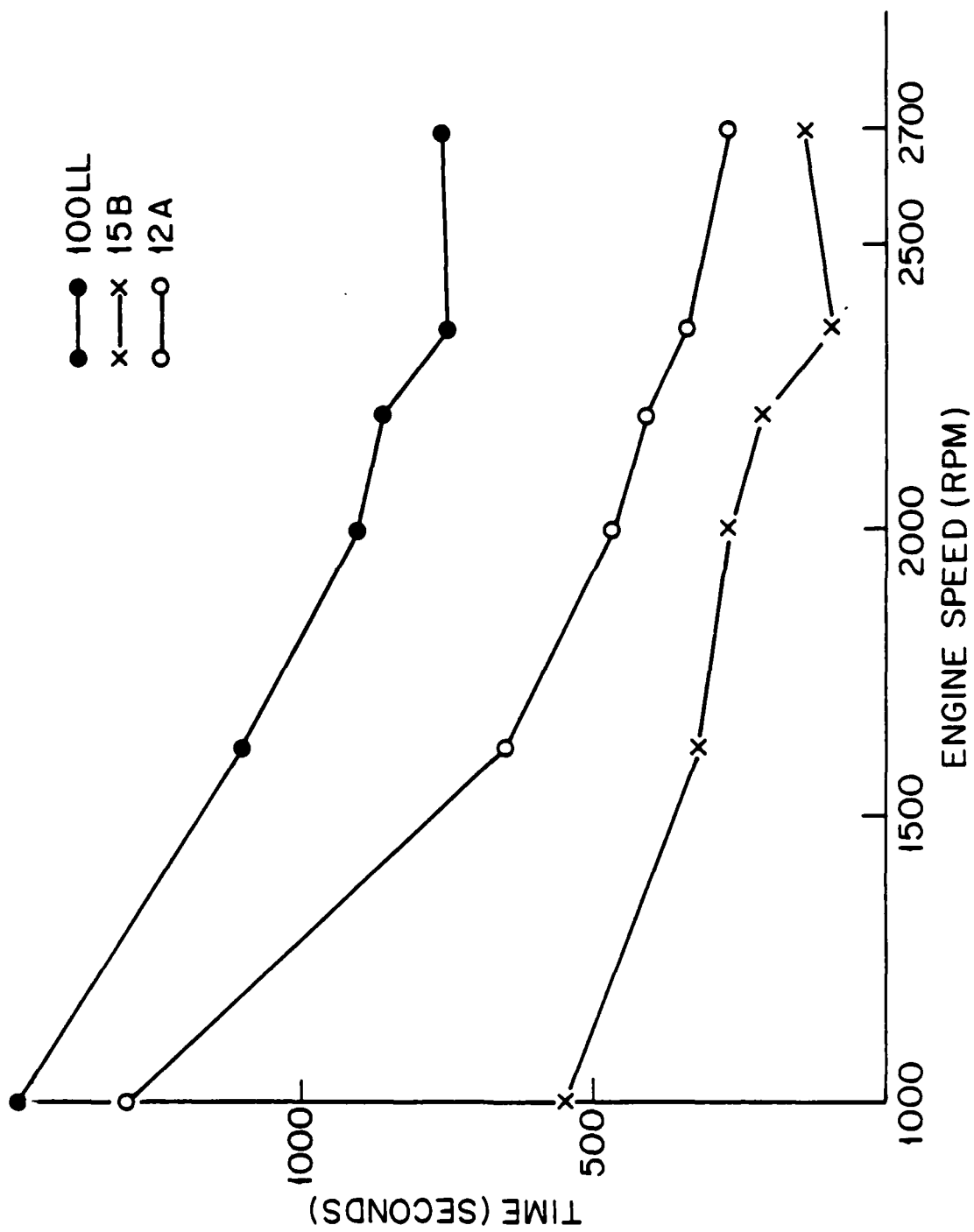


FIGURE 18. TIME FOR VAPOR LOCK (WITH FUEL PUMP)

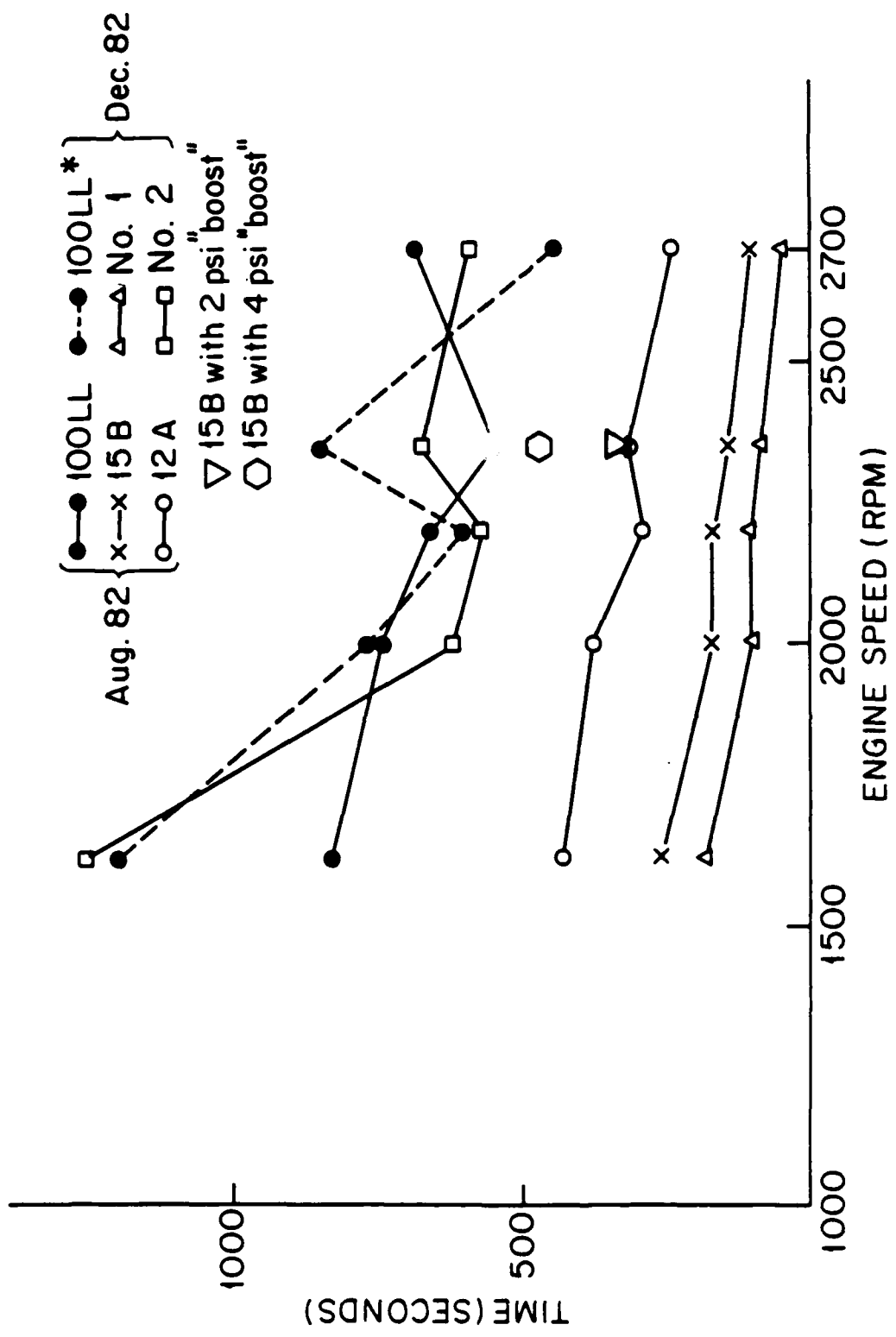


FIGURE 19. TIME FOR VAPOR LOCK (GRAVITY FEED SYSTEM, NO PUMP)

*DIFFERENT BATCH OF 100LL

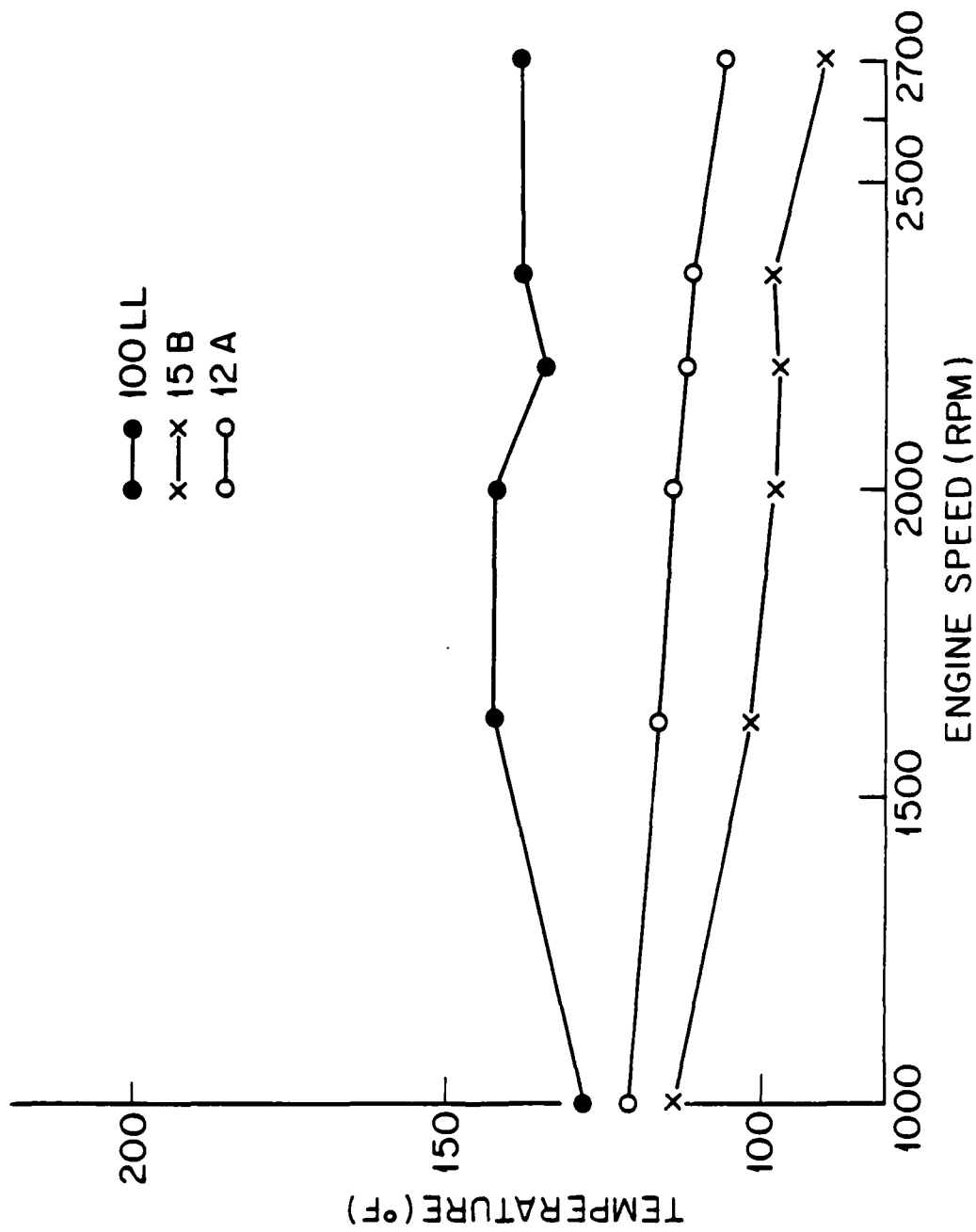


FIGURE 20. FUEL TEMPERATURE (BEFORE CARBURETOR INLET) WHEN VAPOR LOCK OCCURS WITH FUEL PUMP.

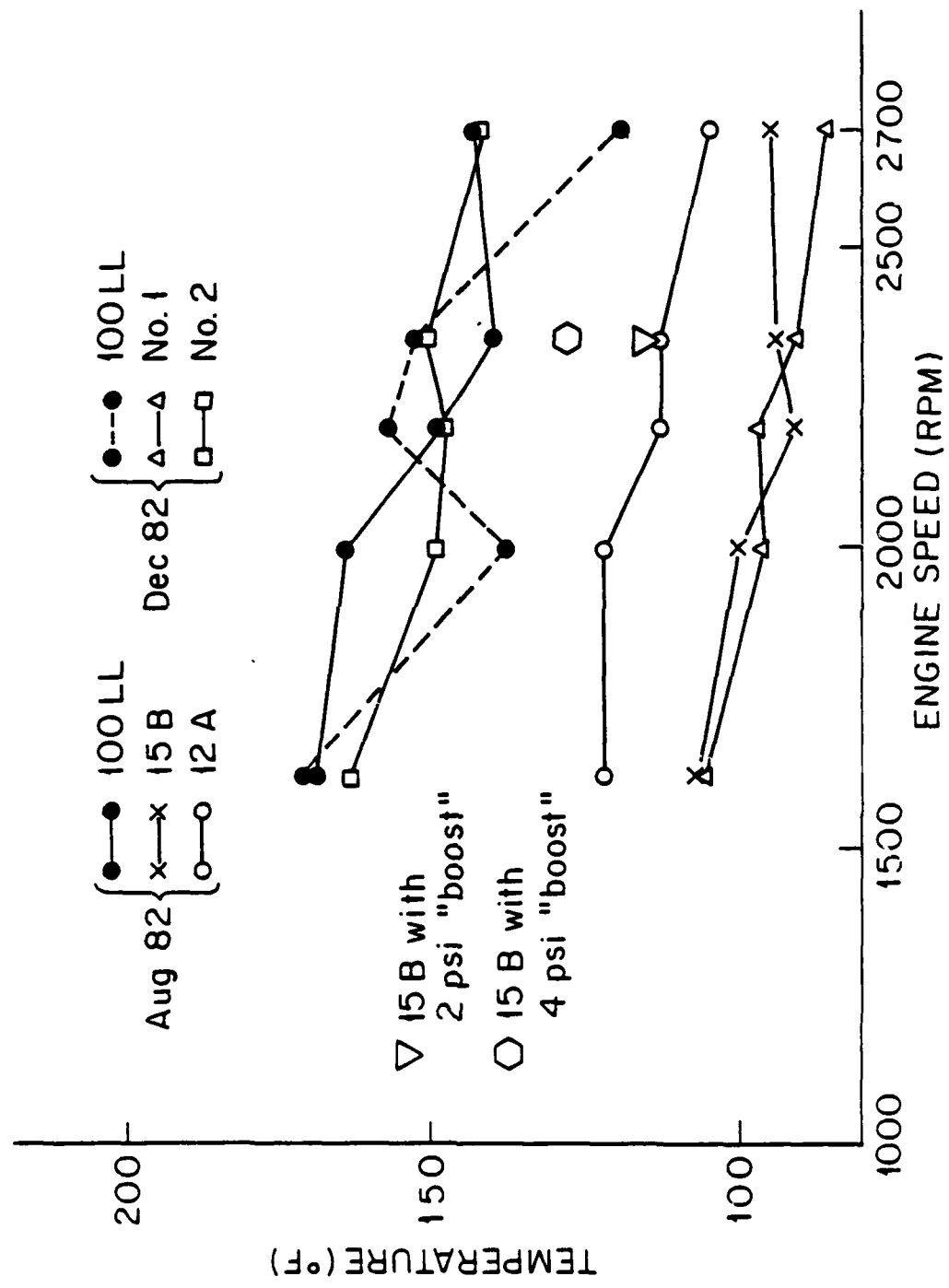


FIGURE 21. FUEL TEMPERATURE (BEFORE CARBURETOR INLET) WHEN VAPOR LOCK OCCURS, GRAVITY FEED SYSTEM, NO PUMP.

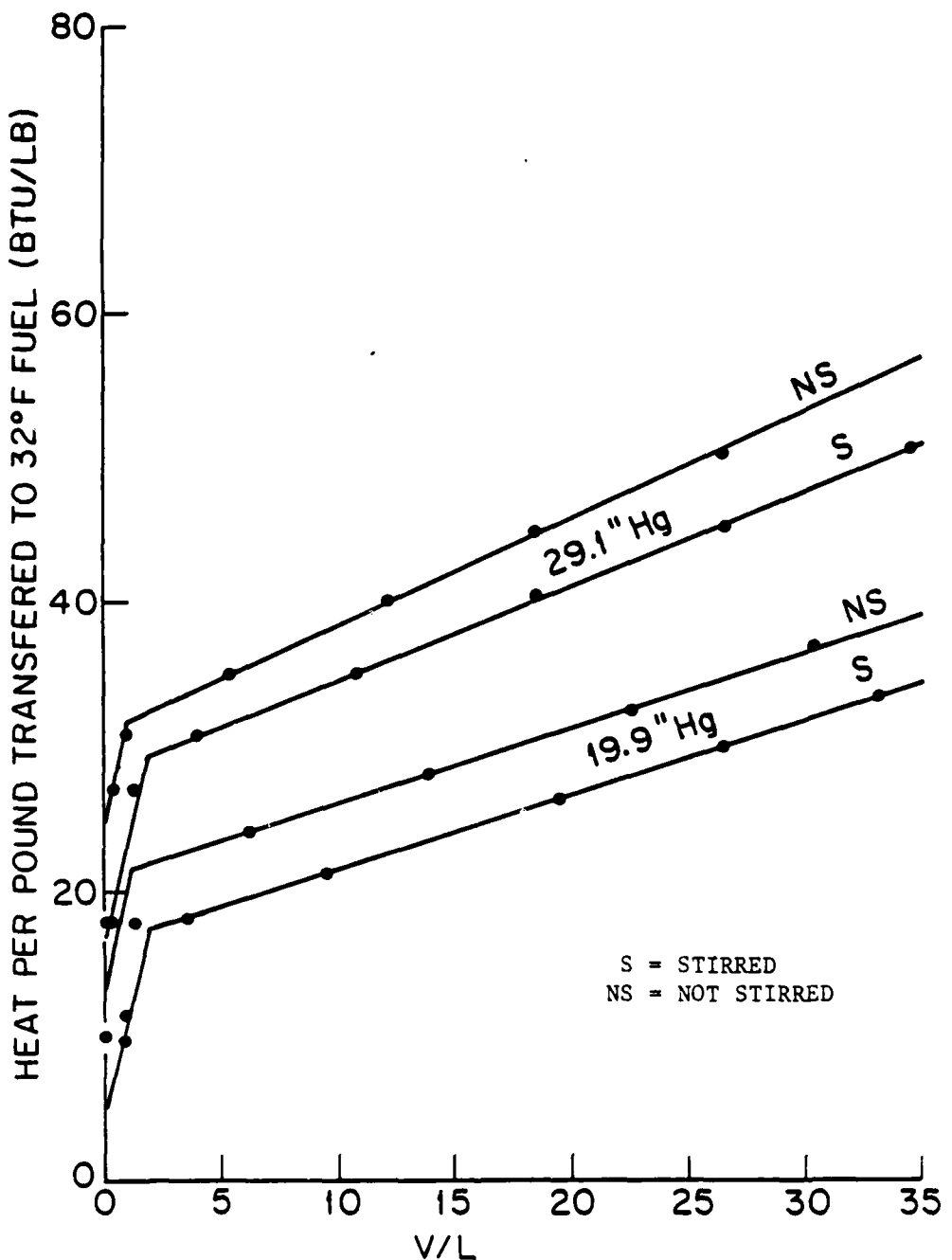


FIGURE 22. HEAT ADDED PER POUND OF FUEL VS VAPOR TO LIQUID RATIO FOR FUEL NO. 1.

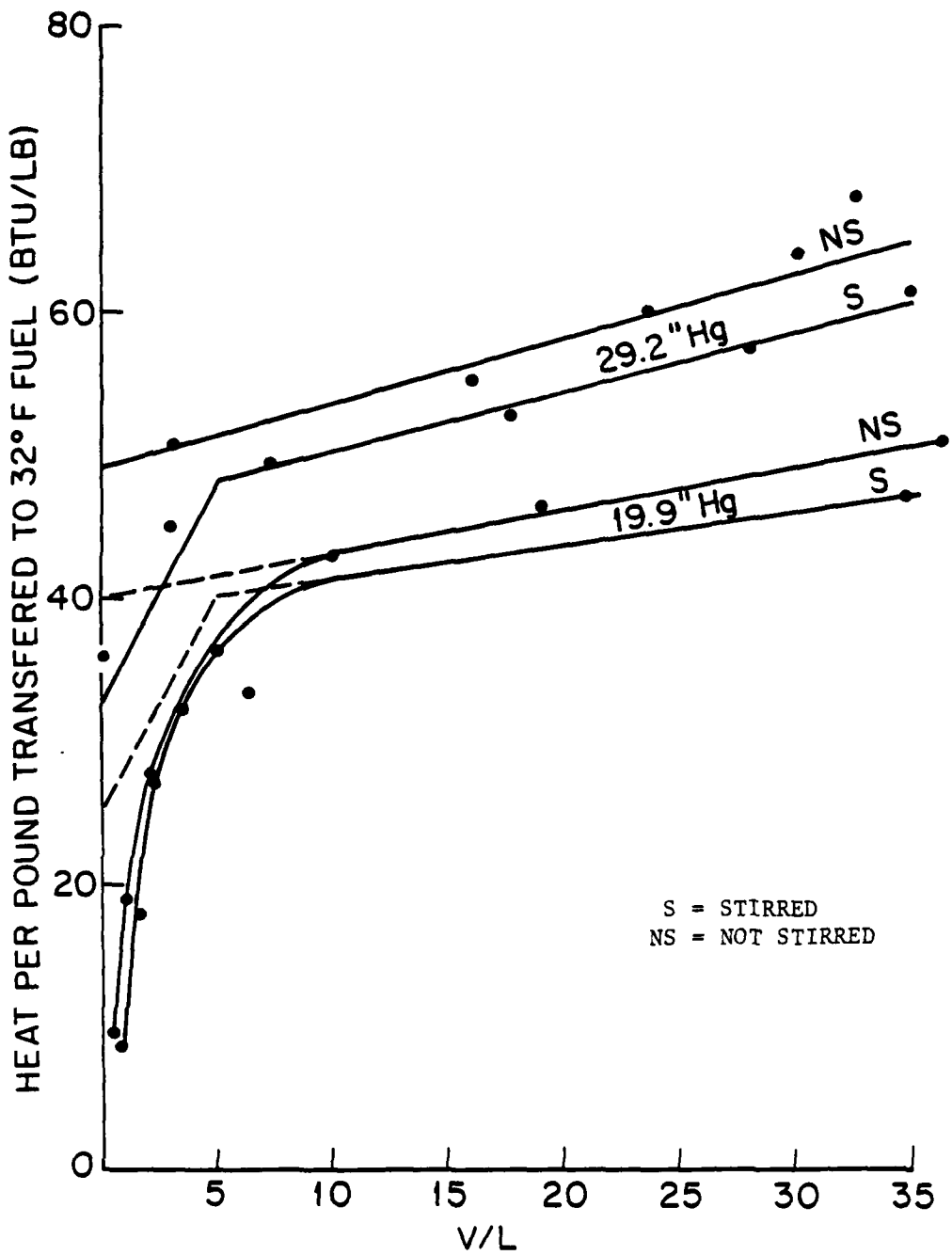


FIGURE 23. HEAT ADDED PER POUND OF FUEL VS VAPOR TO LIQUID RATIO FOR WET 100LL.

Dashed lines represent simplified curve for computer model.

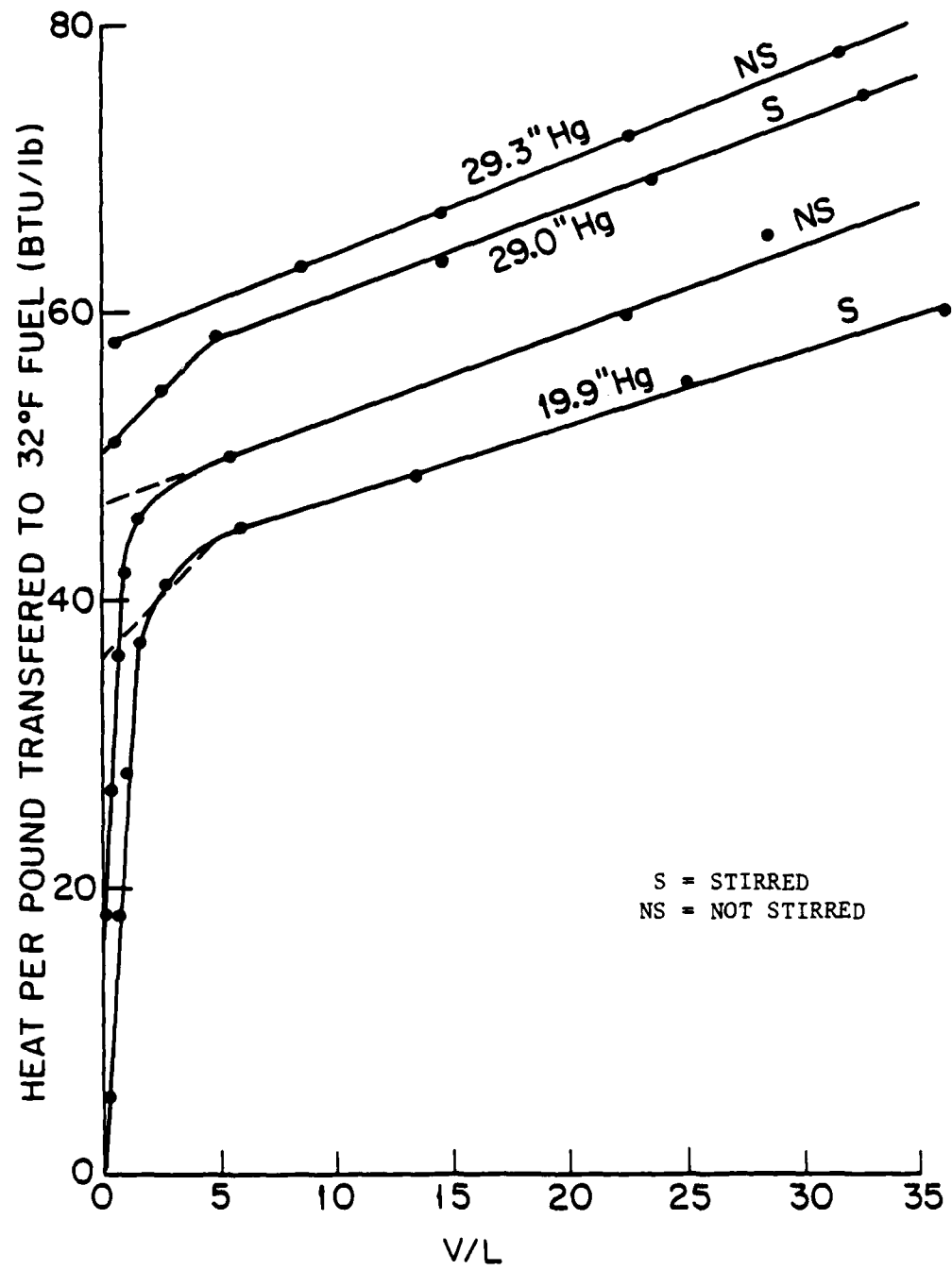


FIGURE 24. HEAT ADDED PER POUND OF FUEL VS VAPOR TO LIQUID RATIO FOR DRY 100LL.

Dashed lines represent simplified curve for computer model.

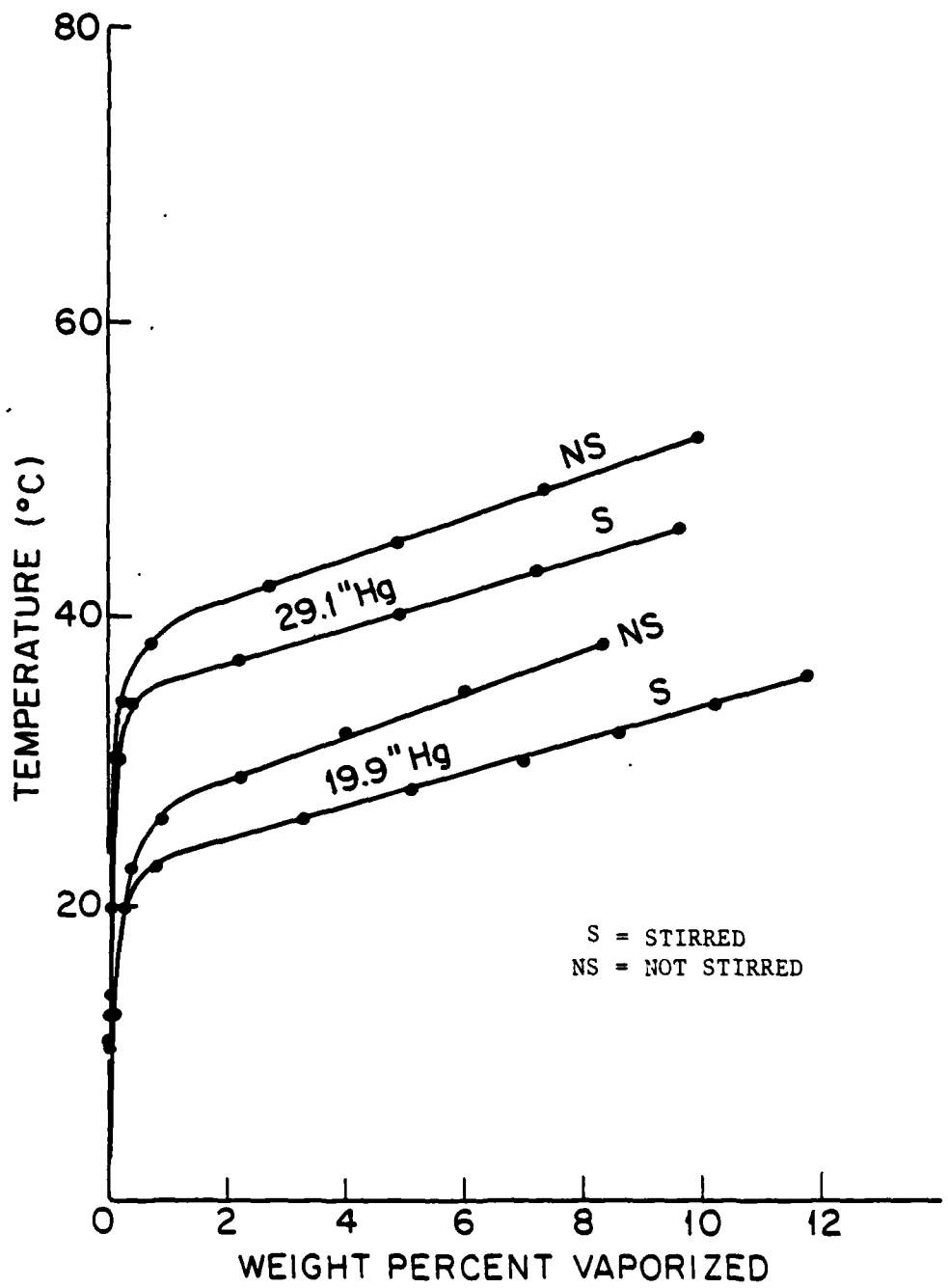


FIGURE 25. WEIGHT PERCENT VAPORIZED VS TEMPERATURE FOR NO. 1 FUEL.

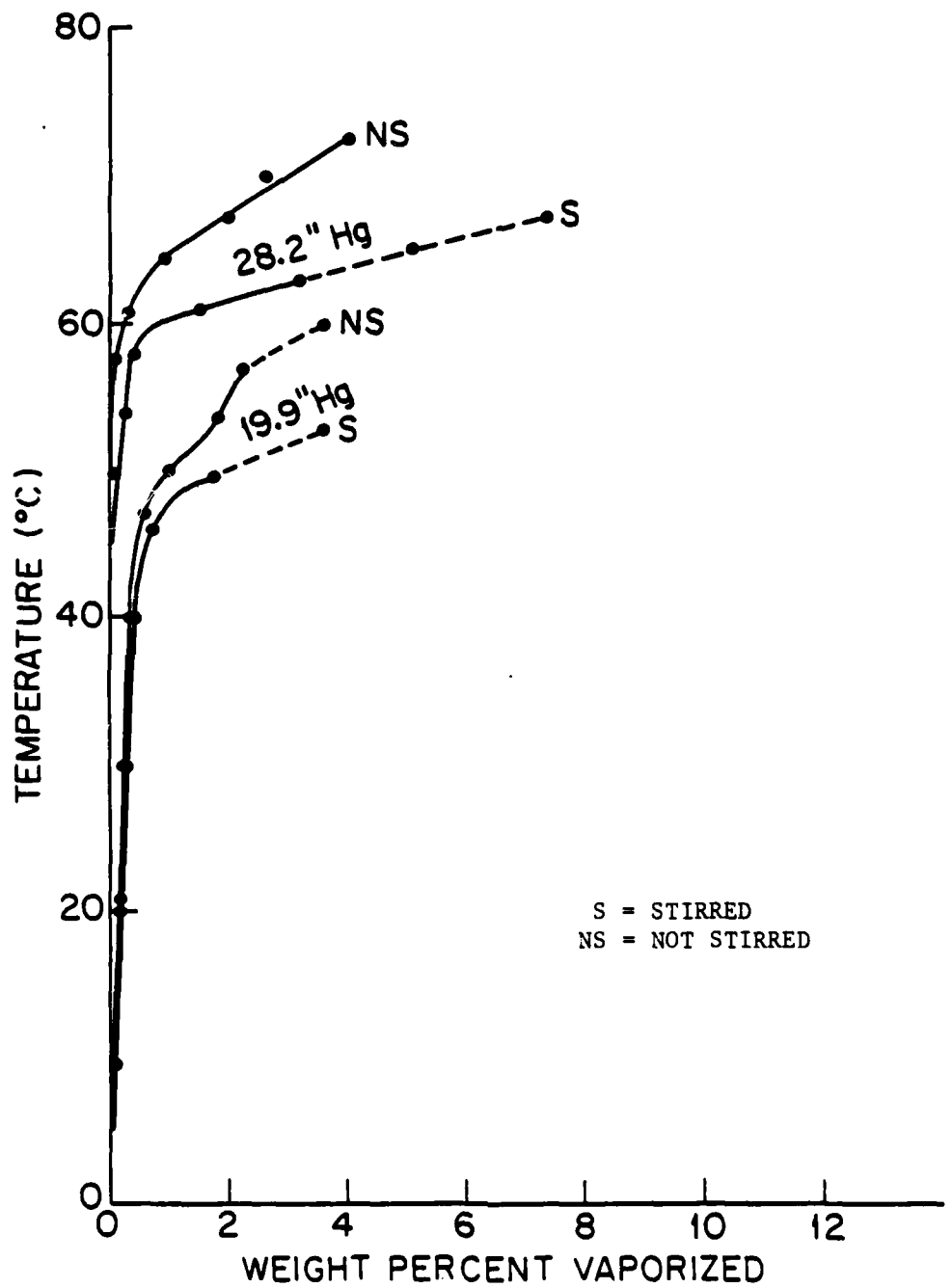


FIGURE 26. WEIGHT PERCENT VAPORIZED VS TEMPERATURE FOR WET 100LL

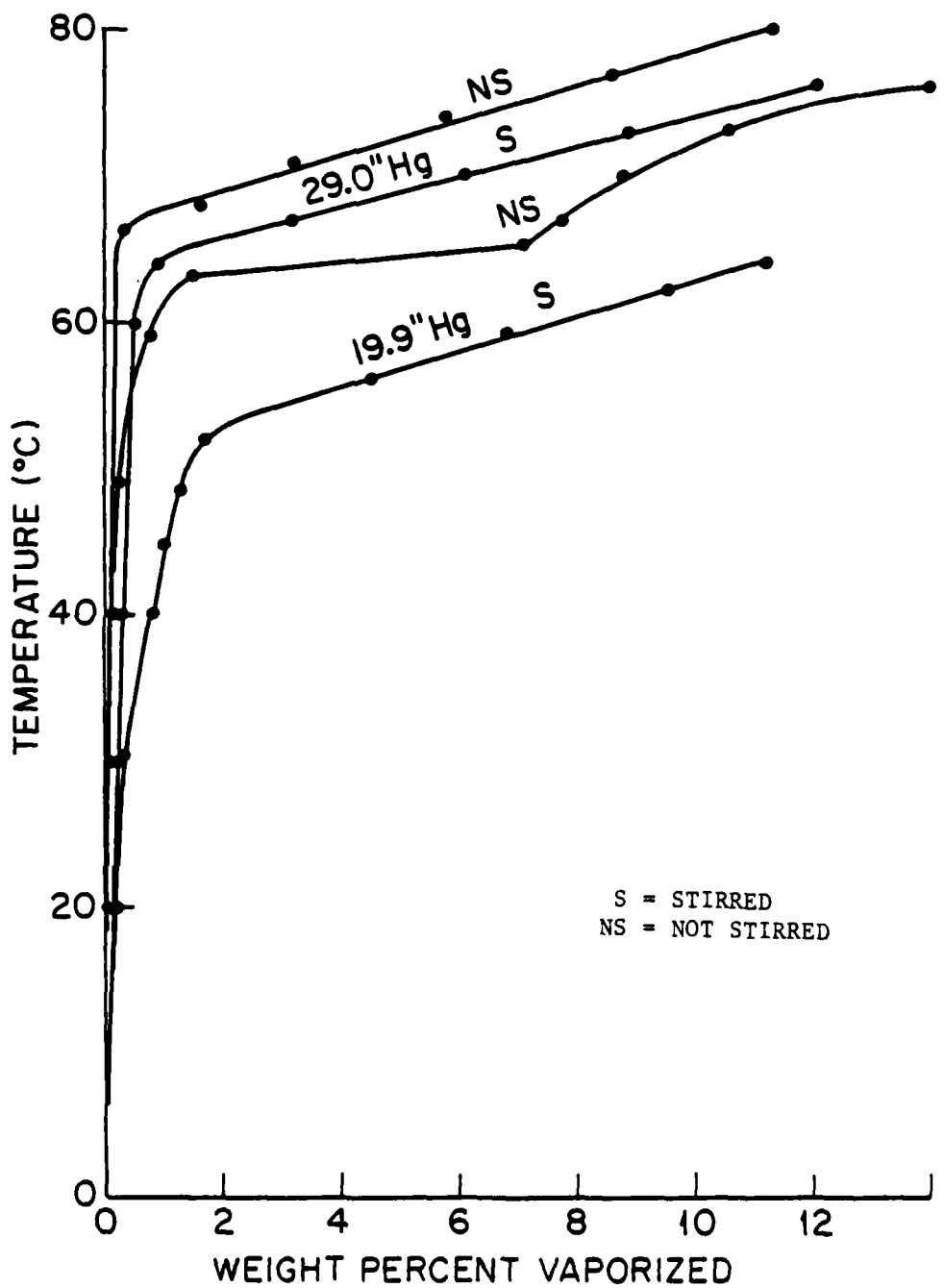


FIGURE 27. WEIGHT PERCENT VAPORIZED VS TEMPERATURE FOR DRY 100 LL.

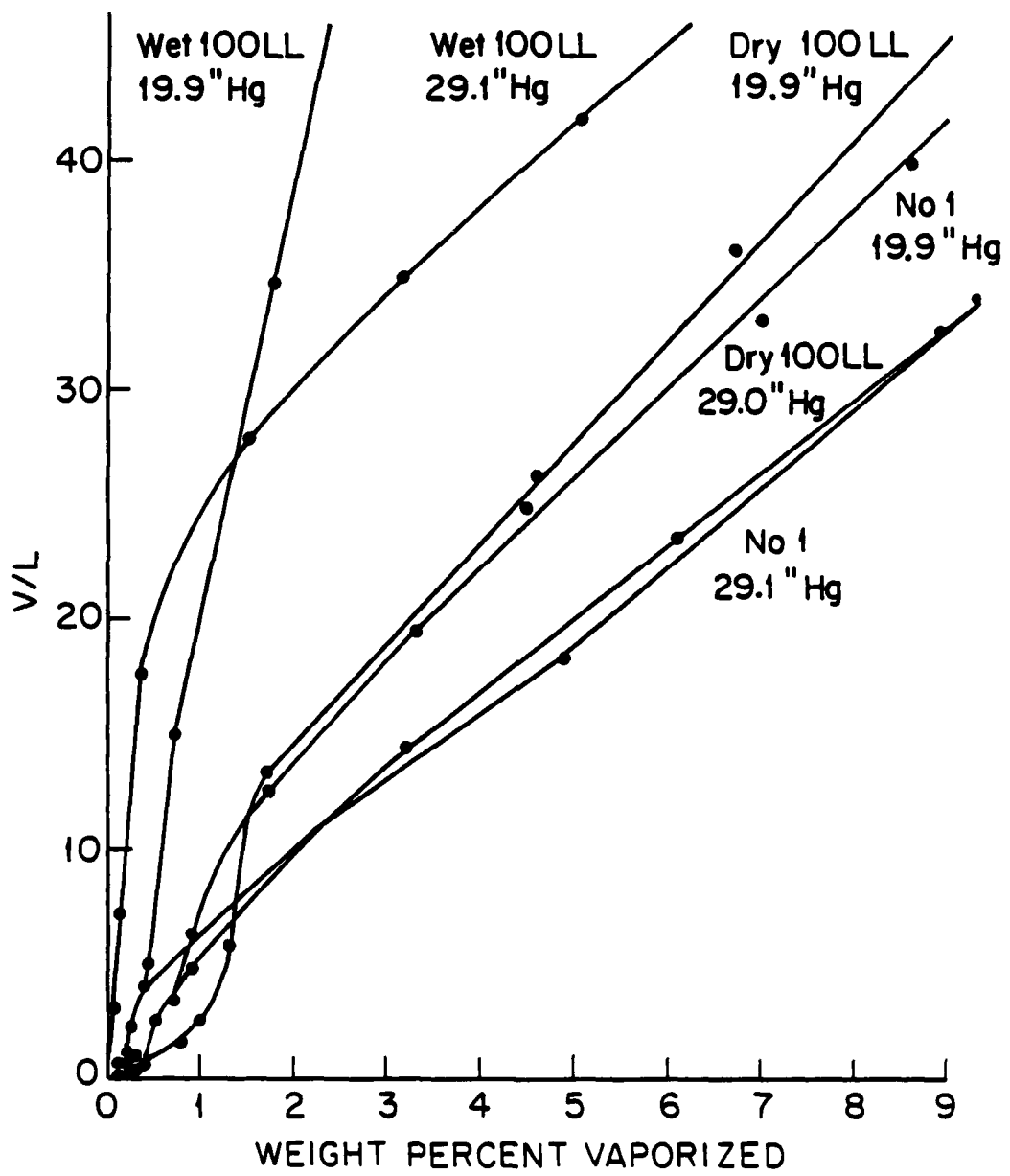


FIGURE 28. VAPOR TO LIQUID RATIO VS WEIGHT PERCENT VAPORIZED

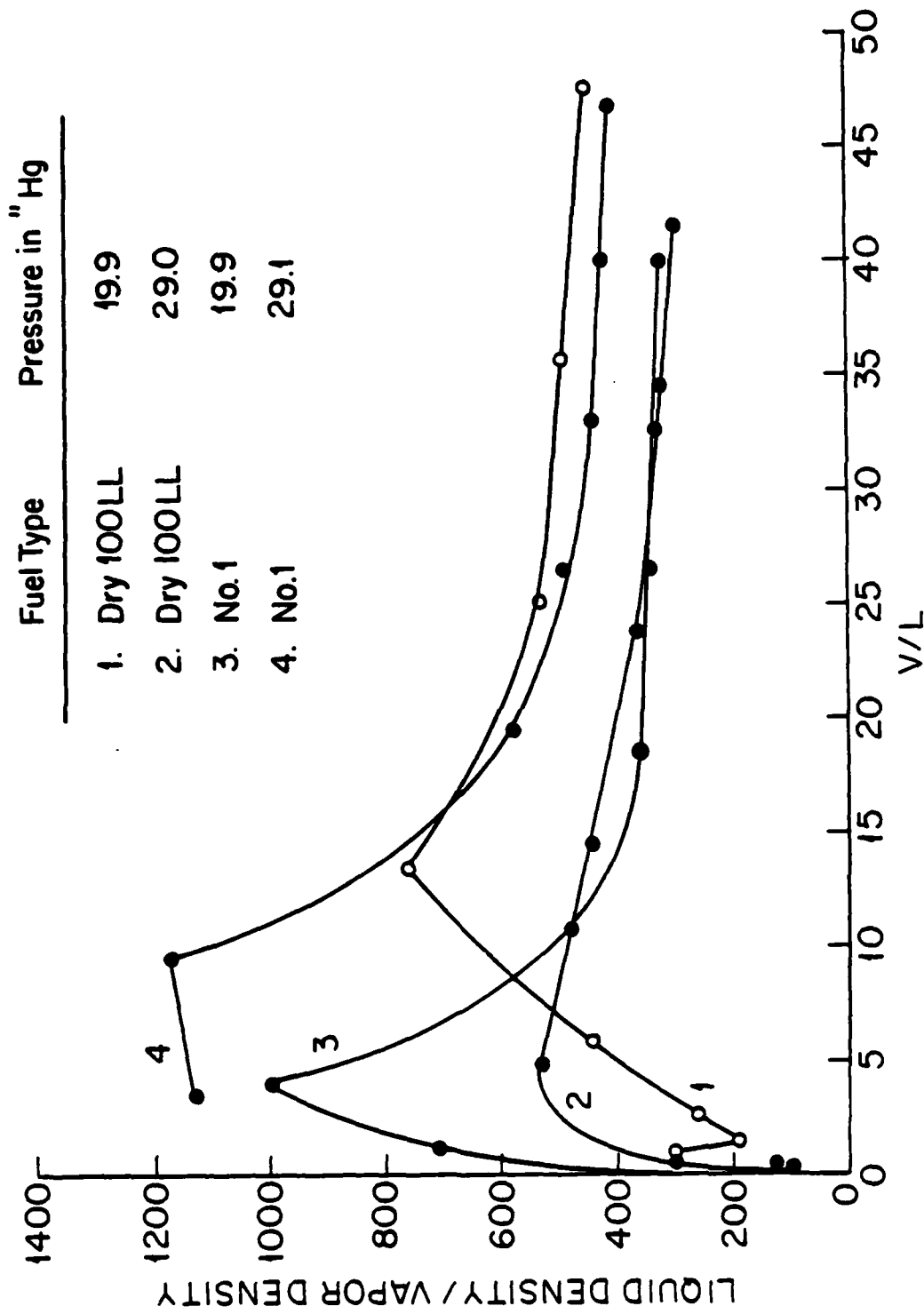


FIGURE 29. DENSITY RATIO BETWEEN LIQUID AND TOTAL VAPOR EVOLVED UP TO DIFFERENT VAPOR TO LIQUID RATIOS - No. 1 fuel and dry 100LL.

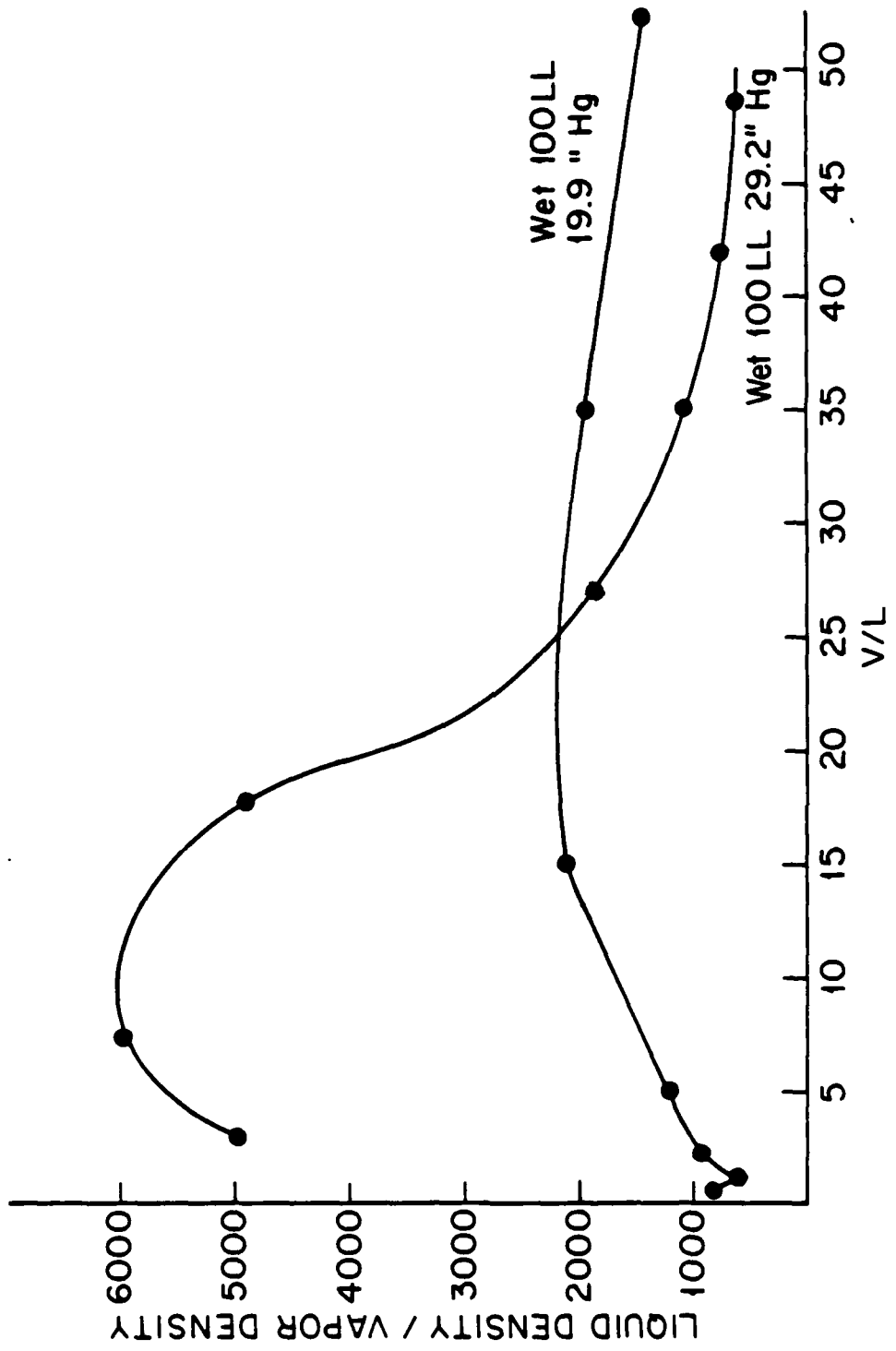


FIGURE 30. DENSITY RATIO BETWEEN LIQUID AND TOTAL VAPOR EVOLVED UP TO DIFFERENT VAPOR TO LIQUID RATIOS - wet 100LL

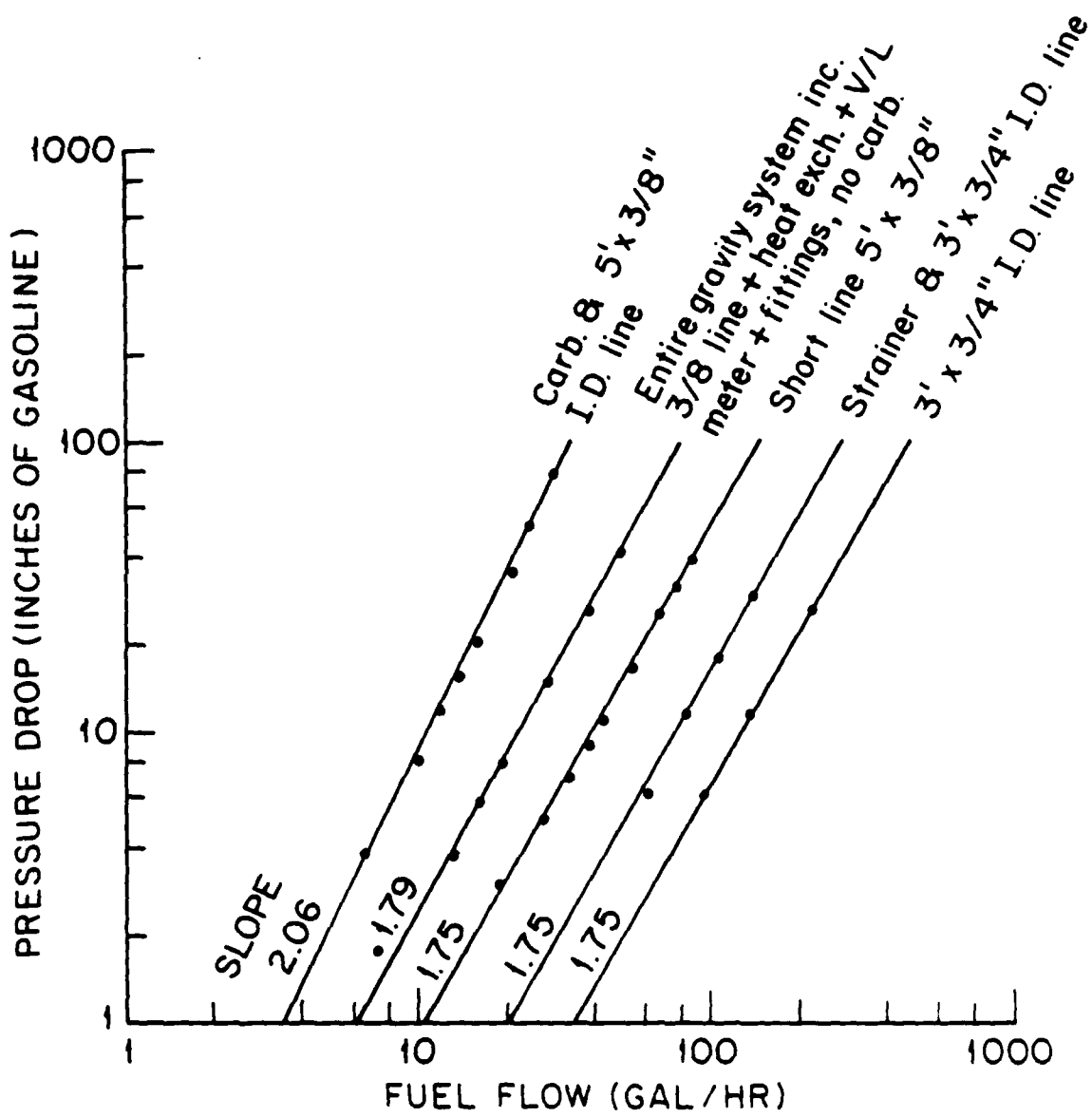


FIGURE 31. MEASURED FLOW CHARACTERISTICS OF GRAVITY FUEL SYSTEM COMPONENTS.

Tested with cold 100LL fuel.

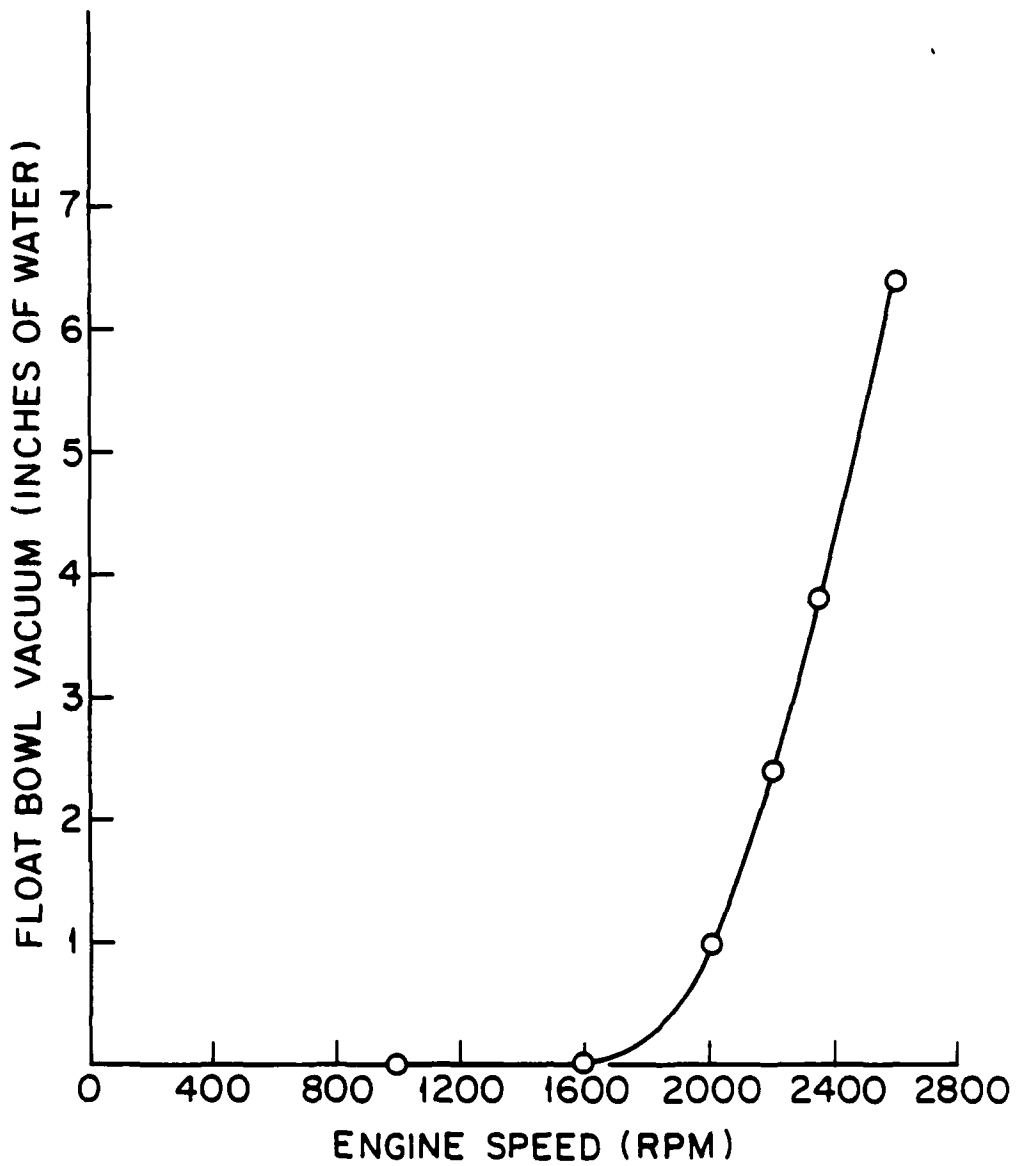


FIGURE 32. FLOAT BOWL VACUUM VS ENGINE SPEED.

No air filter, 3 inch diameter, 8 foot long intake plenum.

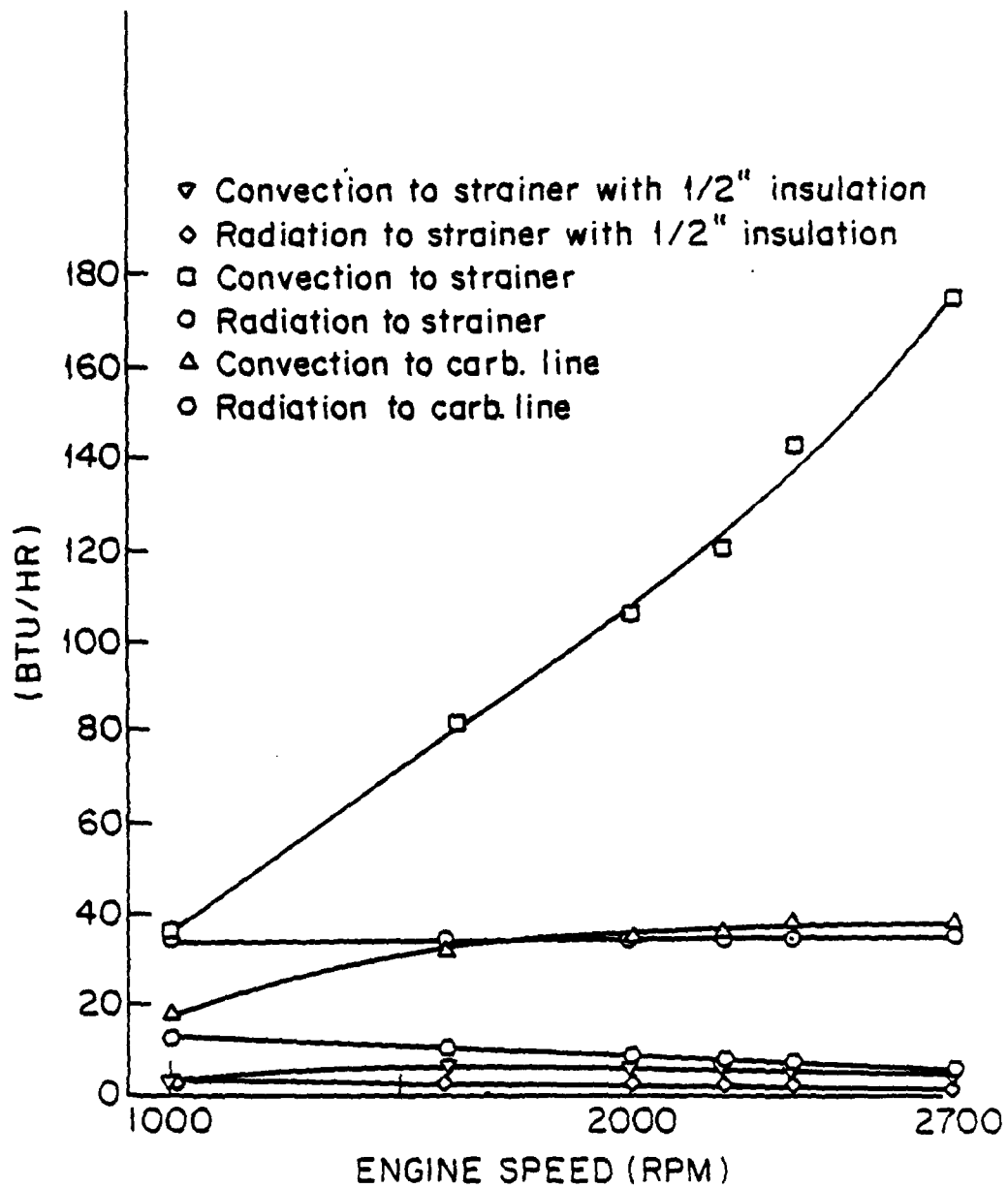


FIGURE 33. CALCULATED RADIANT AND CONVECTIVE HEAT TRANSFER TO STRAINER (BASELINE AND INSULATED) AND CARBURETOR LINE.

Baseline strainer (2-1/4 x 3-1/4 uninsulated), .25 inch inside diameter carburetor line with .15 inch polymeric wall.

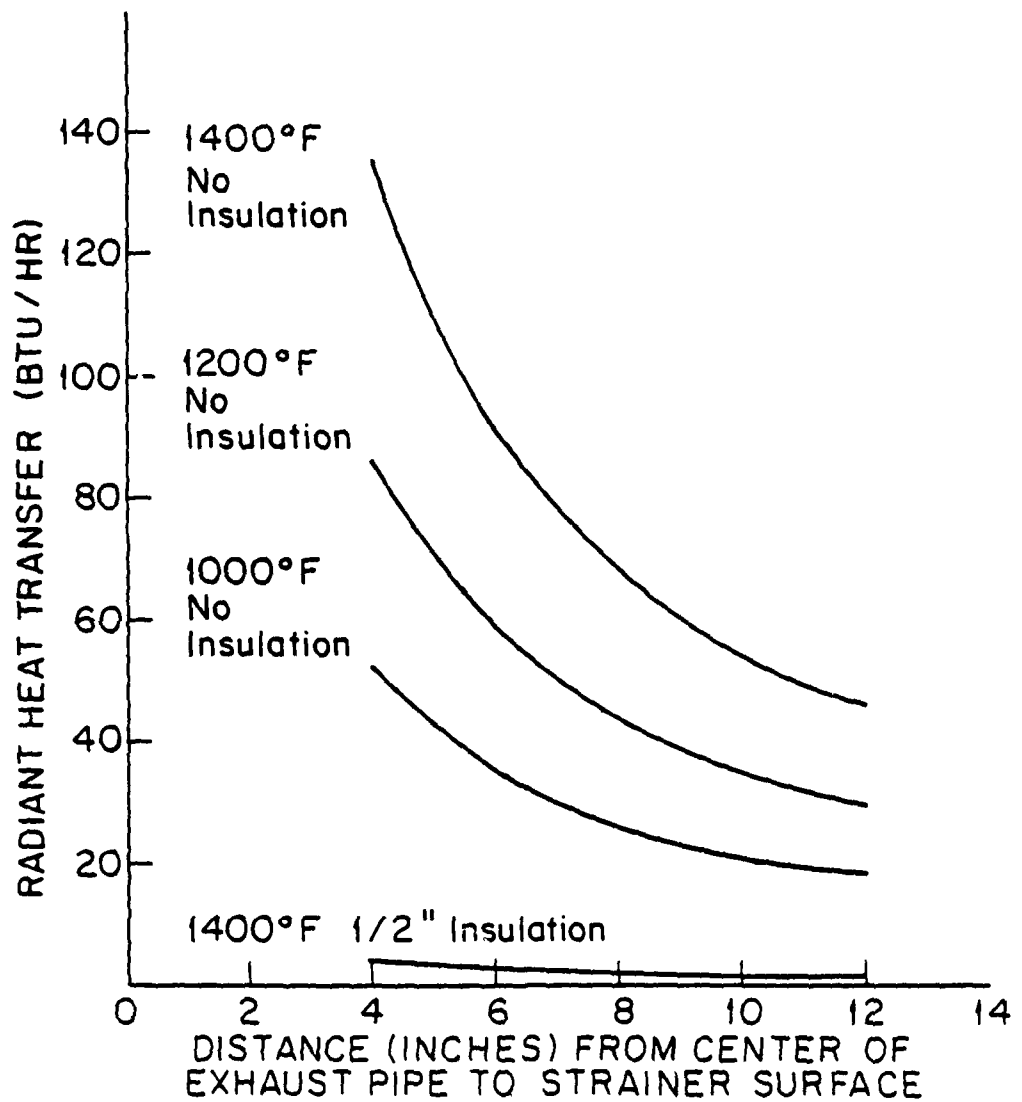


FIGURE 34. CALCULATED RADIANT HEAT TRANSFER TO STRAINER (BASELINE AND INSULATED) VERSUS DISTANCE FROM EXHAUST PIPE FOR VARIOUS SURFACE TEMPERATURES.

2 inch diameter exhaust pipe, 2-1/4 inch diameter by 3-1/4 inch fuel strainer, with uninsulated aluminum surface and covered with 1/2 inch of fiberglass insulation.

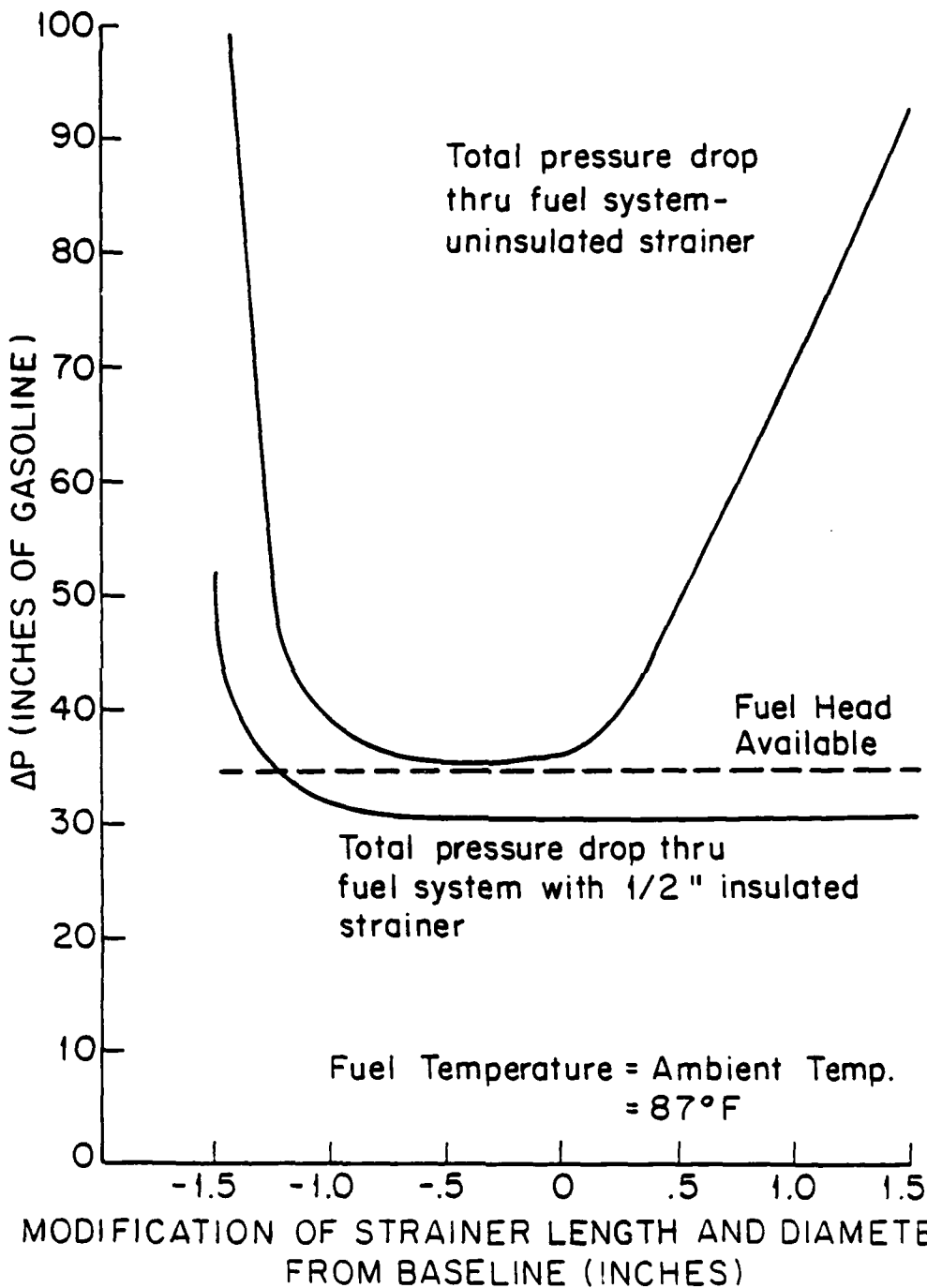


FIGURE 35. EFFECT OF STRAINER SIZE ON FUEL SYSTEM PRESSURE DROP-CALCULATED

Fuel temperature = ambient temperature = 87°F (vapor lock critical temperature for baseline 2700 rpm point), fuel no. 1, no agitation of fuel in tank.

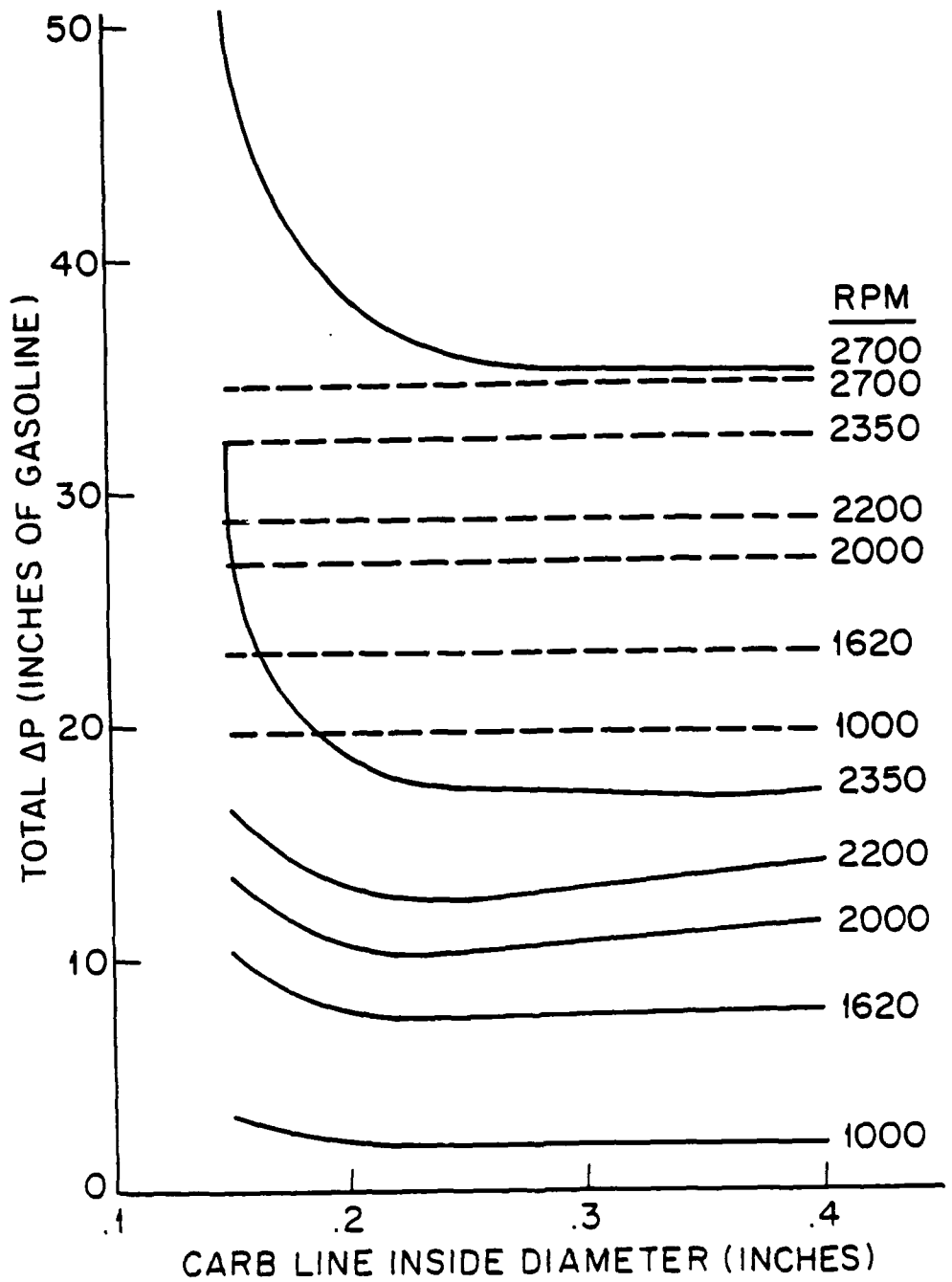


FIGURE 36. EFFECT OF CARBURETOR LINE INSIDE DIAMETER ON TOTAL SYSTEM PRESSURE DROP AND TOTAL PRESSURE HEAD AVAILABLE WITH UNINSULATED STRAINER.

Baseline conditions, .15 inch carburetor line wall thickness of polymeric material. Fuel temperature = ambient temperature = 85°F (critical for 2700 rpm condition), fuel no. 1, no agitation of fuel in tank.

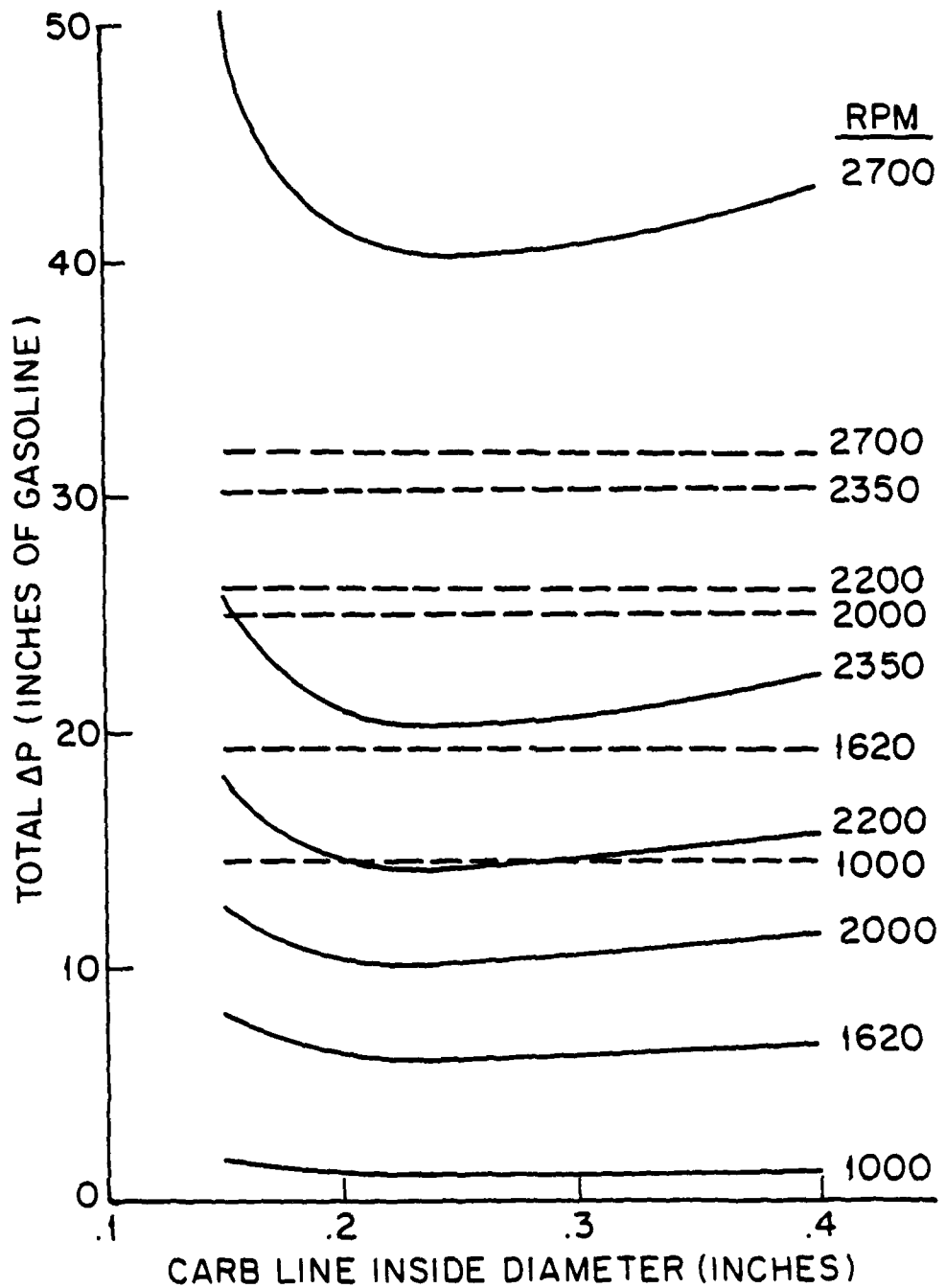


FIGURE 37. EFFECT OF CARBURETOR LINE INSIDE DIAMETER ON TOTAL SYSTEM PRESSURE DROP AND TOTAL PRESSURE HEAD AVAILABLE WITH INSULATED STRAINER.

1/2 inch fiberglass insulated strainer with baseline conditions.
 .15 inch carburetor line wall thickness of polymeric material,
 fuel no. 1, fuel temperature = ambient temperature = 94°F,
 no agitation of fuel in tank.

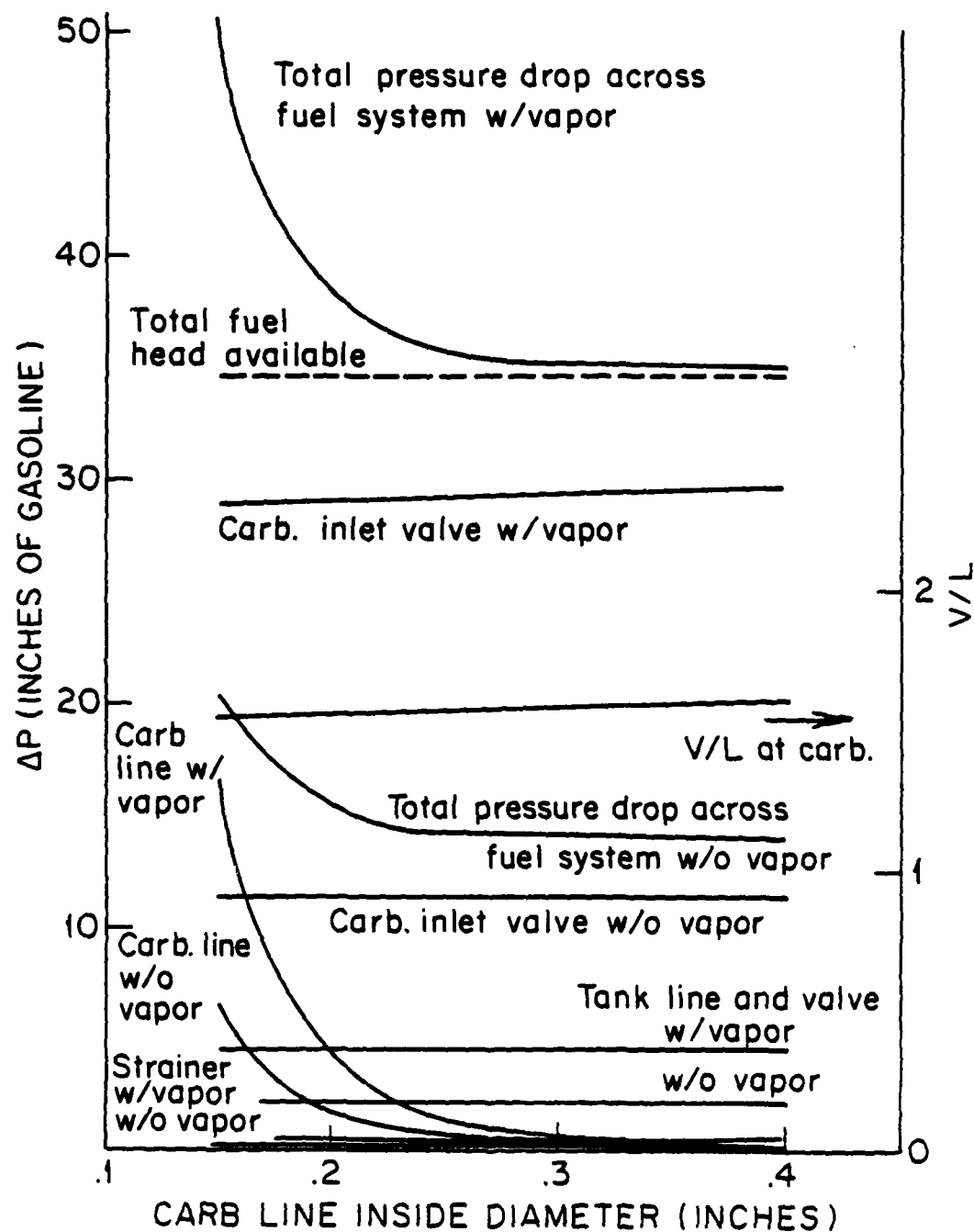
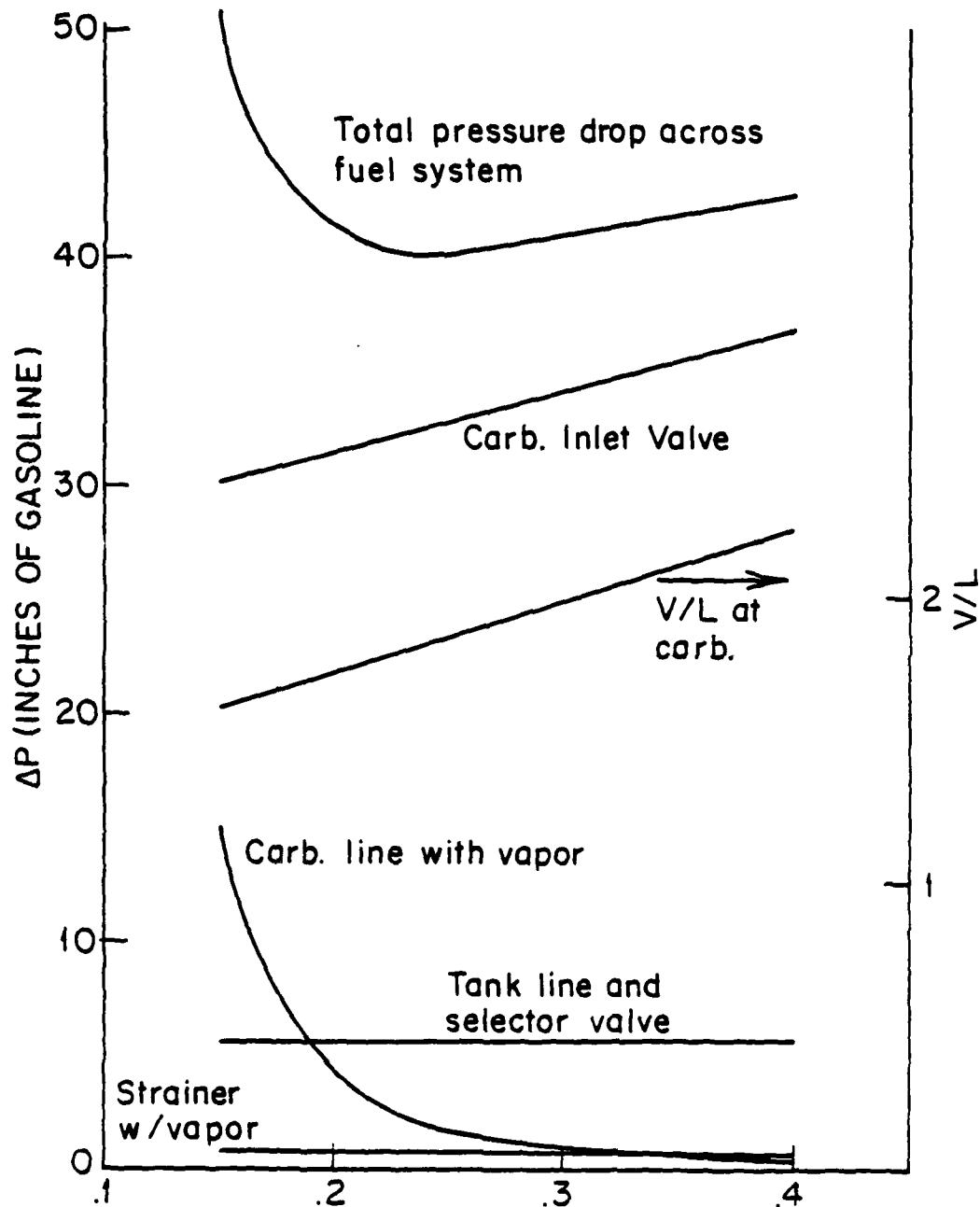


FIGURE 38. SOURCE OF PRESSURE DROPS AS CARBURETOR LINE INSIDE DIAMETER IS CHANGED WITH UNINSULATED STRAINER.

Baseline conditions, .15 inch carburetor line wall thickness of polymeric material, fuel no. 1, fuel temperature = ambient temperature = 85°F, no agitation of fuel in tank (2700 rpm at critical fuel temperature).



CARB LINE INSIDE DIAMETER (INCHES)

FIGURE 39. SOURCE OF PRESSURE DROPS AS CARBURETOR LINE INSIDE DIAMETER IS CHANGED WITH INSULATED STRAINER.

1/2 inch insulated strainer, baseline conditions, .15 inch wall thickness polymeric material, fuel no. 1, fuel temperature = ambient temperature = 94°F, no agitation of fuel in tank (2700 rpm at critical fuel temperature).

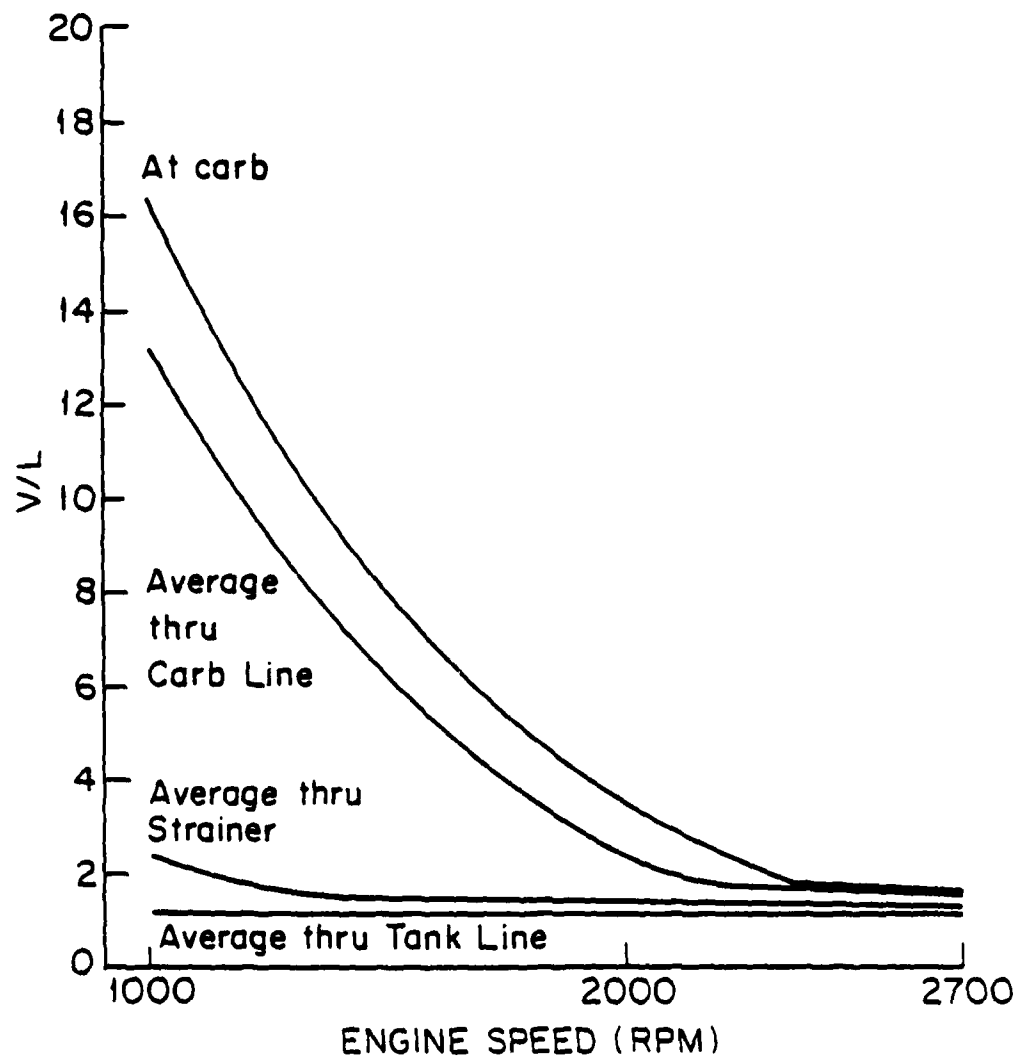


FIGURE 40. VAPOR TO LIQUID RATIOS PRESENT AT VARIOUS PLACES IN FUEL SYSTEM VS ENGINE SPEED WITH UNINSULATED STRAINER.

Baseline conditions, fuel no. 1, fuel temperature = ambient temperature = 85°F (critical for 2700 rpm condition), no agitation of fuel in tank.

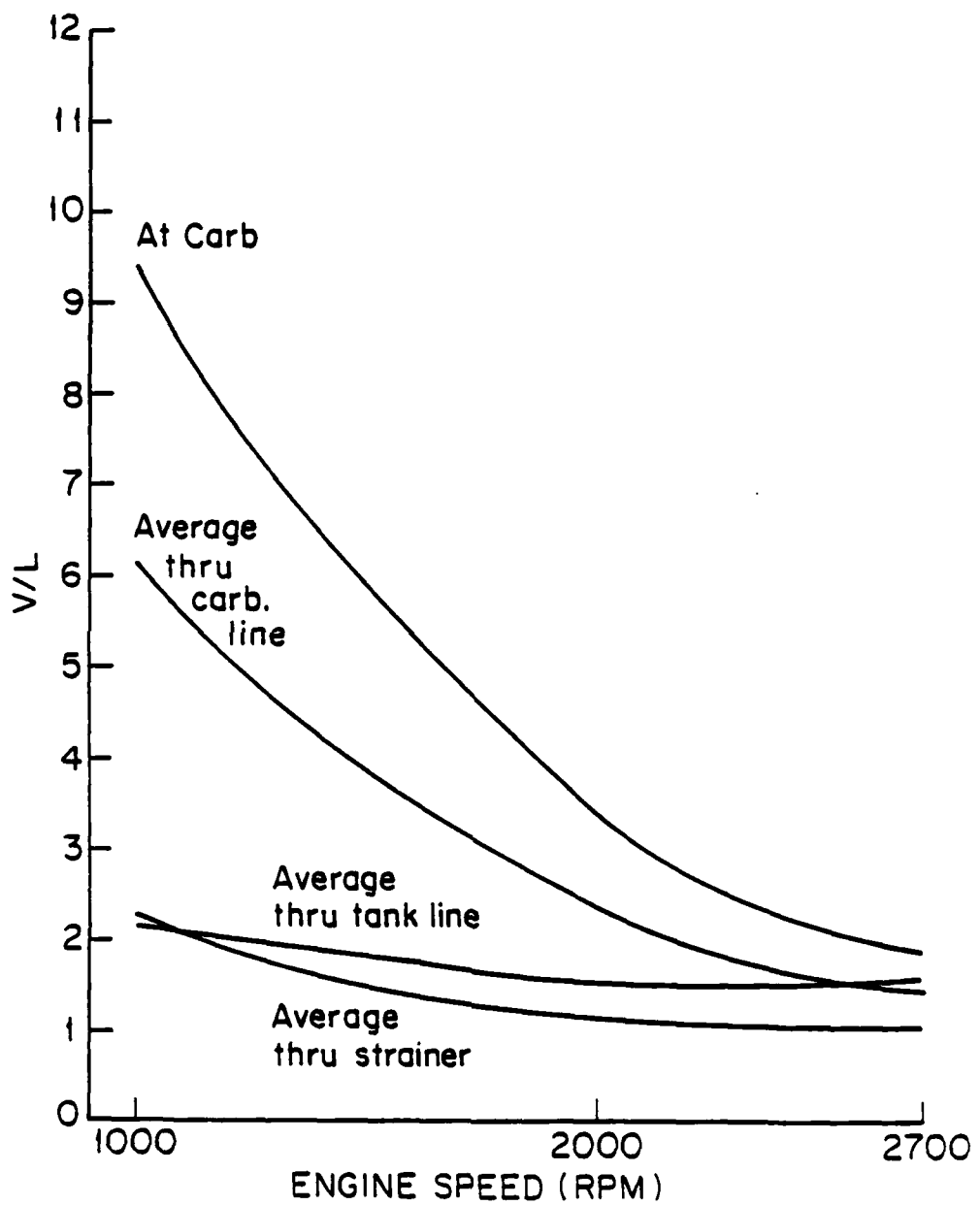


FIGURE 41. VAPOR TO LIQUID RATIOS PRESENT AT VARIOUS PLACES IN FUEL SYSTEM VS ENGINE SPEED WITH INSULATED STRAINER.

1/2 inch insulated strainer, baseline conditions, fuel no. 1, fuel temperature = ambient temperature = 94°F (critical for 2700 rpm condition), no agitation.

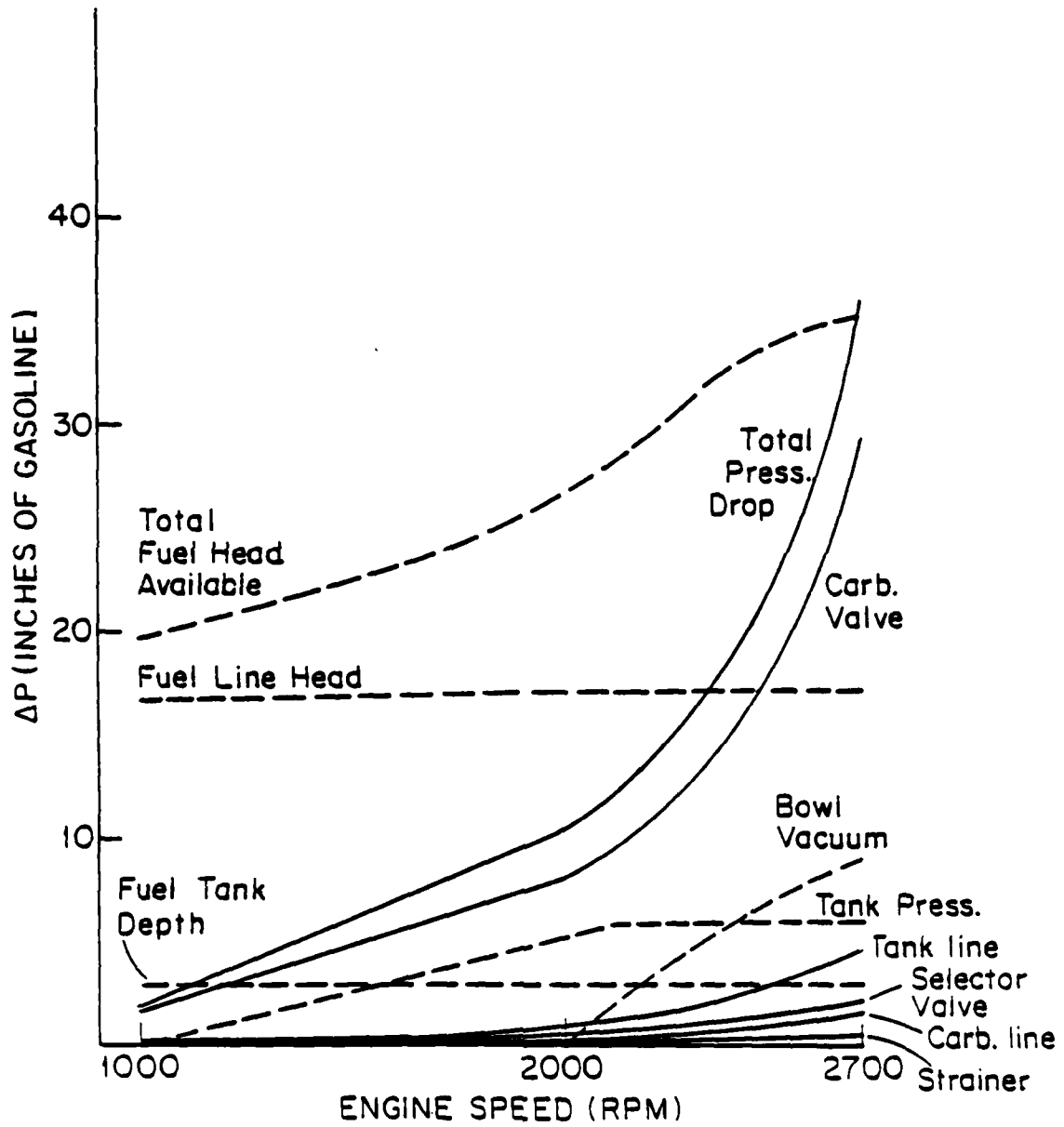


FIGURE 42. BREAKDOWN OF SOURCES OF FUEL HEAD AVAILABLE AND PRESSURE DROPS WITH UNINSULATED STRAINER.

Baseline conditions, fuel no. 1, fuel temperature = ambient temperature = 85°F (critical for 2700 rpm condition) no agitation of fuel in tank.

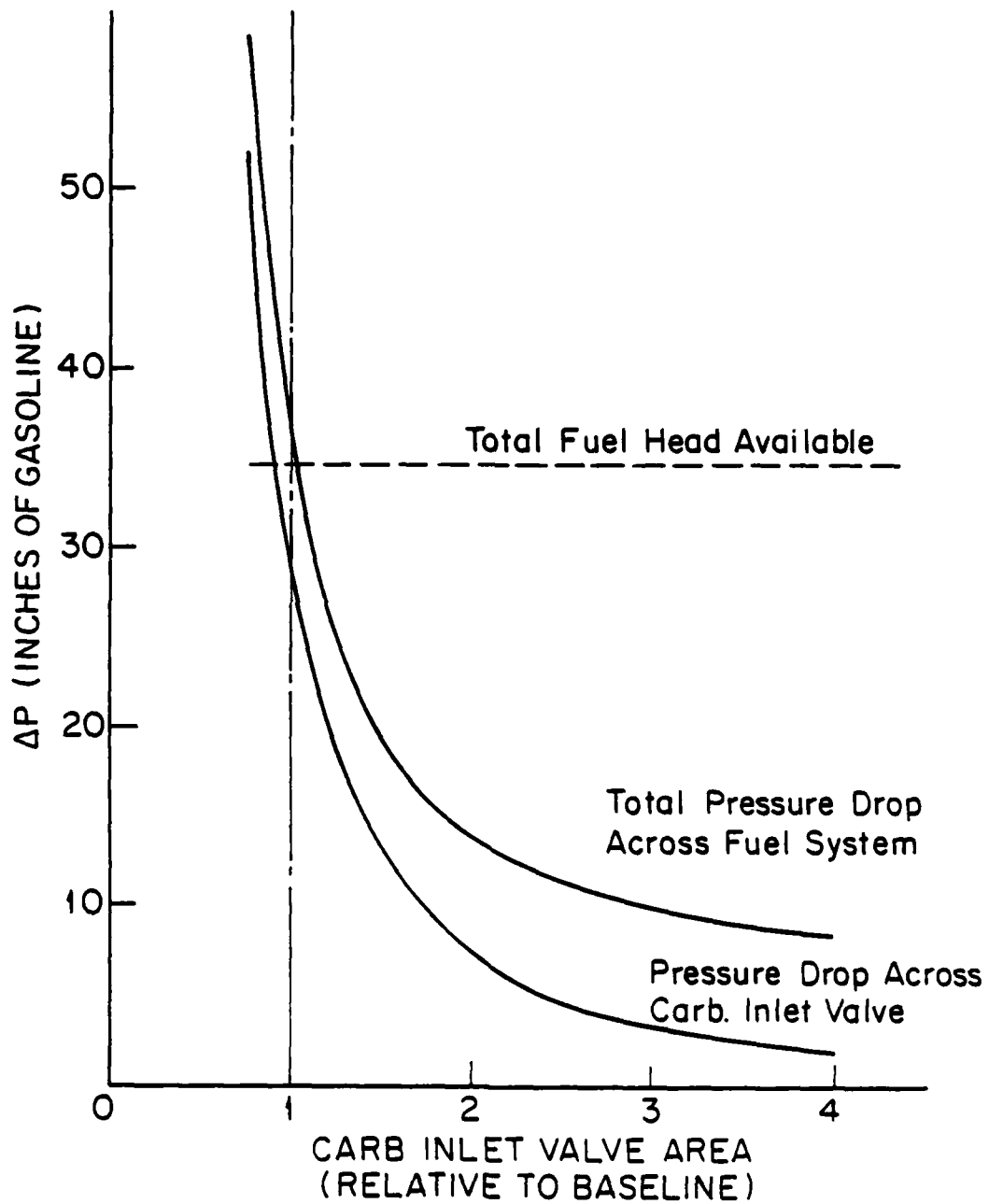


FIGURE 43. EFFECT OF CARBURETOR INLET VALVE AREA ON PRESSURE DROP.

Uninsulated strainer, baseline conditions, fuel no. 1, no agitation, fuel temperature = ambient temperature = 85°F (2700 rpm at critical fuel temperature).

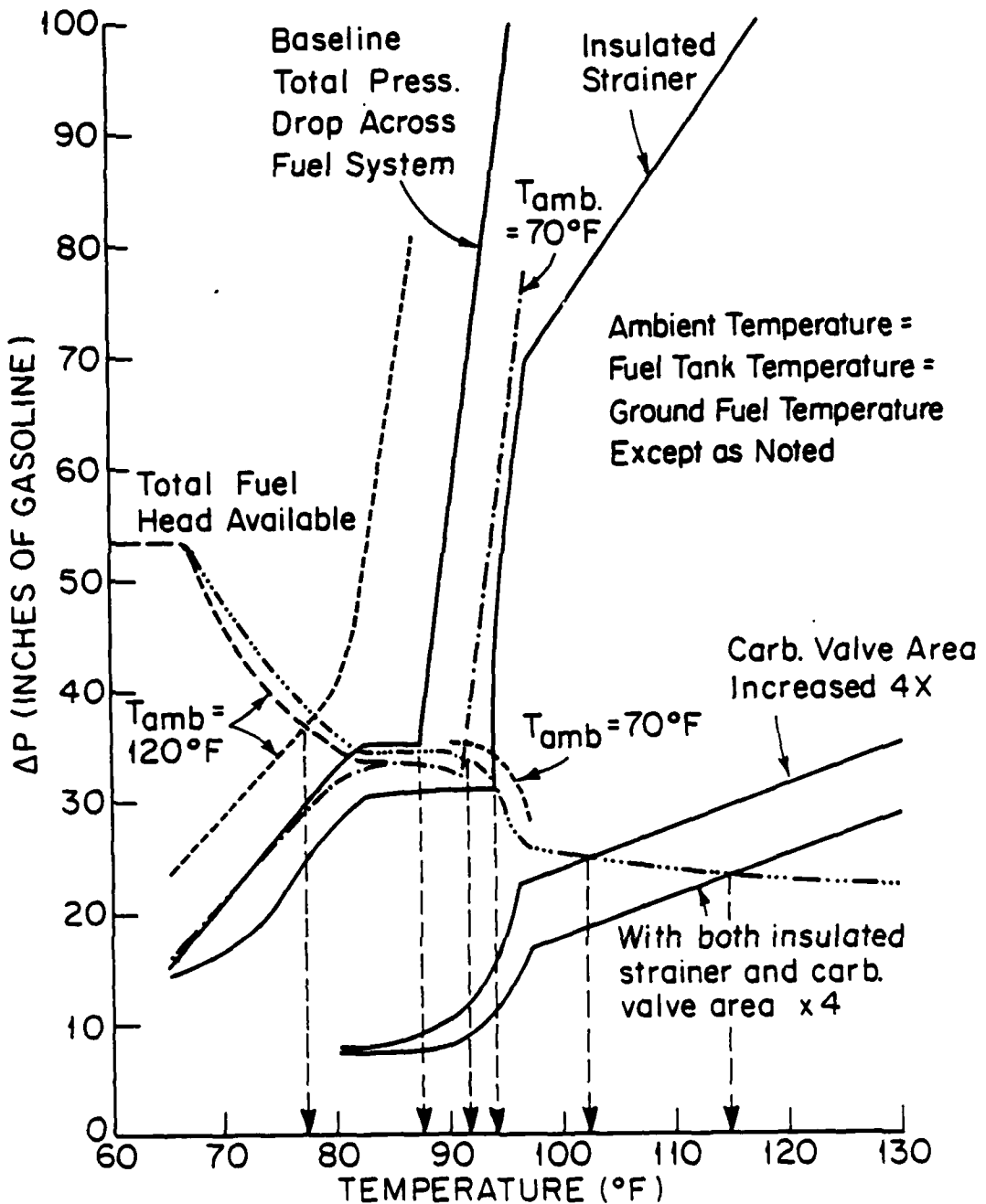


FIGURE 44. EFFECT OF FUEL SYSTEM MODIFICATIONS ON INITIAL FUEL TEMPERATURE PRODUCING VAPOR LOCK.

Fuel no. 1, no agitation of fuel in tank, 2700 rpm.

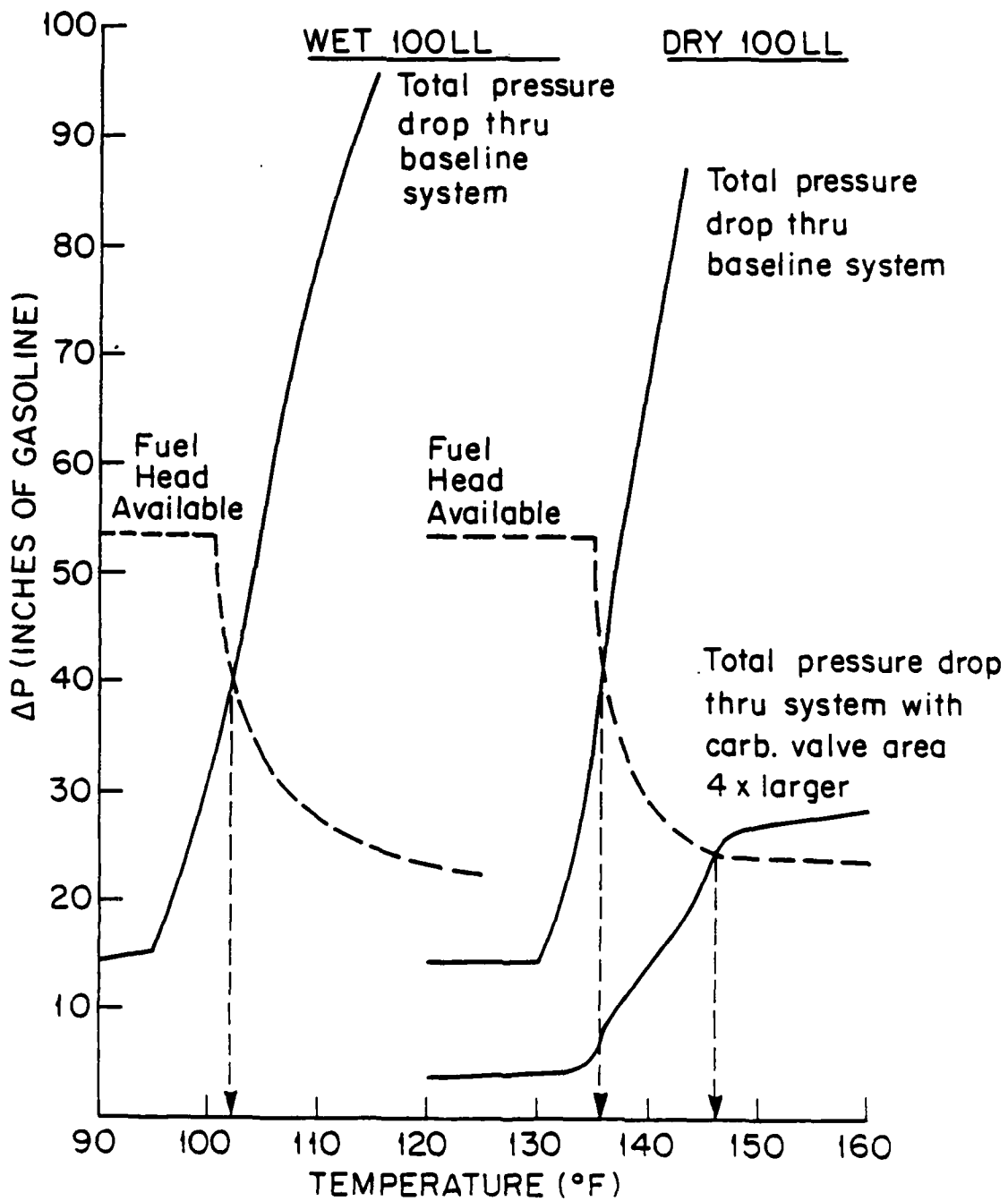


FIGURE 45. EFFECT OF WATER IN 100 LL FUEL AND EFFECT OF CARBURETOR INLET VALVE MODIFICATION ON INITIAL FUEL TEMPERATURE PRODUCING VAPOR LOCK.

No agitation of fuel in tank, 2700 rpm.

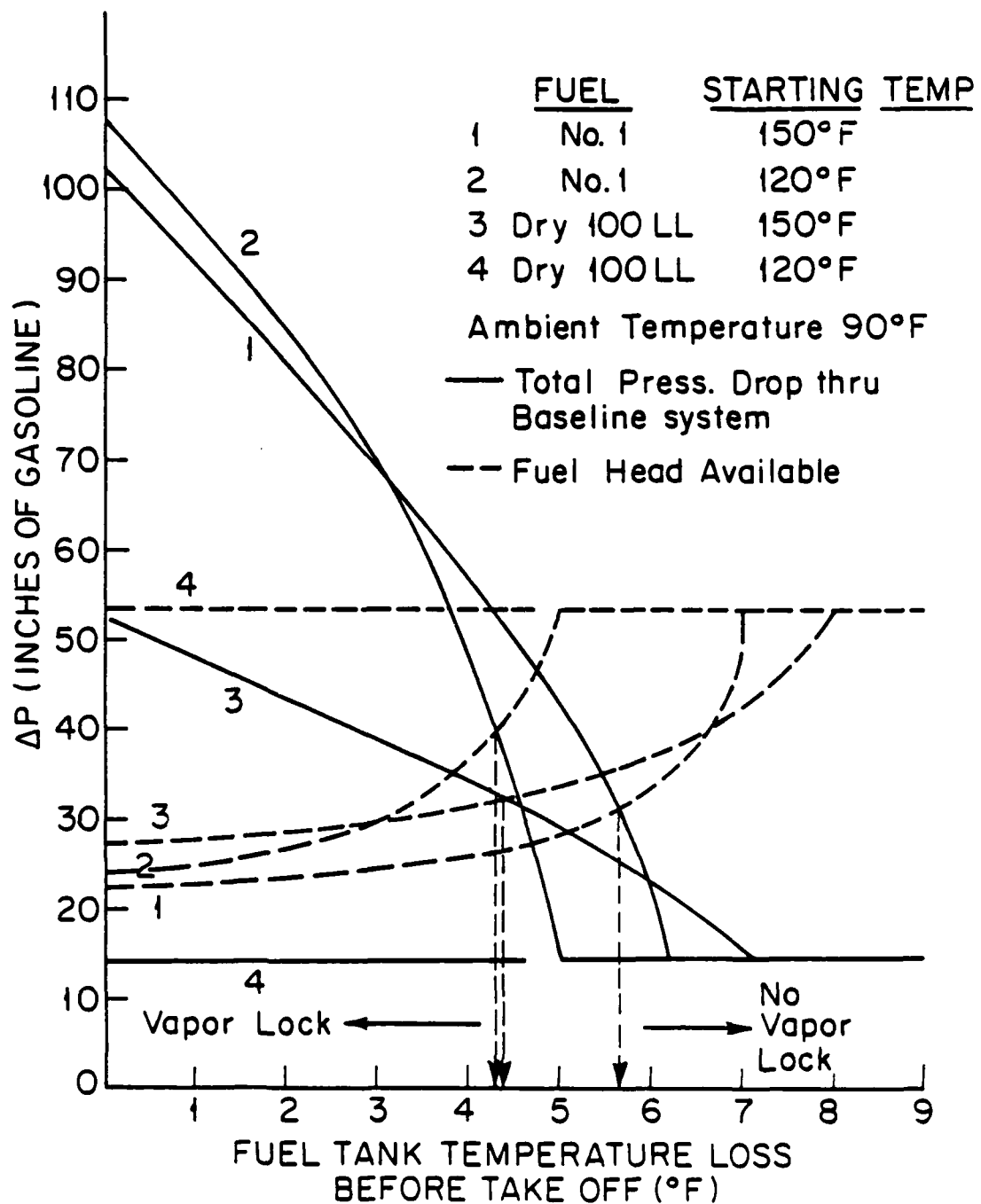


FIGURE 46. EFFECT OF FUEL TANK TEMPERATURE DROP BEFORE HOT FUEL HANDLING TEST.

No agitation of fuel in tank, 2700 rpm.

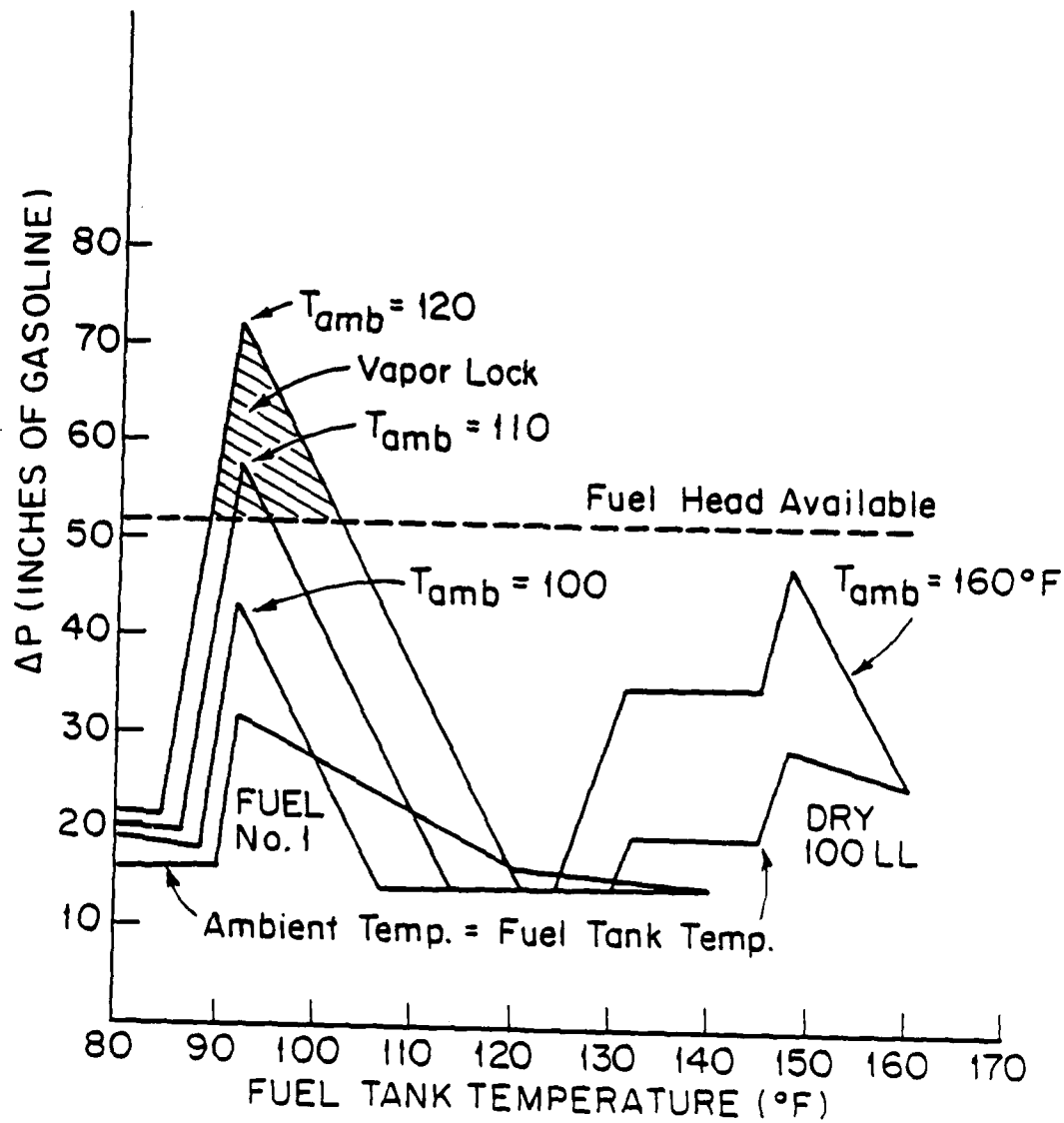


FIGURE 47. EFFECT OF AGITATION OF FUEL IN TANK.

Solid lines represent total pressure drop thru fuel system at various temperatures indicated, 2700 rpm.

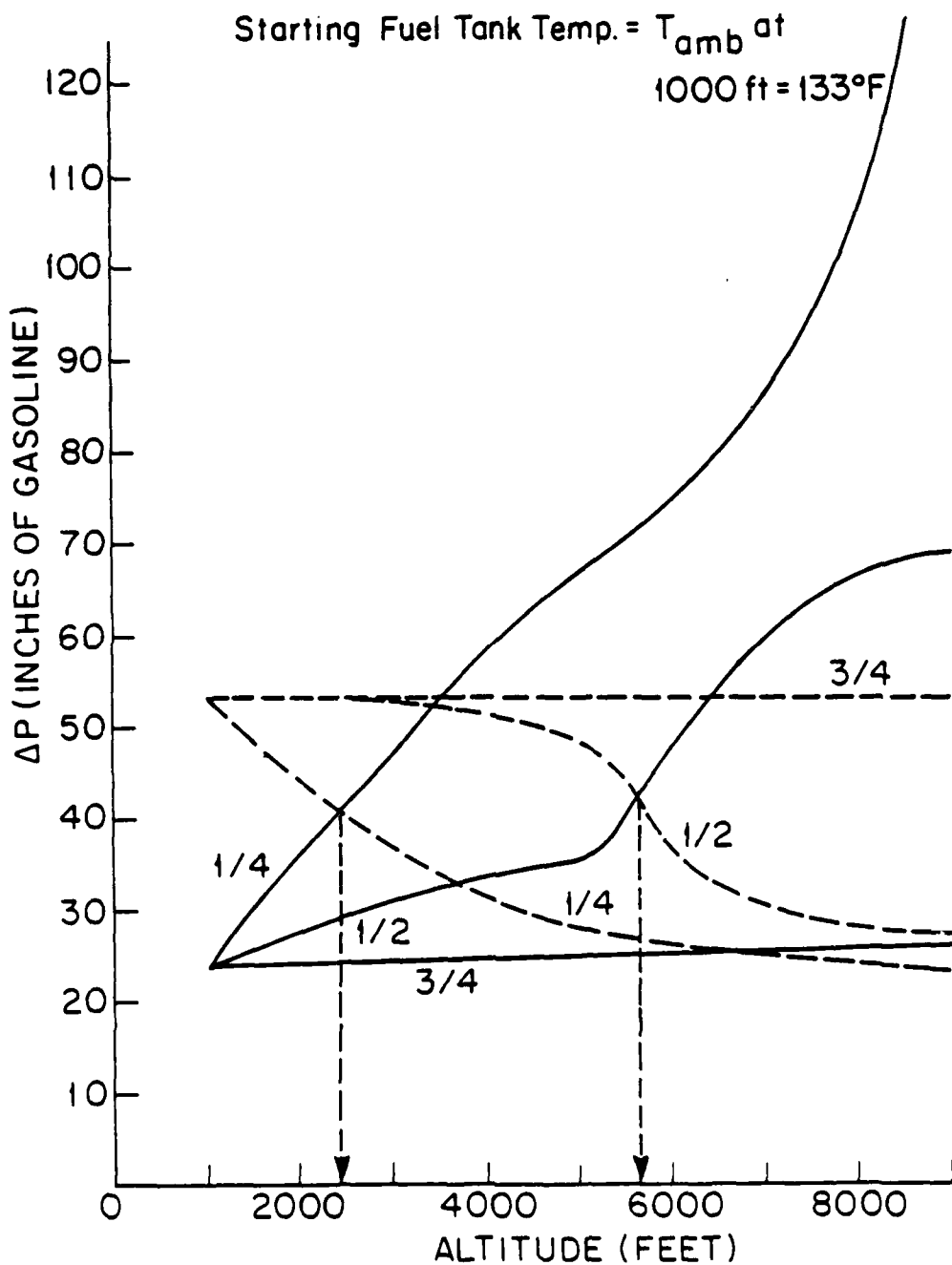


FIGURE 48. EFFECT OF ALTITUDE ON VAPOR LOCK WITH DIFFERENT FUEL TANK COOLING RATES.

Solid lines are total pressure drop thru baseline fuel system, dashed lines are fuel head available, fractions represent rate fuel temperature drops with altitude, divided by the rate which atmospheric temperature drops with altitude (3.5°F/1000 ft., dry 100LL fuel, 2700 rpm).

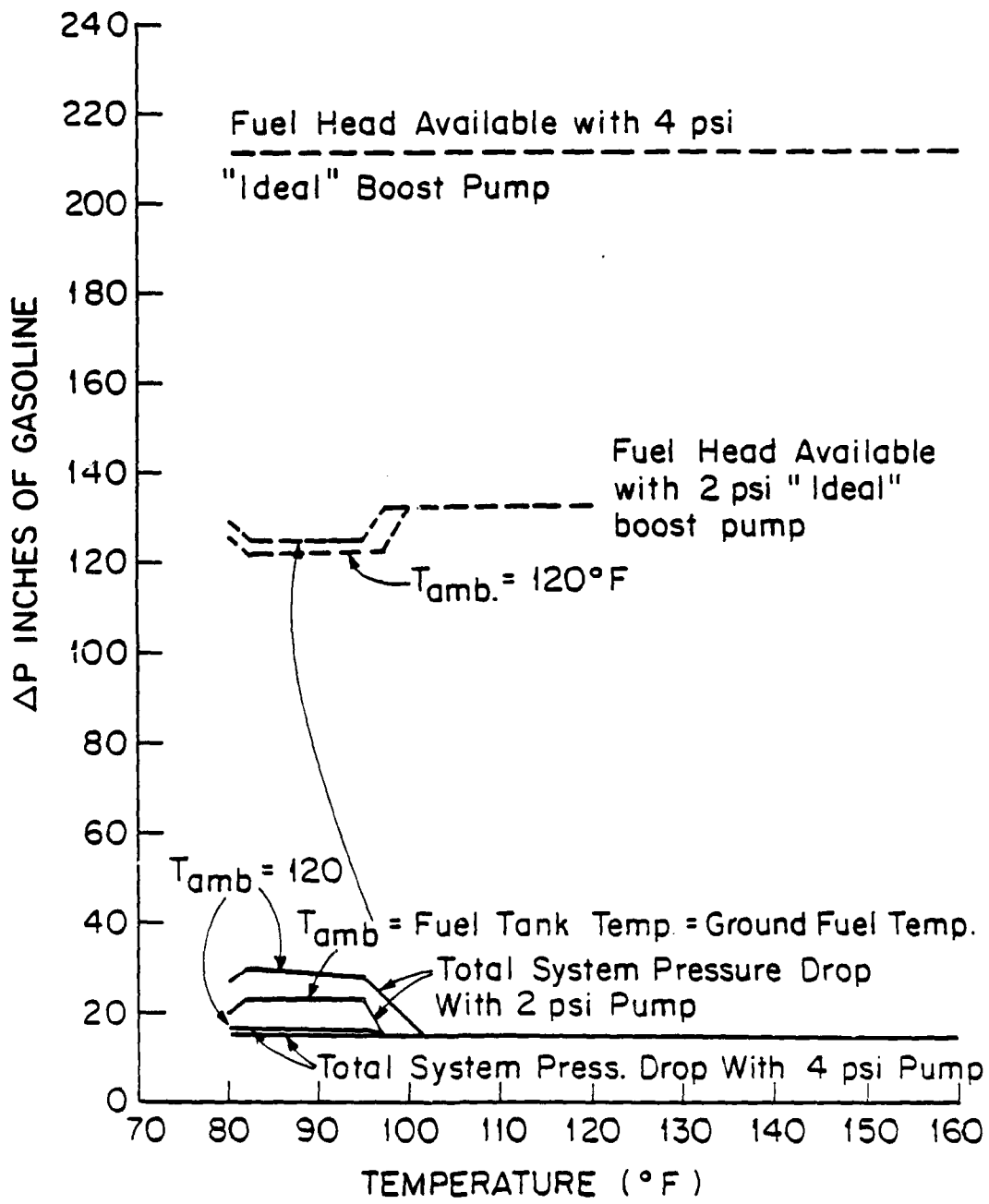


FIGURE 49. EFFECTIVENESS OF "IDEAL" BOOST PUMP.

(Pump submerged in fuel tank which raises fuel pressure entering supply line without generating vapor itself), no. 1 fuel, no agitation of fuel in tank, 2700 rpm.

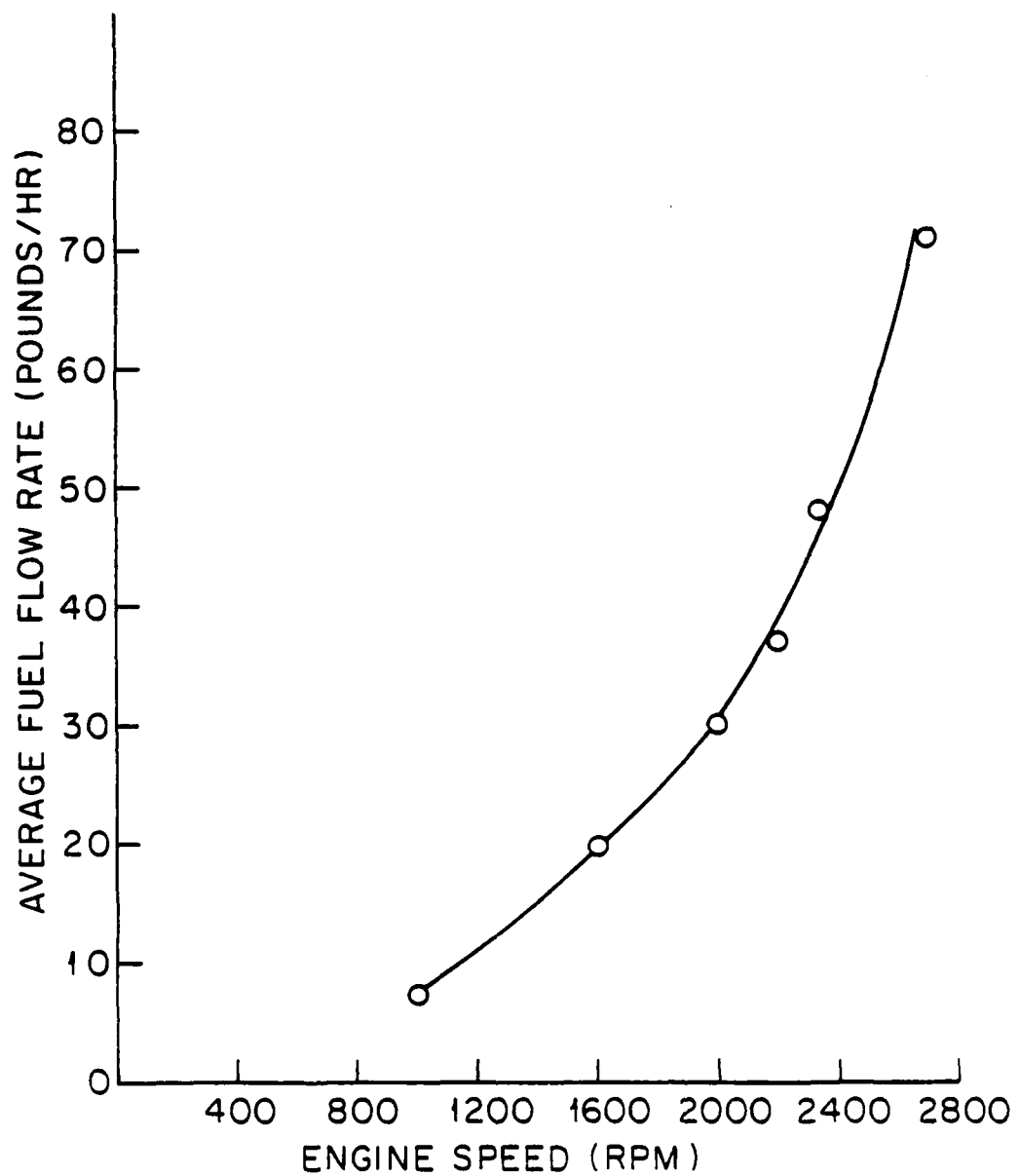


FIGURE 50. MEASURED FUEL CONSUMPTION RATE VS ENGINE SPEED

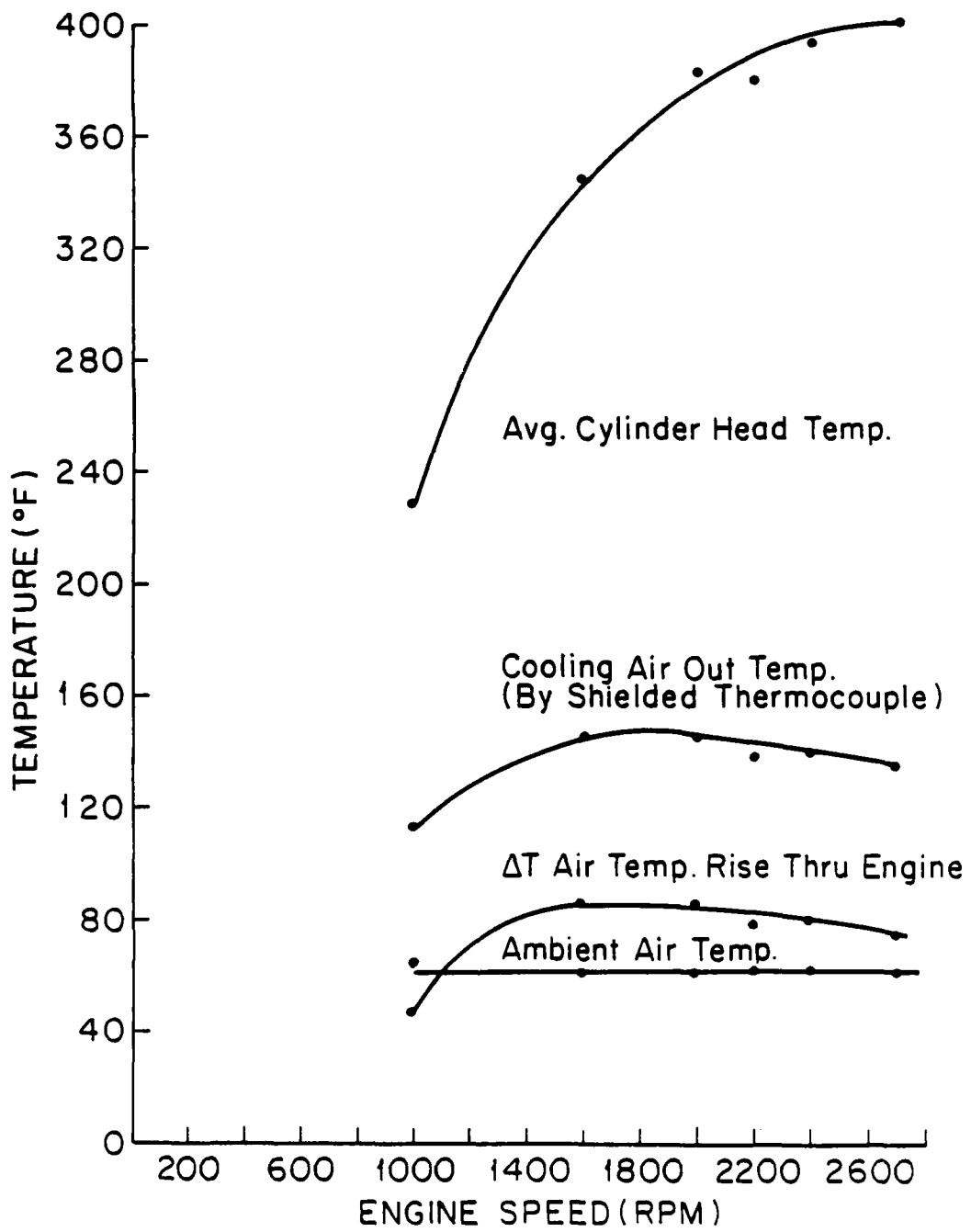


FIGURE 51. MEASURED CYLINDER HEAD AND COOLING AIR TEMPERATURES VS ENGINE SPEED.

APPENDIX B

COMPUTER PROGRAM TO CALCULATE VAPOR TO LIQUID RATIOS FROM FUEL INSPECTION DATA
(ASTM METHOD D439x1.2, reference 7)

```
10 'COMPUTER PROGRAM TO CALCULATE VAPOR TO LIQUID RATIOS FROM
20 'FUEL INSPECTION DATA. (ASTM METHOD D439 XI.2, REFERENCE 7)
30 INPUT"DISTILLATION TEMPERATURE AT 10% EVAPORATED";E
40 INPUT"DISTILLATION TEMPERATURE AT 20% EVAPORATED";F
50 INPUT"DISTILLATION TEMPERATURE AT 50% EVAPORATED";G
60 H=G-E
70 INPUT"RIED VAPOR PRESSURE, PSI";P
80 Q=F-E
90 R=H/Q
100 IF R>6.7 THEN R=6.7
110 A=217.147-16.9527*P+.822909*(P[2]-.0166849*(P[3]+54.0436/P
120 B=-9.66363+.91054*Q-.022326*(Q[2]+.000178314*(Q[3]+.823553/Q
130 S=-.00525449-.0532486/((P-1.4)[2]-.01709/((P-1.4)[2]+.0009677*R-.0000195828*(R[2]
-.0704753*R/(P[2]+.549224*R/(P[4]-.00961619*(R[2]/P+
.000910603*(R[3]/P+.00203879*(R[2]/(P[2]
140 C=4.245*P+1.0/S
150 D=1.1246-1.24135*R+.238875*(R[2]-.012675*(R[3]+10.5273/R
160 M7=A+B
170 T45=F+.125*H+C
180 U10=M7+.146341*(T45-M7)+D
190 N20=M7+.390244*(T45-M7)+1.46519*D
200 W30=M7+.634146*(T45-M7)+D
210 'NOTE: M7, U10, N20, W30, T45 ARE ESTIMATED TEMPERATURES
220 'AT V/L RATIOS 4, 10, 20, 30, 45
230 PRINT"TEMPERATURE (DEG F) = ";M7;" AT V/L = 4"
240 PRINT"TEMPERATURE (DEG F) = ";U10;" AT V/L = 10"
250 PRINT"TEMPERATURE (DEG F) = ";N20;" AT V/L = 20"
260 PRINT"TEMPERATURE (DEG F) = ";W30;" AT V/L = 30"
270 PRINT"TEMPERATURE (DEG F) = ";T45;" AT V/L = 45"
280 LPRINT" FUEL VAPOR PRESSURE = ";P
290 LPRINT" TEMPERATURE (DEG F) = ";M7;" AT V/L = 4"
300 LPRINT" TEMPERATURE (DEG F) = ";U10;" AT V/L = 10"
310 LPRINT" TEMPERATURE (DEG F) = ";N20;" AT V/L = 20"
320 LPRINT" TEMPERATURE (DEG F) = ";W30;" AT V/L = 30"
330 LPRINT" TEMPERATURE (DEG F) = ";T45;" AT V/L = 45"
```

APPENDIX C
VAPOR LOCK ANALYSIS COMPUTER PROGRAM

```

10 'COMPUTER PROGRAM FOR VAPOR LOCK ANALYSIS OF AIRCRAFT FUEL SYSTEM
20 '
30 INPUT "FUEL TYPE, 1 FOR #1, 100 FOR DRY 100LL, 200 FOR WET 100LL";FUEL
40 INPUT "GROUND ALTITUDE OF AIRPORT IN FT (1 TO 10000)";GA
50 INPUT "ALTITUDE OF AIRCRAFT IN FT (1 TO 10000)";AL
60 INPUT "AIRSPEED IN KNOTS";AR
70 INPUT "FUEL FLOW RATE IN POUNDS PER HOUR";M
80 INPUT "AIR TEMP RISE ABOVE AMBIENT, ACROSS ENGINE IN DEG F";TA
90 INPUT "MAXIMUM TEMPERATURE FUEL IN TANK HAS EXPERIENCED";TG
100 INPUT "HAS FUEL IN TANK BEEN AGITATED WHILE AT THIS TEMPERATURE, Y OR N";AS
110 INPUT "FUEL TANK TEMPERATURE AT ALTITUDE IN DEG F";TF
120 INPUT "AMBIENT TEMPERATURE IN DEG F";TB
130 INPUT "MEAN CROSS SECTIONAL AIRFLOW AREA OVER FUEL SYSTEM PARTS IN SQ FT";MA
140 INPUT "THERMAL CONDUCTIVITY OF CARB LINE, K FOR FIBER GLASS = .02, POLYMERIC
        MATERIAL (RUBBER) = .08, ALUMINUM = 130, BTU/HR/SQ FT/DEG F ";K
150 INPUT "DISTANCE FROM EXHAUST PIPE TO FUEL LINE IN INCHES";EF
160 INPUT "DISTANCE FROM EXAUST PIPE TO STRAINER IN INCHES";ES
170 INPUT "DIAMETER OF EXHAUST PIPE IN INCHES";ED
180 INPUT "EXHAUST PIPE SURFACE TEMPERATURE IN DEG F";EP
190 INPUT "SPECIFIC GRAVITY OF FUEL";SG
200 INPUT "STRAINER THERMAL CONDUCTIVITY";SK
210 INPUT "STRAINER WALL THICKNESS IN INCHES";WT
220 INPUT "BASELINE STRAINER DIAMETER IN INCHES";BD
230 INPUT "BASELINE STRAINER LENGTH IN INCHES";BL
240 INPUT "NEW STRAINER DIAMETER IN INCHES";SD
250 INPUT "NEW STRAINER LENGTH IN INCHES";LS
260 INPUT "CARB LINE INSIDE DIAMETER IN INCHES";T
270 INPUT "CARB LINE WALL THICKNESS IN INCHES";W
280 INPUT "CARB LINE LENGTH IN FEET";LG
290 INPUT "NUMBER OF FUEL TANKS TURNED ON";NT
300 INPUT "TANK LINE LENGTH(S) FROM TANK TO SELECTOR VALVE, IN FT";LK
310 INPUT "LINE LENGTH FROM SELECTOR VALVE TO STRAINER IN INCHES";LV
320 INPUT "BASELINE TANK LINE OUTSIDE DIAMETER IN INCHES";KD
330 INPUT "NEW TANK LINE OUTSIDE DIAMETER IN INCHES";ND
340 INPUT "TANK LINE WALL THICKNESS";KW
350 INPUT "FUEL TANK DEPTH IN INCHES FROM FUEL SURFACE TO OUTLET POINT";FD
360 INPUT "FLOW RATE FOUND BY BREAKING FUEL SUPPLY LINE BEFORE STRAINER, GAL/HR";KQ
370 INPUT "FUEL HEAD FROM TANK LIQUID LEVEL TO BREAK LEVEL IN INCHES";KH
380 INPUT "FLOW RATE BY BREAKING LINE AFTER STRAINER, GAL/HR";SQ
390 INPUT "FUEL HEAD, TANK LEVEL TO STRAINER OUTLET, IN INCHES";SH
400 INPUT "FLOW RATE THRU CARB INLET VALVE AFTER REMOVING CARB BOWL, GAL/HR";CQ
410 INPUT "FUEL HEAD, TANK LEVEL TO CARB INLET VALVE SEAT, IN INCHES";CH
420 INPUT "CARB FLOAT NEEDLE VALVE FLOW AREA, ABOVE 1 IS LARGER THAN STANDARD, LESS
        THAN 1 IS SMALLER";CF
430 INPUT "CARB BOWL VACUUM IN INCHES OF WATER";BV
440 INPUT "TOTAL RISER HIGHTS IN INCHES, (DISTANCE FROM TOP OF ISOLATED HIGH SPOTS
        TO NEXT LOWER LEVEL, MULTIPLE RISERS ARE ADDITIVE)";RH
450 REM *** CALCULATION OF VOLUME FUEL FLOW RATE IN GAL/HR
460 Q=M/(8.3*SG)
470 REM *** CALCULATION OF FUEL TANK PRESSURE DUE TO VENT RAM PRESSURE,
480 REM 1/2 RO V SQUARE, IN INCHES OF GASOLINE
490 TP=.000458/SG*AR[2
500 REM *** PRESSURE HEAD DUE TO CARB BOWL VACUUM
510 BH=BV/SG

```

```

520 REM *** EXHAUST PIPE RADIUS, DIAMETER/2
530 ER=ED/2
540 REM *** ABSOLUTE EXHAUST PIPE SURFACE TEMP IN DEG R
550 ET=EP+460
560 REM *** STRAINER TO CARB LINE INSIDE DIAMETER IN FT
570 D1=T/12
580 REM *** OUTSIDE RADIUS OF CARB LINE IN FT
590 R2=(T/2+W)/12
600 REM *** INSIDE DIAMETER OF STRAINER IN INCHES
610 S2=(SD/2-W)*2
620 REM *** STRAINER OUTSIDE DIAMETER IN FT
630 D2=SD/12
640 REM *** STRAINER INSIDE RADIUS IN FT
650 RI=S2/2/12
660 REM *** FUEL FLOW VELOCITY THRU CARB LINE IN FT/SEC
670 FV=Q/3600*4/3.14/D1[2/7.48
680 REM *** FUEL DENSITY IN LB/CUBIC FT
690 RO=SG*62.4
700 REM *** GASOLINE VISCOSITY IN ENGLISH UNITS (CENTIPOISES * .000672)
710 U=.34*.000672
720 REM *** PRESSURE DROP THRU CARB LINE IN PSI, BY PIGOTT'S EQUATION
730 DP=3.417E-5*U[.25*LG*RO[.75*FV[1.75/D1[1.25
740 REM *** CONVERSION FROM PSI PRESS DROP TO INCHES OF GASOLINE HEAD
750 DP=DP*27.7/SG
760 REM *** REYNOLDS NUMBER OF FLOW THRU CARB LINE
770 RE=D1*FV*RO/U
780 REM *** AVERAGE AIR VELOCITY OVER FUEL SYSTEM PARTS IN FT/MIN
790 REM BASED ON VOLUME FLOW OF AIR (RAISED IN TEMPERATURE TO MEASURED
800 REM DELTA T, DELTA T = AMBIENT TEMP - COOLING AIR OUT TEMPERATURE)
810 REM REQUIRED TO CARRY AWAY A COOLING LOAD OF ONE THIRD THE
820 REM TOTAL FUEL ENERGY INPUT TO THE ENGINE, AND THE AVERAGE CROSS SECTION
830 REM AREA FOR AIR FLOW OVER THE FUEL SYSTEM PARTS.
840 REM COOLING AIR OUT TEMPERATURE IS MEASURED WITH THERMOCOUPLE SHIELDED
850 REM FROM EXHAUST PIPE RADIATION. ASSUMED FUEL HEATING VALUE = 20,000 BTU
860 REM PER LB, SPECIFIC HEAT OF AIR = .24 BTU/LB DEG F, SPECIFIC VOLUME OF
870 REM AIR =14.0 CU FT/LB
880 VA=M/3*20000/60/.24/TA*14.0/MA
890 REM *** REYNOLDS NUMBER OF AIRFLOW OVER CARB LINE
900 RL=VA/60*2*R2/.239E-3
910 REM *** REYNOLDS NUMBER OVER STRAINER
920 RN=VA*D2/60/.239E-3
930 REM *** NUSSELT NUMBER OF AIRFLOW OVER CARB LINE
940 NL=.174*RL[.618
950 REM *** NUSSELT NUMBER OVER STRAINER
960 NS=.174*RN[.618
970 REM *** HEAT TRANSFER COEFFICIENT FOR AIR TO CARB LINE
980 REM IN BTU PER HR, PER DEG F AND PER SQ FT
990 HL=.0174*N/(2*R2)
1000 REM *** HEAT TRANSFER COEFFICIENT FOR AIR TO STRAINER
1010 REM IN BTU PER HR, PER DEG F AND PER SQ FT
1020 HS=.0174*NS/D2
1030 REM *** CONVECTION HEAT TRANSFER TO CARB LINE IN BTU/HR PER FOOT
1040 QT=(TA+TB-TF)/(1/(3.14*D1*500)+LOG(2*R2/D1)/(2*3.14*K)+1/(2*3.14*R2*HL))

```

```

1050 REM *** CONVECTION HEAT TRANSFER TO STRAINER CYLINDRICAL SURFACE IN BTU/HR
1060 QS=(TA+TB-TF)/(1/(3.14*S2/12*LS/12*500)+LOG(SD/S2)/(2*3.14*SK*LS/12)+1/(3.14
* $D2^2$ *LS/12*HS))
1070 REM *** RADIANT HEAT TRANSFER TO CARB LINE IN BTU/HR PER FT
1080 REM * VIEW FACTOR , CARB LINE TO EXHAUST PIPE
1090 F1=ER/EF
1100 REM * FIND CARB LINE OUTSIDE SURFACE TEMPERATURE, T1, WHICH WILL
1110 REM MAKE E=F(T1)=0, BY USING NEWTONS METHOD. FOR INITIAL TRIAL T1=85
1120 T1=85
1130 C9=.17E-8*.5*F1*2*3.14*R2
1140 L1=D1/2*500*LOG(R2/D1*2)/K
1150 E=2*3.14*R2*HL*((TB+TA)-T1)+C9*(ET[4-(T1+460)[4]-2*3.14*K/(LOG(R2/D1*2))*(T1-
(T1+L1*TF)/(1+L1))
1160 REM * TEST TO SEE IF E IS CLOSE ENOUGH TO ZERO
1170 IF E>-.05 AND E<.05 THEN1270
1180 REM * DERIVITIVE OF F(T1)
1190 DE=2*3.14*R2*HL*(-1)+C9*(-4*T1[3]-2*3.14*K/(LOG(R2/D1*2))*(1-1/(1+L1))
1200 REM * NEW ESTIMATE OF T1
1210 T1=T1-E/DE
1220 T9=T1
1230 GOTO1150
1240 REM * WHEN THE CARB LINE SURFACE TEMP IS FOUND THEN CALCULATE THE
1250 REM HEAT TRANSFER. ASSUMPTION: COMBINED RADIANT AND CONVECTION
1260 REM OVER 1/3 OF OUTSIDE SURFACE AREA, CONVECTION ONLY ON THE OTHER 2/3
1270 CR=2*3.14*R2*HL*((TB+TA)-T1) + C9*(ET[4-(T1+460)[4]
1280 RT=1/3*(CR-QT)
1290 REM *** RADIANT HEAT TRANSFER TO STRAINER IN BTU/HR
1300 REM * VIEW FACTOR, STRAINER TO EXHAUST PIPE
1310 F2=ER/ES
1320 REM * DETERMINE STRAINER SURFACE TEMP, T1 IN DEG F
1330 T1=85
1340 C8=.17E-8*.5*F2*3.14*D2
1350 L1=RL*500*LOG(D2/2/RI)/SK
1360 E=3.14*D2*HS*((TB+TA)-T1)+C8*(ET[4-(T1+460)[4]-2*3.14*SK/(LOG(D2/2/RI))*(T1-
(T1+L1*TF)/(1+L1))
1370 IF E>-.05 AND E<.05 THEN1410
1380 DE=3.14*D2*HS*(-1)+C8*(-4*T1[3]-2*3.14*SK/(LOG(D2/2/RI))*(1-1/(1+L1))
1390 T1=T1-E/DE
1400 GOTO1360
1410 RC=(3.14*D2*HS*((TA+TB)-T1) + C8*(ET[4-(T1+460)[4])*LS/12
1420 RS=1/3*(RC-QS)
1430 REM *** TOTAL HEAT TRANSFER TO CARB LINE IN BTU/HR
1440 Q1=LG*(QT+RT)
1450 REM *** TOTAL CONVECTION HEAT TRANSFER TO STRAINER IN BTU/HR, INCLUDING
1460 REM ENDS = HEAT TRANSFER TO CYLINDER SURFACE (QS) TIMES
1470 REM (AREA OF CYLINDER + 2 END AREAS)/AREA OF CYLINDER
1480 QS=QS*(3.14*SD*LS+2*3.14*SD[2/4]/(3.14*SD*LS)
1490 REM *** TOTAL HEAT TRANSFER TO STRAINER IN BTU/HR
1500 Q2=QS+RS
1510 REM *** TOTAL HEAT TRANSFER TO TANK LINE IN BTU/HR, ASSUMPTIONS:
1520 REM ALUMINUM TUBING AND A HEAT TRANSFER COEFFICIENT
1530 REM FOR NATURAL CONVECTION OF 1.5 BTU/HR/DEG F/SQ FT

```

```

1540 Q3=ND/12*3.14*(LK*NT+LV)*(TB-TF)*1.5
1550 REM *** HEAT TRANSFERED THRU CARB LINE PER POUND OF FUEL IN BTU/LB
1560 A1=Q1/M
1570 REM *** HEAT TRANSFERED THRU STRAINER PER POUND OF FUEL IN BTU/LB
1580 B1=Q2/M
1590 REM *** HEAT TRANSFERED THRU TANK LINE PER POUND OF FUEL IN BTU/LB
1600 C1=Q3/M
1610 REM *** TOTAL HEAT TRANSFERED PER POUND OF FUEL, UP TO CARB
1620 REM INLET VALVE, IN BTU/LB. FOR FINDING VAPOR TO LIQUID
1630 REM RATIO AT THIS POINT
1640 CC=A1+B1+C1
1650 REM *** 1/2 OF HEAT TRANSFER THRU CARB LINE + HEAT TRANSFER THRU STRAINER +
1660 REM HEAT TRANSFER THRU TANK LINE, PER POUND OF FUEL FLOW IN BTU/LB
1670 REM TO FIND V/L IN CARB LINE
1680 LL=A1/2+B1+C1
1690 REM *** 1/2 HEAT TRANSFER THRU STRAINER+ HEAT TRANSFER THRU TANK LINE
1700 REM IN BTU/LB TO FIND AVERAGE V/L IN STRAINER
1710 SS=B1/2+C1
1720 REM *** 1/2 HEAT TRANSFER THRU TANK LINE, BTU/LB, TO FIND AVERAGE
1730 REM V/L IN STRAINER
1740 ZZ=C1/2
1750 REM *** ITERATE TO FIND PRESSURE HEAD IN TANK LINE, WHICH, ALONG WITH FUEL
1760 REM HEAD IN GAS TANK, IS ASSUMED TO PROVIDE ALL GRAVITY HEAD (STRAINER
1770 REM AND CARB INLET AT SAME LEVEL). THIS PRESSURE AFFECTS V/L RATIOS.
1780 REM 20 INCHES OF HEAD HAS APPROX THE SAME EFFECT AS 1000 FT ALTITUDE
1790 REM * INITIALIZE "VT" TO A VALUE LARGER THAN EXPECTED
1800 VT=100
1810 FOR I=1 TO 7 STEP 1
1820 REM * TANK LINE PRESSURE HEAD AFTER DENSITY REDUCTION FROM VAPOR IN
1830 REM INCHES OF GASOLINE
1840 PH=(KH-FD)/(1+VT)
1850 REM * PRESSURE ABOVE ATMOSPHERIC IN CARB LINE AND STRAINER, INCHES OF MERC
1860 HG=(PH+FD+TP)*SG/13.6
1870 REM * AVERAGE PRESSURE ABOVE ATMOSPHERIC IN TANK LINE IN INCHES OF MERCURY
1880 HH=(PH/2+FD+TP)*SG/13.6
1890 REM *** SELECT V/L VS BTU/LB CURVE FIT FOR FUEL WANTED
1900 IF FUEL=1 THEN 1950
1910 IF FUEL=100 THEN 2370
1920 IF FUEL=200 THEN 2670
1930 PRINT "WRONG FUEL NUMBER"
1940 GOTO 30
1950 REM *** ADJUST HEAT CONTENT PER POUND OF FUEL #1 TO REFLECT CHANGES
1960 REM TO BTU/LB VS V/L CURVE CAUSED BY DIFFERENT INITIAL FUEL
1970 REM TEMPERATURE (FUEL TEMP - 32 DEG)*SPECIFIC HEAT OF FUEL, AND
1980 REM ALTITUDE ( DEGREES F THAT BTU VS V/L CURVE IS LOWERED PER THOUSAND
1990 REM FT*SPECIFIC HEAT) , ASSUMED SPECIFIC HEAT OF GASOLINE = .5
2000 C=CC+(TF-32)*.5+(AL/1000-HG)*2.5*.5
2010 L=LL+(TF-32)*.5+(AL/1000-HG)*2.5*.5
2020 S=SS+(TF-32)*.5+(AL/1000-HG)*2.5*.5
2030 Z=ZZ+(TF-32)*.5+(AL/1000-HH)*2.5*.5
2040 G=(TG-32)*.5+GA/1000*2.0*.5
2050 V=(TF-32)*.5+(AL/1000-TP*SG/13.6)*2.0*.5

```

```

2060 REM *** FIND V/L RATIO AT CARB INLET, VC, WITH FUEL NO. 1, RVP=14.4
2070 IF C<=18 THEN VC=0
2080 IF C>18 AND C<31 THEN VC=(C-18)*.154
2090 IF C>=31 THEN VC=(C-31)*(1.53+(AL/1000-HG)*.041)+2
2100 REM *** FIND AVERAGE V/L IN CARB LINE, VL
2110 IF L<=18 THEN VL=0
2120 IF L>18 AND L<31 THEN VL=(L-18)*.154
2130 IF L>=31 THEN VL=(L-31)*(1.53+(AL/1000-HG)*.041)+2
2140 REM *** FIND AVERAGE V/L IN STRAINER, VS
2150 IF S<=18 THEN VS=0
2160 IF S>18 AND S<31 THEN VS=(S-18)*.154
2170 IF S>=31 THEN VS=(S-31)*(1.53+(AL/1000-HG)*.041)+2
2180 REM *** FIND AVERAGE V/L THRU TANK LINE
2190 IF Z<=18 THEN VK=0
2200 IF Z>18 AND Z<31 THEN VK=(Z-18)*.154
2210 IF Z>=31 THEN VK=(Z-31)*(1.53+(AL/1000-HH)*.041)+2
2220 REM *** FIND VOLUMES OF VAPOR VENTED FROM FUEL TANK(S) ON GROUND
2230 REM * HAS MORE VAPOR POTENTIAL BEEN ELIMINATED IN THE TANK BY AGITATION?
2240 IF A$="Y" THEN 2250 ELSE 2290
2250 IF G<=18 THEN VG=0
2260 IF G>18 AND G<31 THEN VG=(G-18)*.154
2270 IF G>=31 THEN VG=(G-31)*(1.53+(GA/1000)*.041)+2
2280 GOTO2320
2290 IF G<=26 THEN VG=0
2300 IF G>26 AND G<33 THEN VG=(G-26)*.154
2310 IF G>=33 THEN VG=(G-33)*(1.30+(GA/1000)*.064)+1
2320 REM *** FIND VOLUMES OF VAPOR VENTED FROM FUEL TANK(S) AT ALTITUDE
2330 IF V<=26 THEN VV=0
2340 IF V>26 AND V<33 THEN VV=(V-26)*.154
2350 IF V>=33 THEN VV=(V-33)*(1.30+(AL/1000-TP*SG/13.6)*.064)+1
2360 GOTO 2940
2370 REM *** SAME AS ABOVE BUT WITH DRY 100LL FUEL, RVP =6.8
2380 C=CC+(TF-32)*.5+(AL/1000-HG)*2.8*.5
2390 L=LL+(TF-32)*.5+(AL/1000-HG)*2.8*.5
2400 S=SS+(TF-32)*.5+(AL/1000-HG)*2.8*.5
2410 Z=ZZ+(TF-32)*.5+(AL/1000-HH)*2.8*.5
2420 G=(TG-32)*.5+GA/1000*2.1*.5
2430 V=(TF-32)*.5+(AL/1000-TP*SG/13.6)*2.1*.5
2440 IF C<=51 THEN VC=0
2450 IF C>51 AND C<59 THEN VC=(C-51)*.625
2460 IF C>=59 THEN VC=(C-59)*(1.65+(AL/1000-HG)*.023)+5
2470 IF L<=51 THEN VL=0
2480 IF L>51 AND L<59 THEN VL=(L-51)*.625
2490 IF L>=59 THEN VL=(L-59)*(1.65+(AL/1000-HG)*.023)+5
2500 IF S<=51 THEN VS=0
2510 IF S>51 AND S<59 THEN VS=(S-51)*.625
2520 IF S>=59 THEN VS=(S-59)*(1.65+(AL/1000-HG)*.023)+5
2530 IF Z<=51 THEN VK=0
2540 IF Z>51 AND Z<59 THEN VK=(Z-51)*.625
2550 IF Z>=59 THEN VK=(Z-59)*(1.65+(AL/1000-HH)*.023)+5
2560 IF A$ ="Y" THEN 2570 ELSE 2610
2570 IF G<=51 THEN VG=0
2580 IF G>51 AND G<59 THEN VG=(G-51)*.625
2590 IF G>=59 THEN VG=(G-59)*(1.65+(GA/1000)*.023)+5

```

```

2600 GOTO2630
2610 IF G<=59 THEN VG=0
2620 IF G>59 THEN VG=(G-59)*(1.57+(GA/1000)*.019)
2630 IF V<=59 THEN VV=0
2640 IF V>59 THEN VV=(V-59)*(1.57+(AL/1000-TP*SG/13.6)*.019)
2650 GOTO 2940
2660 REM *** SAME AS ABOVE BUT WITH WET 100LL FUEL
2670 C=CC+(TF-32)*.5+(AL/1000-HG)*1.5*.5
2680 L=LL+(TF-32)*.5+(AL/1000-HG)*1.5*.5
2690 S=SS+(TF-32)*.5+(AL/1000-HG)*1.5*.5
2700 Z=ZZ+(TF-32)*.5+(AL/1000-HH)*1.5*.5
2710 G=(TG-32)*.5+GA/1000*1.7*.5
2720 V=(TF-32)*.5+(AL/1000-TP*SG/13.6)*1.7*.5
2730 IF C<=34 THEN VC=0
2740 IF C>34 AND C<49 THEN VC=(C-34)*.50
2750 IF C>=49 THEN VC=(C-49)*(2.26+(AL/1000-HG)*.20)+5
2760 IF L<=34 THEN VL=0
2770 IF L>34 AND L<49 THEN VL=(L-34)*.50
2780 IF L>=49 THEN VL=(L-49)*(2.26+(AL/1000-HG)*.20)+5
2790 IF S<=34 THEN VS=0
2800 IF S>34 AND S<49 THEN VS=(S-34)*.50
2810 IF S>=49 THEN VS=(S-49)*(2.26+(AL/1000-HG)*.20)+5
2820 IF Z<=34 THEN VK=0
2830 IF Z>34 AND Z<49 THEN VK=(Z-34)*.50
2840 IF Z>=49 THEN VK=(Z-49)*(2.26+(AL/1000-HH)*.20)+5
2850 IF A$="Y"THEN 2860 ELSE 2900
2860 IF G<=34 THEN VC=0
2870 IF G>34 AND G<49 THEN VG=(G-34)*.50
2880 IF G>=49 THEN VG=(G-49)*(2.26+(GA/1000)*.20)+5
2890 GOTO 2920
2900 IF G<=50 THEN VG=0
2910 IF G>50 THEN VG=(G-50)*(2.11+(AL/1000)*.12)
2920 IF V<=50 THEN VV=0
2930 IF V>50 THEN VV=(V-50)*(2.11+(AL/1000-TP*SG/13.6)*.12)
2940 REM *** CORRECT V/L RATIOS FOR VOLUMES OF VAPOR VENTED FROM FUEL TANK
2950 REM SUBTRACT THE LARGER OF VG OR VV FROM THE V/L RATIOS
2960 IF VG>VV THEN VW=VG ELSE VW=VV
2970 VT=VK-VW
2980 IF VT<0 THEN VT=0
2990 NEXT I
3000 VC=VC-VW
3010 VL=VL-VW
3020 VS=VS-VW
3030 VK=VK-VW
3040 IF VC<0 THEN VC=0
3050 IF VL<0 THEN VL=0
3060 IF VS<0 THEN VS=0
3070 IF VK<0 THEN VK=0
3080 REM *** PRESSURE DROP ACROSS CARB INLET VALVE IN INCHES OF
3090 REM GASOLINE HEAD
3100 DC=1/CF[2*(CH/CQ[2*Q[2 - SH/SQ[1.75*Q[1.75)*(1+VC)
3110 REM *** PRESSURE DROP ACROSS CARB LINE IN INCHES OF GASOLINE
3120 DL=DP*(1+VL)

```

```

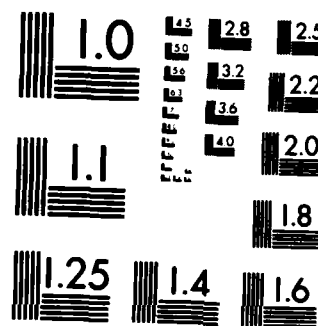
3130 REM *** PRESSURE DROP ACROSS STRAINER IN INCHES OF GASOLINE
3140 REM ASSUMPTION: PRESSURE DROP ACROSS STRAINER DECREASES INVERSELY
3150 REM WITH THE SQUARE OF THE INSIDE CYLINDER SURFACE AREA.
3160 REM DELTA P NEW = DELTA P BASELINE *(AB/AN) SQUARED, WHERE BASELINE
3170 REM SURFACE AREA = AB, NEW AREA = AN
3180 AB=3.14*(BD-2*WT)*(BL-2*WT)+(2*3.14*(BD-2*WT)[2/4]
3190 AN=3.14*(SD-2*WT)*(LS-2*WT)+(2*3.14*(SD-2*WT)[2/4]
3200 DS=AB[2/AN[2*(SH/SQ[1.75 - KH/KQ[1.75)*Q[1.75*(1+VS)
3210 REM *** PRESSURE DROP ACROSS FUEL TANK TO STRAINER LINE,
3220 REM INCLUDING SELECTOR VALVE
3230 DK=KH/KQ[1.75*Q[1.75*(1+VK)
3240 REM *** CALCULATE NEW PRESSURE DROP ACROSS TANK LINE PRODUCED WITH
3250 REM NEW LINE SIZE, AND DETERMINE PRESSURE DROP DUE TO SELECTOR VALVE
3260 REM * TANK LINE INSIDE DIAMETERS IN FEET
3270 KI=(KD-2*KW)/12
3280 NI=(ND-2*KW)/12
3290 REM * CALCULATED TANK LINE PRESSURE DROP BY PIGOTT'S EQUATION
3300 KV=KQ/NT/3600*4/3.14/KI[2/7.48
3310 RK=SG*62.4
3320 UK=.34*.000672
3330 DB=3.417E-5*UK[.25*LK*RK[.75*KV[1.75/KI[1.25
3340 DB=DB*27.7/SG
3350 REM * PRESSURE DROP ACROSS TANK LINE(S) (WITHOUT SELECTOR VALVE) WITH THE
3360 REM NEW TUBING SIZE = CALCULATED BASELINE/MEASURED BASELINE PRESS DROPS
3370 REM (FOR FLOW RATE 'KQ) TIMES TOTAL TANK LINE & SELECTOR DROP (DK) TIMES
3380 REM THE RATIO OF THE INSIDE LINE DIAMETERS TO THE 4.75 POWER
3390 DM=DB/KH*DK*(KI/NI)[4.75
3400 REM * SELECTOR PRESS DROP = (MEASURED - CALCULATED)/MEASURED PRESS DROPS
3410 REM (AT THE MEASURED FLOW RATE 'KQ) TIMES THE TANK TO STRAINER PRESS
3420 REM DROP (DK). SELECTOR PRESSURE DROP INCLUDES ELBOWS, FITTINGS, AND THE
3430 REM DROP THRU THE LINE FROM SELECTOR TO STRAINER (NO DIAMETER CHANGE).
3440 DV=(KH-DB)/KH*DK
3450 REM * TOTAL TANK LINE PRESS DROP= TANK LINE + SELECTOR VALVE PRESSURE DROPS
3460 DN=DM+DV
3470 REM *** TOTAL PRESSURE DROP IN INCHES OF GASOLINE
3480 DT=DC+DL+DS+DN
3490 REM *** TOTAL PRESSURE HEAD AVAILABLE IN INCHES OF GASOLINE
3500 TH=TP+FD+PH+BII-RH
3510 REM *** PRINT RESULTS
3520 LPRINT "FUEL=";FUEL;"SG=";SG;"M=";M;"Q=";Q;"AL=";AL;"AR=";AR;"MA=";MA;"TA=";TA
;"TF=";TF;"TB=";TB
3530 LPRINT "GA=";GA;"TG=";TG;"EF=";EF;"ES=";ES;"ED=";ED;"EP=";EP
3540 LPRINT "KD=";KD;"ND=";ND;"KW=";KW;"NT=";NT;"LK=";LK;"LV=";LV
3550 LPRINT "SK=";SK;"WT=";WT;"BD=";BD;"BL=";BL;"SD=";SD;"LS=";LS
3560 LPRINT "K=";K;"T=";T;"W=";W;"LG=";LG;"CF=";CF;"AGITATION=";AS
3570 LPRINT "CQ=";CQ;"CH=";CH;"SQ=";SQ;"SH=";SH;"KQ=";KQ;"KH=";KH
3580 LPRINT "QT=";QT;"QS=";QS;"Q3=";Q3
3590 LPRINT "RT=";RT;"RS=";RS;"T9=";T9;"T1=";T1
3600 LPRINT "FV=";FV;"RE=";RE;"KV=";KV;"VA=";VA;"HL=";HL;"HS=";HS
3610 LPRINT "C=";C;"L=";L;"S=";S;"Z=";Z;"G=";G;"V=";V
3620 LPRINT "VC=";VC;"VL=";VL;"VS=";VS;"VK=";VK;"VV=";VV;"VG=";VG
3630 LPRINT "DC=";DC;"DL=";DL;"DS=";DS;"DV=";DV;"DK=";DK;"DN=";DN;"DB=";DB;"DP=";DP
3640 LPRINT "RH=";RH;"BH=";BH;"PH=";PH;"FD=";FD;"TP=";TP;"TH=";TH
3650 LPRINT "A1=";A1;"B1=";B1;"C1=";C1;"HG=";HG;"HH=";HH;"BV=";BV
3660 LPRINT " "
3670 GOTO30

```

| | | | | |
|------|-------|---|--------------------|--|
| 3680 | 'FUEL | = FUEL TYPE | | |
| 3690 | 'SG | = FUEL SPECIFIC GRAVITY | | |
| 3700 | 'M | = FUEL MASS FLOW RATE | LB/HR | |
| 3710 | 'Q | = VOLUMETRIC FUEL FLOW RATE | GAL/HR | |
| 3720 | 'AL | = ALTITUDE | FT | |
| 3730 | 'AR | = AIR SPEED | KNOTS | |
| 3740 | 'MA | = MEAN AREA OF AIR DUCTNG OVER FUEL SYSTEM | SQ FT | |
| 3750 | 'TA | = AIR TEMP RISE ABOVE AMBIENT, ACROSS ENGINE | DEG F | |
| 3760 | 'TF | = TEMPERATURE OF FUEL IN FUEL TANK | DEG F | |
| 3770 | 'TB | = AMBIENT TEMPERATURE | DEG F | |
| 3780 | 'GA | = ALTITUDE OF AIRPORT | FT | |
| 3790 | 'TG | = MAXIMUM TEMPERATURE THAT FUEL IN FUEL TANK HAS BEEN DEG F | | |
| 3800 | 'EF | = DISTANCE FROM EXHAUST PIPE TO CARB LINE | INCHES | |
| 3810 | 'ES | = DISTANCE FROM EXHAUST PIPE TO STRAINER | INCHES | |
| 3820 | 'ED | = EXHAUST PIPE DIAMETER | INCHES | |
| 3830 | 'EP | = EXHAUST PIPE TEMPERATURE | DEG F | |
| 3840 | 'KD | = BASELINE TANK TO STRAINER LINE, OUTSIDE DIAMETER | INCHES | |
| 3850 | 'ND | = NEW TANK TO STRAINER LINE, OUTSIDE DIAMETER | INCHES | |
| 3860 | 'KW | = TANK LINE WALL THICKNESS | INCHES | |
| 3870 | 'SK | = STRAINER WALL THERMAL CONDUCTIVITY | BTU/HR/FT SQ/DEG F | |
| 3880 | 'WT | = STRAINER WALL THICKNESS | INCHES | |
| 3890 | 'BD | = BASELINE STRAINER DIAMETER | INCHES | |
| 3900 | 'BL | = BASELINE STRAINER LENGTH | INCHES | |
| 3910 | 'SD | = NEW STRAINER DIAMETER | INCHES | |
| 3920 | 'LS | = NEW STRAINER LENGTH | INCHES | |
| 3930 | 'NT | = NUMBER OF FUEL TANKS TURNED ON | | |
| 3940 | 'LK | = TANK LINE LENGTH(S) FROM TANK TO SELECTOR VALVE | FT | |
| 3950 | 'LV | = LINE LENGTH FROM SELECTOR VALVE TO STRAINER | FT | |
| 3960 | 'K | = CARB LINE THERMAL CONDUCTIVITY | BTU/HR/FT SQ/DEG F | |
| 3970 | 'T | = CARB LINE INSIDE DIAMETER | INCHES | |
| 3980 | 'W | = CARB LINE WALL THICKNESS | INCHES | |
| 3990 | 'LG | = CARB LINE LENGTH | FT | |
| 4000 | 'CF | = CARB FLOAT NEEDLE VALVE AREA, RELATIVE TO BASELINE | | |
| 4010 | 'CQ | = MEASURED FLOW RATE THROUGH CARB FLOAT VALVE | GAL/HR | |
| 4020 | 'CH | = FUEL HEAD, FUEL LEVEL TO CARB FLOAT VALVE | INCHES | |
| 4030 | 'SQ | = MEASURED FLOW RATE, FUEL TANK TO STRAINER OUTLET | GAL/HR | |
| 4040 | 'SH | = FUEL HEAD, FUEL LEVEL TO STRAINER OUTLET | INCHES | |
| 4050 | 'KQ | = MEASURED FLOW RATE, FUEL TANK TO STRAINER INLET | GAL/HR | |
| 4060 | 'KH | = FUEL HEAD, FUEL LEVEL TO STRAINER INLET | INCHES | |
| 4070 | 'QT | = CONVECTION HEAT TRANSFER TO CARB LINE | BTU/HR/FT | |
| 4080 | 'QS | = CONVECTION HEAT TRANSFER TO STRAINER | BTU/HR | |
| 4090 | 'Q3 | = HEAT TRANSFER TO TANK LINE | BTU/HR | |
| 4100 | 'RT | = RADIANT HEAT TRANSFER TO CARB LINE | BTU/HR/FT | |
| 4110 | 'RS | = RADIANT HEAT TRANSFER TO STRAINER | BTU/HR | |
| 4120 | 'T9 | = CARB LINE OUTSIDE SURFACE TEMPERATURE | DEG F | |
| 4130 | 'T1 | = STRAINER OUTSIDE SURFACE TEMPERATURE | DEG F | |
| 4140 | 'V | = FUEL VELOCITY IN CARB LINE | FT/SEC | |
| 4150 | 'RE | = CARB LINE FUEL FLOW REYNOLDS NUMBER | | |
| 4160 | 'KV | = FUEL VELOCITY IN TANK LINE AT MEAS FLOW 'KQ | FT/SEC | |
| 4170 | 'VA | = AVERAGE AIR VELOCITY OVER FUEL SYSTEM PARTS | FT/MIN | |
| 4180 | 'HL | = HEAT TRANSFER COEFFICIENT, AIR TO CARB LINE | BTU/HR/FT/DEG F | |
| 4190 | 'HS | = HEAT TRANSFER COEFFICIENT, AIR TO STRAINER | BTU/HR/FT/DEG F | |

AD-A150 336 SOME CHARACTERISTICS OF AUTOMOTIVE GASOLINES AND THEIR 2/2
PERFORMANCE IN A L. (U) MICHIGAN UNIV ANN ARBOR DEPT OF
MECHANICAL ENGINEERING AND AP. K M MORRISON ET AL.
UNCLASSIFIED NOV 84 DOT/FAR/CT-84/12 DOT-FAR79NA-6083 F/G 21/4 NL





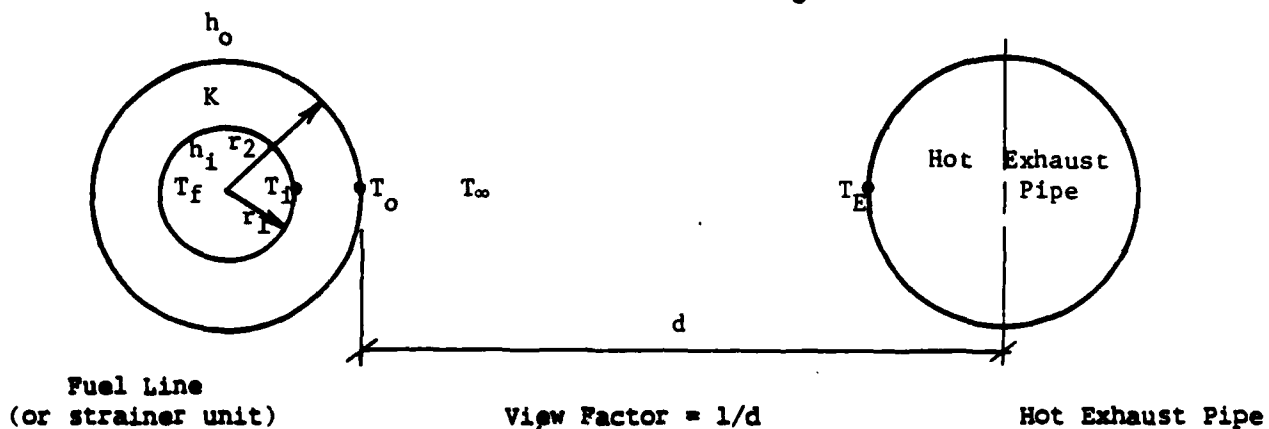
MICROCOPY RESOLUTION TEST CHART
NATIONAL BUREAU OF STANDARDS-1963-A

| | | |
|----------|---|--------------------|
| 4200 'C | = HEAT CONTENT PER POUND OF FUEL AT CARB INLET | BTU/LB |
| 4210 'L | = HEAT CONTENT PER POUND OF FUEL THRU CARB LINE | BTU/LB |
| 4220 'S | = HEAT CONTENT PER POUND OF FUEL THRU STRAINER | BTU/LB |
| 4230 'Z | = HEAT CONTENT PER POUND OF FUEL THRU TANK LINE | BTU/LB |
| 4240 'V | = HEAT CONTENT PER POUND OF FUEL IN TANK AT ALTIT. BTU/LB | |
| 4250 'VC | = VAPOR TO LIQUID RATIO AT CARB INLET VALVE | |
| 4260 'VL | = AVERAGE VAPOR TO LIQUID RATIO IN CARB LINE | |
| 4270 'VS | = AVERAGE VAPOR TO LIQUID RATIO IN STRAINER | |
| 4280 'VK | = AVERAGE VAPOR TO LIQUID RATIO IN TANK LINE | |
| 4290 'VV | = VOLUMES OF VAPOR VENTED AT ALTITUDE | |
| 4300 'VG | = VOLUMES OF VAPOR VENTED ON GROUND | |
| 4310 'DC | = PRESSURE DROP ACROSS CARB INLET VALVE | INCHES OF GASOLINE |
| 4320 'DL | = PRESSURE DROP ACROSS CARB LINE | INCHES OF GASOLINE |
| 4330 'DS | = PRESSURE DROP ACROSS STRAINER | INCHES OF GASOLINE |
| 4340 'DV | = PRESSURE DROP ACROSS SELECTOR VALVE | INCHES OF GASOLINE |
| 4350 'DK | = BASELINE PRESS DROP ACROSS TANK LINE & SELECTOR | INCHES OF GASOLINE |
| 4360 'DN | = NEW PRESSURE DROP ACROSS TANK LINE & SELECTOR | INCHES OF GASOLINE |
| 4370 'DB | = CALCULATED PRESS DROP THRU BASE TANK LINE AT 'KQ | INCHES OF GASOLINE |
| 4380 'DT | = TOTAL PRESSURE DROP ACROSS FUEL SYSTEM | INCHES OF GASOLINE |
| 4390 'RH | = TOTAL RISER HEAD LOSS | INCHES OF GASOLINE |
| 4400 'BH | = ADDITIONAL PRESSURE HEAD DUE TO CARB BOWL VACUUM | INCHES OF GASOLINE |
| 4410 'PH | = TANK LINE PRESSURE HEAD AVAILABLE | INCHES OF GASOLINE |
| 4420 'FD | = FUEL TANK DEPTH, FUEL LEVEL TO OUTLET | INCHES |
| 4430 'TP | = FUEL TANK PRESSURE DUE TO RAM VENT | INCHES OF GASOLINE |
| 4440 'TH | = TOTAL PRESSURE HEAD AVAILABLE | INCHES OF GASOLINE |
| 4450 'A1 | = HEAT TRANSFERED THRU CARB LINE PER POUND OF FUEL | BTU/LB |
| 4460 'B1 | = HEAT TRANSFERED THRU STRAINER PER POUND OF FUEL | BTU/LB |
| 4470 'C1 | = HEAT TRANSFERED THRU TANK LINE PER POUND OF FUEL | BTU/LB |
| 4480 'HG | = GAGE PRESSURE IN CARB LINE AND STRAINER | INCHES OF MERCURY |
| 4490 'HH | = GAGE PRESSURE IN TANK LINE | INCHES OF MERCURY |
| 4500 'BV | = CARB BOWL VACUUM | INCHES OF WATER |

APPENDIX D

METHOD OF FINDING FUEL LINE SURFACE TEMPERATURE

METHOD OF FINDING FUEL LINE
SURFACE TEMPERATURE (T_o)



$$\text{Eqn. 1: } q_1 = 2\pi r_2 l h_o (T_o - T_o) + C(T_e^4 - T_o^4)$$

$$\text{Eqn. 2: } q_2 = \frac{2\pi k l}{\ln(r_2/r_1)} (T_o - T_i)$$

$$\text{Eqn. 3: } q_3 = 2\pi r_1 l h_i (T_i - T_f)$$

Eqn. 1 is the convection heat transfer from ambient to surface plus the radiation to the surface.

Eqn. 2 is the conductive heat transfer through the wall.

Eqn. 3 is the convection heat transfer from the wall to the fuel under steady-state conditions.

The heat transferred to the surface equals the heat conducted through the wall and equals the heat transferred to the fuel.

$$q_1 = q_2 = q_3$$

Setting Eqn. 2 = Eqn. 3 ($q_2 = q_3$) and solving for T_i

$$\frac{2\pi k l}{\ln(r_2/r_1)} (T_o - T_i) = 2\pi r_1 l h_i (T_i - T_f)$$

$$T_o - T_i = \frac{2\pi r_1 l h_i \ln(r_2/r_1) (T_i - T_f)}{2\pi k l}$$

$$T_i = \frac{\frac{(T_0 + r_i h_i \ln(r_2/r_1) T_f)}{k}}{(1 + \frac{r_i h_i \ln(r_2/r_1)}{k})}$$

Now substituting the expression for T_i derived above into Eqn. 1 and Eqn. 2 and setting Eqn. 1 - Eqn. 2 = 0 ($q_1 = q_2$), we can numerically find the value for T_0 which satisfies this condition.

$$q_1 - q_2 = 0$$

$$2\pi r_2 l h_0 (T_\infty - T_0) + C(T_e^4 - T_0^4) - \frac{2\pi k l}{\ln(r_2/r_1)} (T_0 - T_i) = 0$$

$$f(T_0) = 2\pi r_2 l h_0 (T_\infty - T_0) + C(T_e^4 - T_0^4) - \frac{2\pi k l}{\ln(r_2/r_1)} \frac{T_0 - (T_0 + \frac{r_i h_i \ln(r_2/r_1) T_f}{k})}{(1 + \frac{r_i h_i \ln(r_2/r_1)}{k})} = 0$$

We can now use a numerical method (such as Newton's) to find a value of T_0 such that when substituted into the equation above, $f(T_0)$ will equal 0.

C = Stefan-Boltzman Constant x View Factor x Emissivity of Exhaust Pipe Surface x Area of Cylinder Exposed to Radiation

END

FILMED

3-85

DTIC